ABSTRACT

Title of Dissertation:	SALTWATER INTRUSION ALTERS NITROGEN AND PHOSPHORUS TRANSFORMATIONS IN COASTAL AGROECOSYSTEMS
	Danielle Shoshana Weissman, Doctor of Philosophy, Agroecology, 2020
Dissertation directed by:	Dr. Kate Tully, Department of Plant Science and Landscape Architecture

As sea levels rise, coastal regions are becoming more vulnerable to saltwater intrusion (SWI). In coastal agricultural areas, SWI is causing changes in biogeochemical cycling in soil and waterways. These changes are leading to the release of excess nitrogen (N) and phosphorus (P) from farm fields, which in turn can cause impaired water quality downstream. I explored the effects of saltwater intrusion on N and P concentrations of surface water and soil porewater on Maryland's Eastern Shore in the Chesapeake Bay Watershed on three spatial and temporal scales: 1) a three-year field study through farmland and various surrounding habitats; 2) a one-month laboratory soil incubation study; and 3) a regional study of tidal tributaries (sub-watersheds) along Maryland's Eastern Shore where I utilized 35 years of observational data on nutrient concentrations and salinity from the Chesapeake Bay Water Quality Monitoring Program. The results of the field and incubation studies

suggest that SWI can cause a large release of N and P from the soils of coastal landscapes to downstream water bodies such as tidal creeks and marshes. However, the results of the regional study suggest that the relative magnitude of SWI-driven contributions of N and P to waterways as compared to other sources and drivers of N and P differ depending on the spatial and temporal scale considered. Defining mechanisms through which SWI spurs nutrient release from soils of agricultural fields and surrounding habitats as well as the magnitude of these processes is critical for quantifying N and P export in coastal watersheds. The results of these three studies can potentially be used to inform water quality models for individual tidal tributaries, which would allow for more targeted approaches to nutrient load reductions in sub-watersheds of the Chesapeake Bay and other watersheds globally.

SALTWATER INTRUSION ALTERS NITROGEN AND PHOSPHORUS TRANSFORMATIONS IN COASTAL AGROECOSYSTEMS

by

Danielle Shoshana Weissman

Dissertation submitted to the Faculty of the Graduate School of the
University of Maryland, College Park, in partial fulfillment
of the requirements for the degree of
Doctor of Philosophy
2020

Advisory Committee:
Dr. Kate Tully, Chair
Dr. Keryn Gedan
Dr. Kristal Jones
Dr. Margaret Palmer
Dr. Stephanie Yarwood

Acknowledgements

First and foremost, I would like to thank my mentor, Dr. Kate Tully for her incredible guidance, encouragement, and feedback through my PhD process. I could not have asked for a better mentor. I would also like to thank my committee members: Dr. Keryn Gedan, Dr. Kristal Jones, Dr. Margaret Palmer, Dr. Stephanie Yarwood, for their helpful insight and feedback over the past five years. Dr. Palmer provided me with a wonderful and unique opportunity to work as a Graduate Assistant at the National Socio-Environmental Synthesis Center, where she is the Director.

I would also like to thank Aubrey Wiechecki, Tia Ouyang, John Dietrich, Tony Pham, and the many other undergraduate students that helped me with my research over the years. I simply could not have done this without all of them. I would like to give a special thanks to Quentin Read for the statistical help for Chapter 2 and Christopher Wingate for completing the land cover change analysis for Chapter 3 of this study. Additionally, I appreciate the farmers who generously allowed me to conduct research on their land.

Finally, I would like to acknowledge the funding sources that allowed me to carry out this research. This work was supported by several funding sources: a Seed Grant through the University of Maryland National Science Foundation-ADVANCE Institutional Transformation grant (grant no. HRD-1008117); a USDA National Institute for Food and Agriculture (NIFA) Integrated Agriculture and Natural Resources Extension and Research Program Grant administered through the University of Maryland (project no. MD-PSLA-18496/project accession no. 1016911); a grant from the USDA NIFA Resilient Agroecosystems in a Changing Climate Challenge Area (grant no. 12451226/project accession no. 1015143); a Maryland Sea Grant Coastal Resilience and Sustainability Fellowship (grant no. 20171-002); and the National Socio-Environmental Synthesis Center. The National Socio-Environmental Synthesis Center is supported by an award from the US National Science Foundation (Grant #s DBI-1052875 and DBI-1639145) to the University of Maryland, with additional support from University of Maryland, University of Maryland Center for Environmental Science, and Resources for the Future.

Table of contents

List of Tables

List of Figures

List of Supplemental Figures

Chapter 1: Saltwater intrusion affects nutrient concentrations in soil porewater and surface waters of coastal habitats

Abstract

Coastal ecosystems are undergoing major biogeochemical shifts due to climate change and sea level rise. At the same time, agricultural fertilizer applications are increasing coastal nutrient inputs. In this study, we examine the potential impact of saltwater intrusion (SWI) on nitrogen (N) and phosphorus (P) concentrations in soil porewater and surface water of different habitats within the Chesapeake Bay estuary. Study sites are located along Maryland's Lower Eastern Shore and were monitored over three summers from 2016 to 2018. These sites encompass various habitats on the land-sea interface, consisting of healthy forests, intruded forests, abandoned fields, intruded fields, agricultural ditches, tidal creeks, and tidal salt marshes. Intruded fields were being actively farmed at the time of the study. Soil porewater and surface water grab samples were collected from the habitats and analyzed for electrical conductivity, pH, dissolved organic P (DOP), dissolved inorganic P in the form of soluble reactive P (SRP), dissolved inorganic N as ammonium-N (NH_4-N), and total dissolved iron (TDFe). Electrical conductivity was greatest in the marshes (16.58 mS/cm averaged across all years) and did not significantly differ among intruded forests, intruded fields, and agricultural ditches. As a legacy of heavy fertilizer use, DOP concentrations exceeded 0.45 mg P/l in all habitats. Concentrations of inorganic N and P differed significantly by habitat. Concentrations of NH_4-N were significantly higher in salt marsh soil porewater than

in any other habitat measured. Overall, SRP concentrations were highest in the soil porewater of intruded fields and marshes and in the surface water of agricultural ditches (0.30, 0.29, and 0.33 mg P/l averaged across all years, respectively). These concentrations greatly exceeded recommended U.S. Environmental Protection Agency nutrient pollution thresholds for the region. In its oxidized state, dissolved iron can bind to SRP and prevent it from becoming bioavailable. However, TDFe concentrations in the ditches, tidal creeks, and marshes were too low to adequately buffer against SRP loss to downstream areas. As SWI moves salts inland and increases hydrologic connectivity across coastal landscapes, it is important to consider the mechanisms through which nutrients may be released from coastal soils and their potential to impact downstream water quality.

Introduction

Coastal agricultural landscapes are changing rapidly in response to climate change. Low-lying farmland is particularly vulnerable to saltwater intrusion (SWI) and coastal flooding. In many areas of the world, cultivated landscapes, forests, and other ecosystems are transforming into tidal salt marshes as sea levels rise (Smith 2013; Moomaw et al. 2018; Kirwan and Gedan 2019). As a result, extensive upland area will be lost rapidly in coming decades (Wasson et al. 2013). This phenomenon is spurring radical shifts in ecosystem dynamics, including biogeochemical cycling in soils and water bodies (Bhattachan et al. 2018).

Though the effects of SWI on coastal forests have been studied (Hussein and Rabenhorst 2010; Marton et al. 2012; White and Kaplan 2017), little research has focused on its impact on farmland. Salinization of agricultural soils has been studied

widely (Allison et al. 1954; Hanin et al. 2016). However, soil salinization studies only consider well-drained inland soils that receive salts via irrigation water (e.g. they are saline but not saturated) and have very different biogeochemical processes than SWI-affected soils in coastal areas (e.g. they are saline and frequently saturated).

Globally, accelerating rates of sea level rise are increasing the amount of coastal upland area that is affected each year (White and Kaplan 2017). The combination of agricultural land use legacies, sea level rise, and SWI has large and measurable effects on soil biogeochemical processes (Ardón et al. 2013; Helton et al. 2014; Sharpley et al. 2014). Thus, it is critical to develop an understanding of how SWI affects these processes in coastal regions in order to determine how to best help communities adapt to this phenomenon. In this study we explore interactions between SWI, nitrogen (N), and phosphorus (P) that can lead to nutrient pollution in waterways.

As sea levels rise, SWI into freshwater ecosystems has increased in frequency, duration, and spatial extent. This phenomenon can enhance nutrient export from watersheds (Ardón et al. 2013, 2017; Williams et al. 2014). Prior studies indicate that salts and sulfate (SO_4^{2-}) in saltwater can lead to N and P release from inundated soils as ammonium (NH_4^+), nitrate (NO_3^-), and phosphate (PO_4^{3-}) due to mechanisms of ion exchange (Ardón et al. 2013, 2017; Williams et al. 2014). These ionic forms are inorganic and readily bioavailable. Phosphorus is often retained in farm soils after decades of excessive fertilizer use (legacy P) by binding to metals such as iron (Fe) and aluminum (Al; Sharpley et al. 2014, Tully et al. 2019b). Pools of P tend to be recalcitrant in the aerobic upper soil layers of agricultural fields but can become

mobile and bioavailable due to Fe transformations associated with saturated and reducing conditions as fields undergo SWI (Tully et al. 2019b). Ammonium can be released from inundated soil through cation exchange with salts (Ardón et al. 2013), and studies have demonstrated that N and P export is enhanced in oxygen depleted soils saturated with saltwater (Brand-Klibanski et al. 2007; Dierberg et al. 2011; Ardón et al. 2017). Since coastal groundwater tables in the study region are typically shallow (< 3 m; Sharpley et al. 2014), SWI and tidal inundation can create anaerobic conditions in upper soil layers. Although wetlands typically serve as nutrient filters and sinks (Tanner and Sukias 2011), they may become net sources of nutrients to water bodies downstream as they receive high concentrations of legacy nutrients from flooded agricultural soils upstream (Weston et al. 2006; Nair et al. 2013). Effective nutrient management requires a better understanding of the role that SWI plays in transporting nutrients off farm fields and into nearby habitats.

This study focuses on differences in nutrient concentrations in the soil porewater and surface water of farmland and surrounding hydrologically connected habitats undergoing SWI in the Chesapeake Bay, which is the largest estuary in the United States (Boesch 2006) and is situated along the Atlantic Coastal Plain region. Our study took place in Somerset County, Maryland along its border with the Chesapeake Bay, where the primary drivers of SWI are land subsidence and sea level rise (Ezer and Corlett 2012; Tully et al. 2019a).

By 2050, sea level is projected to rise anywhere from 28 to 65 cm along the mid-Atlantic Coastal Plain under most emissions scenarios (Miller et al. 2013). In response, tidal marshes are predicted to migrate into upland forest and farmland

(Glick et al. 2008). Agricultural fields in coastal areas of the Atlantic Coastal Plain are bounded by ditches on one or more sides to allow for drainage (e.g. removing water from fields). However, these ditches are often connected to tidal creeks that drain into tidal salt marshes and larger tributaries such as rivers, bays, and subestuaries (Bhattachan et al. 2018; Tully et al. 2019a). Sea level rise can convert them into conduits for saltwater moving onto fields. Tide gates, which allow water to flow unidirectionally (i.e. off of a farm field into an agricultural ditch; Roman & Burdick, 2012) are sometimes installed to allow fields to drain during low tide and prevent saltwater from moving onto fields during high tide (Walsh and Miskewitz 2013). As sea levels rise, maintaining functional tide gates on low lying farmland has become challenging (Walsh and Miskewitz 2013). Due to high soil salinity, farmers and landowners have stopped planting crops on a significant portion of fields in Somerset County (Maryland Department of Natural Resources and NOAA 2008). These fields have been overtaken by novel plant communities, which include a mixture of agricultural weeds, native and non-native wetland vegetation, and upland species (Gedan and Fernández-Pascual 2019). Nearby forested areas are also undergoing SWI. In this study, our main objective was to determine how soil porewater and surface water electrical conductivity (EC; a proxy for salinity), N, and P concentrations change in distinct yet connected habitats across the land-sea interface. We also measured pH and total dissolved iron (TDFe) to allow us to better interpret our findings as they are important controls on some of the processes that affect N and P cycling in systems undergoing SWI (Chambers and Odum 1990; Tully et al. 2019b).

This goal of this research was to determine how agricultural fertilizer inputs and legacy nutrients affect concentrations of N and P in habitats within coastal agroecosystems undergoing SWI. To accomplish this, we first identified seven distinct habitats: (1) forest; (2) intruded forest; (3) abandoned field; (4) intruded field (actively farmed); (5) ditch (agricultural ditch); (6) tidal creek; and (7) marsh (tidal salt marsh). We measured dissolved inorganic N and P in the form of ammonium nitrogen (NH_4-N), nitrate nitrogen (NO_3-N), soluble reactive phosphorus (SRP), and dissolved organic P (DOP) in soil porewater and surface water collected from these habitats. We expected dissolved inorganic N to be primarily in the form of NH_4^+ as NO_3^- is rapidly converted to other forms under low oxygen conditions that form in saturated soils. We hypothesized that SRP concentrations would be highest on intruded fields and in their surrounding ditches due to active farming and P applications on these fields. We also expected to observe high concentrations of SRP and DOP that had moved off of farm fields in downstream tidal creeks and salt marshes. Finally, we also considered the potential that a proportion of the different forms of N and P measured in each habitat were estuarine-derived through analysis of concentration data from the Chesapeake Bay Program at water quality monitoring stations located near our study sites (Chesapeake Bay Program 2019). We hypothesized that this contribution would be minor compared to concentrations we observed in our selected habitats. Measurements of nutrient concentrations in different areas of SWI-affected agroecosystems can indicate which habitats are net sources of N and P to downstream waterways and lead to an improved understanding of key biogeochemical controls on N and P transformations in these systems.

Methods

Study site

We studied a suite of biogeochemical responses to SWI along the coast of Somerset County, Maryland, located in the mesohaline zone of the Chesapeake Bay. From 1985 to 2006, mean annual surface water salinities along the coastline of Somerset County ranged from 7.6-18 parts per thousand (ppt; 11.9-28.1 mS/cm) in the spring and 12.6-18 ppt (19.7-28.1 mS/cm) in the winter (Weinberg 2008).

Our study sites are located near Princess Anne in Somerset County, the southernmost county in Maryland (38.2° N, 75.7° W; Figure 1-1A and 1-1B). Somerset County is a major producer of poultry, grains, oilseeds, and beans (USDA-NASS 2012). The area receives an average of 1085 mm of precipitation annually. The mean annual high temperature is 19°C and the mean annual low temperature is 10.2°C (NOAA-NCEI 2018). Over the course of the study, conditions were wet and warm relative to an average year. Total annual precipitation ranged from 1370 to 1610 mm, mean high temperatures ranged from 20.7 to 20.9°C, and mean low temperatures ranged from 8.8 to 9.5°C (2016-2018).

This region has a land use history of clearcutting and reforestation (Trimble 2008). Until the 1930s, most upland areas of Somerset County were agricultural (Markewich et al. 1990). Now, roughly 32% of the county's land area is in agriculture (USDA-NASS 2012) and approximately 50% is loblolly pine-dominated forest (Kirwan et al. 2007; Lister et al. 2011). Tidal salt marshes cover about 15% of Somerset County and are located along its coastline (Shepard et al. 2013).

In 2017, agricultural runoff contributed to 42% of N and 56% of P loading in the Chesapeake Bay (Chesapeake Bay Program 2018). Excess nutrients can cause hypoxic zones, algal blooms, and fish kills (Boesch et al. 2001; Burgin and Hamilton 2007; Perez 2015). Though many parts of the Bay are showing water quality improvement, as of 2016, 58% of Bay tidal waters did not meet standards for dissolved oxygen, chlorophyll-a, and water clarity, key indicators of good water quality (Zhang et al. 2018). In 2017, the U.S. Geological Survey found increasing N and P loads at several monitoring stations along major tributaries that drain into the Bay (Moyer and Blomquist 2018). In most tributaries within our study area, nutrient concentrations exceed water quality standards set by the U.S. Environmental Protection Agency (EPA; Maryland Department of the Environment 2018). Moreover, P management has been particularly challenging in this area due to the large and intensifying poultry industry and the historic over-application of P-rich poultry litter on farm fields (Kleinman et al. 2011; Sharpley et al. 2014; Waldrip et al. 2015).

Water sample collection and analysis

Water samples were collected four to five times (approximately once a month) over late spring to early fall each year (2016-2018) (n_{total}=13) at five different agroecosystem sites along the west coast of Somerset County. Each site comprised at least four of the following habitats: (1) forest; (2) intruded forest; (3) abandoned field; (4) intruded field; (5) ditch; (6) tidal creek; and (7) marsh (Table 1-1). An illustrated example of the layout of a typical site is shown in Figure 1-2A. Each habitat was represented at a minimum of three sites (Table 1-1). Descriptions of the soil type for

each habitat are included in Table 1-2. Broadly, marshes consisted of Histosols, intruded forests consisted of Alfisols, and all other habitats were silt loam Ultisols (Table 1-2). Complete chemical properties of these soils can be found on the Web Soil Survey website (Soil Survey Staff 2018).

Samples from ditches and tidal creeks were grab samples taken approximately 30 cm below the surface of the water. The total water depth ranged from approximately 1 to 1.5 meters in the creeks and 0.5 to 1 meter in the ditches depending on streamflow conditions at the time. Soil porewater samples from all other habitats were collected using ceramic cup lysimeters (22 mm diameter; Soil Solution Access Tubes, Irrometer, Riverside, California, USA). Lysimeters were installed in three pairs in each habitat. Each pair consisted of a lysimeter at 25 cm and 50 cm depth in the soil profile. All water samples (surface and porewater) were kept at 4°C after collection and transported within 24 hours to the University of Maryland where they were filtered (Whatman No. 42; 2.5 μm), and frozen until analysis. A subsample of each sample to be analyzed for dissolved inorganic P (DIP measured as SRP) was acidified to pH ~ < 2 with hydrochloric acid (HCl) to prevent PO_4^{3-} coprecipitation with Fe upon sample exposure to oxygen. Because we used a larger pore size filter paper, these samples may contain both soluble reactive phosphorus (SRP) and very low concentrations of acid hydrolyzable phosphorus (Chesapeake Bay Program 2019). However, we will refer to this form of DIP as SRP herein. Samples were analyzed colorimetrically on a LACHAT QuikChem (LACHAT Instruments Loveland, CO) using the molybdate-blue method for SRP (detection limit 0.01 mg PO_4-P/l), the salicylate-nitroprusside method for NH_4-N (detection limit 0.02

mg NH_4-N/l), and the sulfanilamide method for NO_3-N (detection limit 0.025 mg NO_3-N/l). Concentrations of NO_3-N were only measured in 2016 water samples. Over 90% of NO_3-N concentrations were below the minimum detection limit of the colorimeter and did not differ significantly by habitat, so we did not continue to measure NO_3-N in 2017 and 2018. We measured EC and pH on unacidified samples (Orion Versa Star Pro, Thermo Fisher Scientific, Hampton, NH USA). In 2018, lysimeters were damaged by a tractor on one of the three abandoned fields we were monitoring, so we were unable to analyze that habitat as part of our statistical model for that year.

Total dissolved P and Fe

Water samples from 2017 were digested to determine total P using potassium persulfate $K_2S_2O_8$-sulfuric acid (H_2SO_4) method, which converted all forms of DOP to measurable SRP. Digested extracts were diluted 2:5 with a 1.0 *M* sodium bicarbonate solution before colorimetric analysis using the molybdate-blue method for PO_4-P (representing TDP) on a LACHAT QuikChem (LACHAT Instruments Loveland, CO). Dissolved organic P was calculated as the difference between TDP and SRP. A subset of water samples from one sampling date (July 5) in 2017 were analyzed for total dissolved Fe (TDFe) using the modified ferrozine method to reduce all dissolved Fe(III) to Fe(II) (Viollier et al. 2000). This sampling date reflected water samples with the highest overall SRP concentrations from 2017. Therefore, we assumed that TDFe concentrations would represent each habitat's potential to form Fe-P complexes during periods of higher SRP concentrations in soil porewater and surface water based on stoichiometric calculations of the molar ratio of TDFe:SRP

present in the sample. Samples were run for Fe, which represents the total dissolved Fe(II) and Fe(III) present in the water samples, on an atomic absorption spectrometer (PinAAcle 900; Perkin Elmer; CT, USA).

Chesapeake Bay Program data processing

To estimate potential estuary-derived contributions of N and P, we analyzed data from the Chesapeake Bay Program from 2016-2018 (CBP; Chesapeake Bay Program 2019). Four monitoring stations were chosen near our study sites in the mainstem portion of the Bay, where tributaries within our study sites drained (stations EE3.1, EE3.2, EE3.3, and EE3.4). We calculated the mean and standard error of the concentrations of NH_4-N and SRP in surface water samples collected at these monitoring stations from late spring through early fall of 2016-2018 (i.e. the same time frame as the study).

Statistical approach

To examine differences in water EC, pH, NH_4-N, SRP, DOP, and TDFe by habitat, we used a linear mixed-effects (LME) model *lme4* package for R (Bates et al. 2018) with a repeated measures design. Habitat was included as a main effect and sampling date and lysimeter identification numbers nested within each agroecosystem site as random effects. We found no significant differences in soil porewater characteristics between each lysimeter pairs (25 cm vs 50 cm below ground surface. Thus, we took the average value of each pair, which were considered replicates of the habitat-level chemistry with habitat as the true replicate. We used *Tukey post-hoc* tests to examine pairwise differences in water chemistry among habitats (*multcomp*

package; Hothorn et al. 2017). We used the Box-Cox method (Box and Cox 1964) to transform the data prior to analysis to meet the assumptions of the statistical model when needed. Less than 10% of values were at or below the detection limit for each analysis. These values were assigned a value of half of the detection limit as it was the best approximation that could be tailored to the datasets based on their non-normal distributions. All statistics were computed in R Studio (R Studio Team 2019).

Results

Results from the LME models show a significant main effect of habitat on EC, pH, NH_4-N, and SRP within each year and across all years and for TDFe for the one date sampled in 2017 (Table 1-3; in all cases $P < 0.001$). Subsequent P values reported in this section are the from the results of *Tukey post-hoc* tests. Across all years we found significantly higher surface water and soil porewater EC levels in the intruded fields and marshes (15.45 and 16.59 mS/cm, respectively) than in forests (2.15 mS/cm; Table 1-4 and Figure 1-3; $P < 0.01$). These EC levels correspond to salinity values of roughly 9.00-9.73 and 1.10 ppt at 25°C. Electrical conductivity was always significantly higher in intruded forests than in forests and in intruded fields than in abandoned fields (Figure 1-3; $P < 0.01$). Across all years, the lowest pH was in the forests and intruded forests (4.95 and 4.95, respectively) and the highest pH was in the marshes and tidal creeks (7.26 and 7.66, respectively; Table 1-4 and Figure 1-4). Marsh pH ranged from 7.06 in 2016 to 8.74 in 2018. In the marshes, pH was consistently significantly higher than in the intruded forests for each year and across all years ($P < 0.01$). Marsh pH was also significantly higher than forest pH in 2017 and 2018 (Figure 1-4; $P < 0.01$).

Ammonium-N concentrations were significantly higher in the marshes than in any other habitat each year and across all years ($P < 0.01$). They ranged from 1.76 mg NH_4-N/l in 2017 to 2.65 mg NH_4-N/l in 2016. There were no other significant differences in NH_4-N concentrations among habitats across the study period. In all habitats except for marshes, NH_4-N concentrations were over three to seven times higher in 2016 as compared to 2017 or 2018. For example, in 2016 forests were 0.98 mg NH_4-N/l but in 2018 they were 0.15 mg NH_4-N/l (Figure 1-5). Because NO_3-N concentrations were very low across habitats in 2016 (in over 90% of samples lower than the method detection limit), we did not continue to measure them in 2017 and 2018. Across study years, SRP concentrations were significantly higher in the ditches (0.33 mg P/l) than on the intruded fields (0.30 mg P/l) but a significant difference was not detected between the ditches and the marshes (0.29 mg P/l; $P < 0.01$). Concentrations of SRP in the intruded fields were approximately three times lower in 2018 than in 2016 (0.12 mg P/l and 0.38 mg P/l respectively). Overall, SRP concentrations were an order of magnitude higher in marshes and ditches than in abandoned fields, forests, and intruded forests (Table 1-4 and Figure 1-6).

Dissolved organic P was measured only in 2017 and ranged from 0.46 to 0.87 mg P/l (Table 1-4). In forests, intruded forests, and abandoned fields, DOP concentrations were an order of magnitude higher than SRP concentrations, but there were no statistically significant differences in DOP concentrations across habitats (Figure 1-7A). For the one sampling date selected in 2017, TDFe concentrations were significantly higher in the intruded forests than in the other habitats ($P < 0.01$).

Overall, TDFe concentrations ranged from 0.14 to 18.08 mg Fe/l (Table 1-4, Figure 1-7B, and 1-7C).

In order to determine if the sources of NH_4-N, SRP, and DOP were estuary-derived, we examined their values at four CBP monitoring stations. These nutrients were all two orders of magnitude lower than the highest values we observed in our habitats (0.028, 0.005 0.010 and mg/l, respectively).

Discussion

This research was conducted on privately-owned land under a wide range of management practices rather than researcher-managed plots, and yet we observed very strong trends in surface water and soil porewater chemistry. Overall, we saw significant differences in EC, NH_4-N, and SRP among habitats, with relatively consistent trends across years (Figure 1-3, 1-5, and 1-6; $P < 0.01$).

The EC threshold tolerances for the survival of widely-planted corn, soy, and wheat, are 1.7 mS/cm, 5.0 mS/cm, and 6.8 mS/cm, respectively (Allison et al. 1954). We observed high EC on intruded fields across all years and sampling dates that were well above these thresholds for crop survival (Figure 1-3). Though fertilizer application can affect EC levels, our previous research on these fields has shown that EC values are low in the center of the fields, where crops are still healthy, and increase dramatically toward the field edges, which are undergoing SWI (Tully et al. 2019b). Therefore, high EC levels were a direct result of SWI. We observed patches of bare soil on the intruded fields where plants did not grow. The formation of these patches was likely due to the combination of SWI and herbicide application that farmers reported using on the edges of the fields to stave off the encroachment of

invasive and native wetland plant species. In turn, plant die-off exposed patches of bare soil, and effectively increased their evaporative surface, further increasing salt levels. In intruded fields, extensive evaporation can cause salts to move to the soil surface through capillarity (Fowler et al. 2014) and form a visible crust (Figure 1-2B). Within these crusts, we measured EC as high as 60 mS/cm and it mostly ranged within 11 to 35 mS/cm (for reference, ocean water is ~55 mS/cm).

The pH of soil porewater on abandoned and intruded fields, and surface water in ditches and tidal creeks ranged from slightly acidic to slightly basic (pH of 5.18-7.66; Figure 1-4). The soils across the intruded field habitats are Ultisols, which typically have a pH of less than 5 (Brady and Weil 2016). A common agricultural practice in this region is the addition of lime ($CaCO_3$ or $CaMg(CO_3)_2$) at 2.1-8.4 Mg/ha, to increase the pH of acidic topsoil (Gascho and Parker 2001). Alkaline saltwater inputs also increase porewater pH. From year to year, pH values may have differed within habitats due partly to varying freshwater and saltwater inputs.

Nitrogen

Nitrogen cycling in soils is complex; therefore, there are several pathways through which N could have been transformed across the study habitats leading to the build-up of NH_4^+ in marshes. Though we did not measure NH_4-N in reference salt marshes, other studies report concentrations in these habitats that range from 0.1-0.5 mg NH_4-N/l (Harvey and Hall 1992; Weston et al. 2011; Wilson and Morris 2012), an order of magnitude lower that the NH_4-N concentrations we observed in marshes receiving drainage from farm fields. We propose that this is due to a combination of effects including: leaching losses of NO_3^-; denitrification; mineralization of organic

marsh soils; dissimilatory NO_3^- reduction to NH_4^+ (DNRA); and inputs of fertilizer N from agricultural fields upstream.

First, NO_3-N concentrations measured in our samples were mostly at or near the method detection limit (< 0.025 mg NO_3-N/l). Since NO_3^- is prone to leaching, particularly in sandy soils (Clarke et al. 2002) like those of our study habitats (Table 1-2), some NO_3^- may have leached into deeper soil layers or groundwater below the depth of our porewater samplers (Clarke et al. 2002; Tanner and Sukias 2011; Jessen et al. 2017). Second, as these systems are frequently inundated, NO_3^- may also be converted to gaseous forms during denitrification (Burgin and Hamilton 2007; Helton et al. 2015). Third, in inundated marsh soils, mineralization of organic soils can lead to NH_4^+ release (Helton et al. 2015; Jia et al. 2017) as the reducing conditions prevent it from being oxidized to NO_3^- (Jia et al. 2017). However, since we did not observe high DIN in the forests and intruded forests, which also contain soil high in organic matter, it is likely that this process does not account for all of the NH_4-N measured in these habitats and in the marshes. Fourth, many studies have shown that while DNRA rates are low in freshwater wetlands, they can be much higher and comparable to rates of denitrification in salt marshes and anoxic marine sediments (Koop-jakobsen and Giblin 2010; Rütting et al. 2011; Giblin et al. 2013). For example, one N tracer study in a salt marsh showed that DNRA converted 30% of the NO_3^- to NH_4^+ while 70% of the NO_3^- was denitrified (Tobias et al. 2001). Finally, as farm fields receive influxes of saltwater, NH_4^+ ions can be released into soil porewater as they are replaced on negatively charged soil surfaces by base cations found in saltwater (Ardón et al. 2013). High NH_4^+ water may then be flushed downstream via tides or

storm events through highly connected ditch networks. This mechanism may partially explain why we measured much higher NH_4-N concentrations in the marshes than in any other habitat (Figure 1-5). Previous studies also report high soil porewater concentrations of NH_4-N (1-10 mg/l) in wetlands bordering agricultural areas (Koretsky et al. 2005; Ardón et al. 2013, 2017), which suggests that agricultural N inputs may increase NH_4-N concentrations in wetlands downstream of SWI-affected farmland.

Phosphorus

The most striking observation during the study period was the magnitude of SRP concentrations in ditches, tidal creeks, and marshes, which suggests that dissolved P may be transported from the intruded fields into agricultural ditches and eventually downstream into tidal creeks and marshes (Figure 1-6 and 1-7A). Even though the intruded fields were not significantly higher in SRP than the intruded forests and abandoned fields in 2016, their mean concentration was much higher (0.29 mg P/l across all years versus 0.03 and 0.05 mg P/l in the intruded forests and abandoned fields; Figure 1-6). The large variability in SRP concentrations in the intruded fields was due to differences in farmer management practices over the course of the study. Based on data from our previous study, intruded fields on Site 2 and Site 3 received less P than on Site 1 in 2017 (Tully et al. 2019b). In 2018, two of the farmers (Site 2 and Site 3) stopped fertilizing their intruded fields as a response to worsening SWI. However, the fact that we still observed high SRP concentrations in the ditches and marshes through all three years of this study (and tidal creeks in 2017 and 2018), indicates that legacy P may still be moving off these fields and serving as

a persistent source of nutrient pollution downstream. For comparison, abandoned fields had low SRP concentrations despite a legacy of agriculture and fertilizer application (Figure 1-6) due to a combination of a lack of new fertilizer inputs to these fields, consistent runoff of SRP downstream, and high biomass agricultural weeds and woody upland wetland plants (Gedan and Fernández-Pascual 2019) that may have assimilated some P into their tissues. In abandoned fields, soil porewater DOP concentrations were 17 times higher than SRP concentrations (Figure 1-7A and Table 1-4), which is another indicator of legacy P. High DOP concentrations in the abandoned fields could be the result of plant residue decomposition and the formation of soil organic matter (Condron et al. 2005).

Dissolved organic P concentrations were not similar to SRP concentrations in water samples of each habitat. Instead, we observed very high DOP concentrations as compared to SRP concentrations across all habitats (Figure 1-7A), which may be partially explained by a legacy of intensive agriculture in these areas. Most of the forested land cover on Maryland's Lower Eastern Shore is secondary growth, and at one time, was under intensive agricultural use before it was converted back to forest (Lister et al. 2011). For comparison, DOP backgrounds concentrations in soil porewater of forests without a legacy of fertilizer inputs are often an order of magnitude lower than those measured in this study (0.02 mg P/l; Qualls and Haines 1991, Qualls et al. 2000, Lilienfein et al. 2004). High DOP concentrations in habitats not actively farmed may also be partially due to lateral movement of DOP through the soil or through surface water flow (Gburek et al. 2005). The high degree of hydrologic connectivity among habitats in this region raises the possibility that some

of the N and P could be contributed by the saltwater itself. However, concentrations of N and P in the Chesapeake Bay mainstem were at least two orders of magnitude lower than concentrations measured in this study. This suggests that the high nutrient concentrations in water are the result of agricultural practices and can cause localized water quality problems.

Iron

Overall, the soil porewater and surface water of the habitats was high in TDFe, which has major implications for how P cycles through the system. We have previously shown that Fe changes from crystalline to poorly-crystalline forms in the soil profile from the center of the SWI intruded fields to their border with tidal salt marshes (Tully et al. 2019b). Poorly-crystalline Fe (Fe(III)) undergoes dissolution and is released as Fe(II) in soil porewater and surface water when the soils are inundated (Kemp et al. 2005; Musolff et al. 2017a). Because wetting and drying cycles occur in the top soil layers (< 50 cm) on the intruded fields, Fe(II) in soil porewater can re-oxidize to Fe(III) when the soils dry and sorb to organic complexes, returning Fe to an oxidized, poorly-crystalline form. Soil organic matter has been shown to have a high affinity for Fe and a tendency to sorb DIP to form Fe-P complexes (Giesler et al. 2005). Though we did not measure Fe(II) and Fe(III) speciation directly, the TDFe concentrations in soil porewater and surface water reflect the ability of TDFe to bind SRP under oxidizing conditions and release it under reducing conditions such as those in soils inundated with saltwater.

High TDFe concentrations in the forests and intruded forests reflect the effects of low soil porewater pH in these habitats (Figure 1-4 and 1-7C; $P < 0.01$). Iron

solubility has been shown to increase as pH decreases (Islam et al. 1980; Johnson and Loeppert 2006). Further, other studies have shown the stoichiometric relationship between dissolved Fe and SRP to be an important control on SRP bioavailability (Chambers and Odum 1990; Hartzell and Jordan 2012). At 0.19 mg Fe/l (Figure 1-7C), the concentration of TDFe measured in the ditch surface water was present at approximately a 1:1 (TDFe:SRP) molar ratio in 2017 (0.23 mg P/l; Figure 1-6). This TDFe concentration is not high enough to bind all of the bioavailable SRP before it moves out to the tidal creeks, marshes, and larger tributaries, even if all of the TDFe were in oxidized form as Fe(III) compounds. Studies show that the molar ratio of TDFe:SRP in a water sample must be greater than 2:1 to allow to all of the Fe to bind all of the SRP under completely oxidized conditions (Gächter and Müller 2003; Jordan et al. 2008). It is well documented that oxygen depleted (reducing) conditions tend to form in the surface water and soil porewater in slow-moving water of agricultural ditches and connected creeks (King et al. 2015) and in marshes (Reddy and DeLaune 2008). Furthermore, in marshes, some of the Fe(II) may have been converted to insoluble iron sulfide (FeS) minerals under reducing conditions, reducing the ability of Fe to bind SRP, as has been documented in many other studies (Dierberg et al. 2011; Kraal et al. 2013; Hartzell et al. 2017). Therefore, TDFe is not present in high enough concentrations in the ditches, tidal creeks, and marshes to adequately buffer against SRP loss to downstream areas.

Each site is located along a minor tributary that drains into a major tributary, or a major tributary that drains into the Chesapeake Bay (Table 1-5). The distances between sites and their major tributaries ranges from just 0.15 to 4.4 km, and the

route is hydrologically linked by ditch networks (Table 1-5). Instead of traveling through forested areas, agricultural fields on the sites drain into ditches that connect directly to tidal creeks. Therefore, forest habitats may not buffer against SWI-related nutrient losses from farm fields. Even though SRP concentrations were low in forest soil porewater, forest soils were high in DOP likely as a result of the legacy of agricultural land use. As saltwater encroaches on forests, DOP can enter waterways, where it may be transformed to inorganic P. Current best management practices to curb P and N pollution in the Bay include creating vegetated buffers of grass, wetland plants, or trees (Sharpley et al. 2006). However, the fact that we found highest inorganic N and P concentrations in marsh soil porewater suggest that tidal salt marshes may be less effective at reducing nutrient pollution downstream if nutrient fertilizer applications on upstream farm fields are not also reduced. This is due to the marshes' ability to convert N and P to bioavailable forms (i.e. NH_4-N and SRP) that tend to remain solubilized in water bodies such as ditches, tidal creeks, and tidal salt marshes.

The excessively high concentrations of P in the focal habitats of this research suggest that coastal agroecosystems should be targeted for nutrient reduction initiatives to prevent nutrient release into waterways and consequent eutrophication (Paerl et al. 2014). Current models of nutrient loading in the Chesapeake Bay do not include potential contributions from legacy and SWI-derived nutrients. As we adapt to sea level rise and SWI, management approaches must take into consideration the potential release of nutrients from inundated soils to prevent problems associated with downstream pollution. Studies that measure legacy nutrient movement through

ecosystems with SWI may help to explain why localized water quality issues persist. These findings can lead to the development of conservation practices adapted to meet water quality improvement goals in watersheds worldwide.

Conclusion

As sea levels rise, SWI will continue to affect coastal agroecosystems. Biogeochemical changes in soil and water due to this process may lead to nutrient export from these areas. Here, we observed this effect on land with a legacy of heavy fertilizer applications. Remarkably, we found consistent patterns in soil porewater and surface water chemistry across study years. Both NH_4-N and SRP concentrations were very high in the marshes as compared to reference conditions. This suggests that these nutrients are moving off farm fields and downstream through connected agricultural ditches and tidal creeks. Concentrations of TDFe support the idea that the habitats have a large capacity to release sorbed P from Fe-P complexes as dissolved oxygen levels decrease in soil porewater and surface water. However, TDFe concentrations are not high enough to rebind released P once it enters waterways with higher levels of dissolved oxygen. Therefore, we show N and P from coastal farmland may end up in high concentrations in nearby marshes and poised for export downstream where it may pose nutrient pollution issues in watersheds.

Tables and figures

Table 1-1

Description and number of habitats (n) measured for each year of study

Habitat	Description	Water sample type	n_{Year}		
			n_{2016}	n_{2017}	n_{2018}
Forest	Forested areas that do not show evidence of saltwater intrusion. (i.e. no tree mortality or encroachment of marsh plant species)	Soil porewater	4	4	4
Intruded forest	Forested areas that show evidence of saltwater intrusion (i.e. displaying tree mortality and encroachment of marsh plant species)	Soil porewater	3	3	3
Abandoned Field	Former agricultural fields in their second year of abandonment as of summer 2016 and not affected by saltwater intrusion. They were left fallow due to being formerly leased to solar companies	Soil porewater	3	3	2
Intruded field	Actively farmed agricultural fields undergoing saltwater intrusion (i.e. displaying crop death and encroachment of native marsh plant species such as *Spartina patens* and *Distichlis spicata*)	Soil porewater	3	3	3
Ditch	Agricultural ditches directly surrounding and draining actively farmed fields	Surface water	5	5	5
Tidal creek	Creeks hydrologically connected to agricultural ditches and larger tributaries	Surface water	0	3	3
Marsh	Tidal *Spartina patens* salt marshes	Soil porewater	5	5	5

Table 1-2

Soil types of each habitat within each agroecosystem site with soil classification in parentheses.

Habitat	Agroecosystem site				
	1	2	3	4	5
Intruded forest	Sunken silt loam (Typic Endoaqualfs)	NA	Sunken silt loam (Typic Endoaqualfs)	NA	Sunken silt loam (Typic Endoaqualfs)
Forest	Quindocqua silt loam (Typic Endoaquults)	Othello silt loam (Typic Endoaquults)	Othello silt loam (Typic Endoaquults)	Quindocqua silt loam (Typic Endoaquults)	Quindocqua silt loam (Typic Endoaquults)
Abandoned field	Quindocqua silt loam (Typic Endoaquults)	NA	NA	Woodstown silt loam (Aquic Hapludults)	NA
Intruded field/Ditch	Manokin/Queponco silt loam (Aquic Hapludults, Typic Hapludults)	Queponco silt loam (Typic Hapludults)	Othello, Fallsington silt loam (Typic Endoaquults, Typic Endoaquults)	Manokin/Queponco silt loam (Aquic Hapludults, Typic Hapludults)	Manokin/Queponco silt loam (Aquic Hapludults, Typic Hapludults)
Tidal creek/Marsh	Transquaking/ Mispillion organic deposits underlain by loamy mineral sediments (Typic Sulfihemists, Terric Sulfihemists)	Transquaking/ Mispillion organic deposits underlain by loamy mineral sediments (Typic Sulfihemists, Terric Sulfihemists)	Honga peat (Terric Sulfihemists)	Transquaking/ Mispillion organic deposits underlain by loamy mineral sediments (Typic Sulfihemists, Terric Sulfihemists)	Transquaking/ Mispillion organic deposits underlain by loamy mineral sediments (Typic Sulfihemists, Terric Sulfihemists)

Note: Table information compiled from the Web Soil Survey (Soil Survey Staff 2018).

Table 1-3

Results of Type III one-way ANOVA with Satterthwaite's method for unbalanced designs for the effect of habitat on each variable. Variables are electrical conductivity (EC), pH, ammonium nitrogen (NH_4-N), and soluble reactive phosphorus (SRP) across all years of the study, dissolved organic phosphorus (DOP) in 2017, and total dissolved iron (TDFe) from the July 5, 2017 sampling date.

Year	Variable	numerator df	denominator df	Sum of squares	*F*-value	*P*
2016	EC	5	80	96.14	18.79	< 0.0001
2017	EC	6	72	104.49	24.18	< 0.0001
2018	EC	5	80	135.00	31.40	< 0.0001
all	EC	5	416	126.22	25.72	< 0.0001
2016	pH	5	80	1411.20	6.33	< 0.0001
2017	pH	6	72	600000	7.62	< 0.0001
2018	pH	5	80	1275.00	10.175	< 0.0001
all	pH	5	416	2665.20	8.04	0.00001
2016	SRP	5	80	125.73	32.85	< 0.0001
2017	SRP	6	72	133.38	20.10	< 0.0001
2018	SRP	5	80	63.75	15.44	< 0.0001
all	SRP	5	416	186.18	42.40	< 0.0001
2016	NH_4-N	5	80	24.75	21.91	< 0.0001
2017	NH_4-N	6	72	76.26	15.18	< 0.0001
2018	NH_4-N	5	80	77.16	22.30	< 0.0001
all	NH_4-N	5	416	91.54	33.19	< 0.0001
2017	DOP	6	72	8.65	3.469	0.03152
2017	TDFe	6	72	154.31	8.921	< 0.0001

Table 1-4

Porewater and surface water concentrations of electrical conductivity (EC), pH, ammonium nitrogen (NH_4-N), and soluble reactive phosphorus (SRP) across all years of the study, dissolved organic phosphorus (DOP) in 2017, and total dissolved iron (TDFe) from the July 5, 2017 sampling date with ± standard error in parentheses for each habitat. Statistically significant differences in means within each variable are indicated by different letters at $P < 0.01$.

Habitat	EC (mS/cm)	pH	NH_4-N (mg N/l)	SRP (mg P/l)	DOP (mg P/l)	TDFe (mg Fe/l)
Abandoned field	2.59 (NA)	7.03 (NA)	0.31 (NA)	0.05 (NA)	0.87 (0.22)	0.29^{a} (0.13)
Ditch	9.71^{b} (0.98)	5.79^{ab} (0.17)	0.38^{a} (0.04)	0.33^{c} (0.04)	0.81 (0.09)	0.19^{a} (0.05)
Forest	2.15^{a} (0.36)	4.95^{b} (0.21)	0.40^{a} (0.12)	0.05^{a} (0.01)	0.49 (0.11)	5.61^{a} (2.74)
Intruded field	15.71^{b} (1.09)	5.18^{ab} (0.23)	0.39^{a} (0.05)	0.30^{b} (0.01)	0.81 (0.27)	1.56^{a} (0.89)
Intruded forest	9.84^{b} (0.36)	4.95^{b} (0.25)	0.37^{a} (0.04)	0.03^{a} (0.01)	0.66 (0.11)	18.08^{b} (5.23)
Tidal creek	9.62 (NA)	7.66 (NA)	0.11 (NA)	0.18 (NA)	0.46 (0.21)	0.14^{a} (0.02)
Marsh	16.58^{c} (0.84)	7.26^{a} (0.04)	2.29^{b} (0.2)	0.29^{c} (0.02)	0.81 (0.10)	0.74^{a} (0.27)

Table 1-5

Distance from center of study site to closest major tributary in kilometers. Sites drain directly into minor tributary listed in this table. If no minor tributary is listed, the site drains directly into the major tributary. Site 5 had one “ditch” habitat that drained to separate major and minor tributaries from the rest of the site.

Agroecosystem site	Minor tributary	Major tributary	Site distance to major tributary (km)
1	---	Manokin River	0.2
2	Monie Creek	Monie Bay	4.4
3	Johnson Creek	Pocomoke Sound	2.7
4	Little Creek	Monie Bay	2.8
5	Back creek	Manokin River	1.4
5 (Ditch)	Coulburn Creek	Big Annemessex	0.7

Figures

Figure 1-1

A: Map of the Chesapeake Bay region, United States. Study area is outlined by the dotted rectangle; B: Map of the study area and agroecosystem site locations, Somerset County, located within Maryland in the Chesapeake Bay.

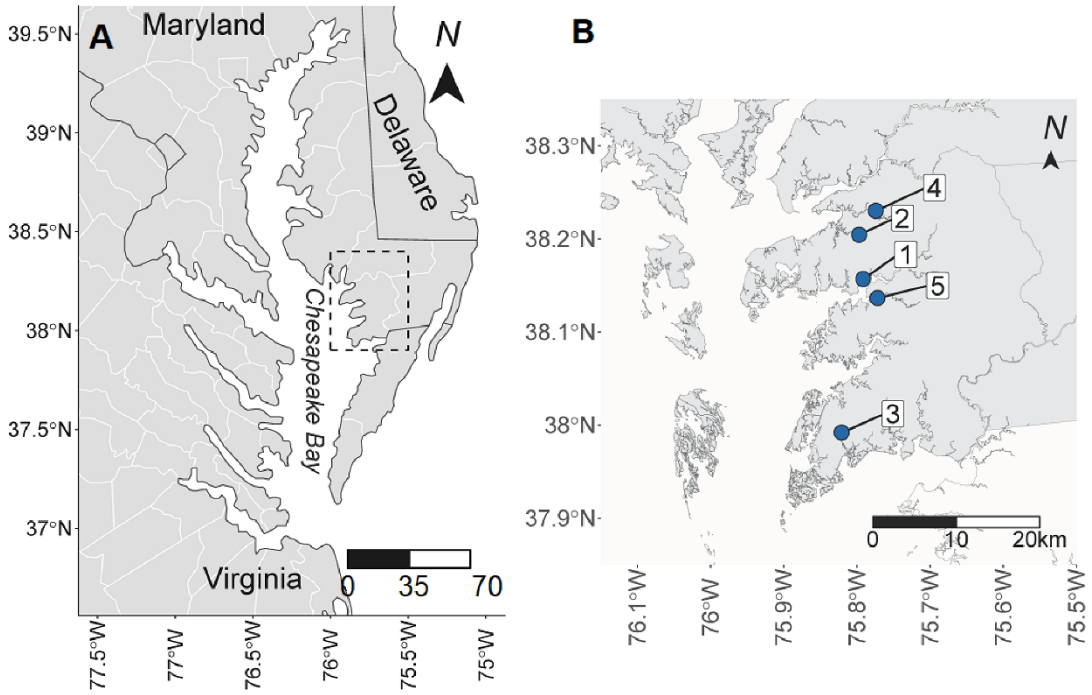

Figure 1-2

A: Satellite imagery of one of the study sites with labeled habitats. B: Salt crust on an intruded farm field at one of the study sites. Note: Figure 1-2A imagery taken from Google Earth (Google Earth 2019)

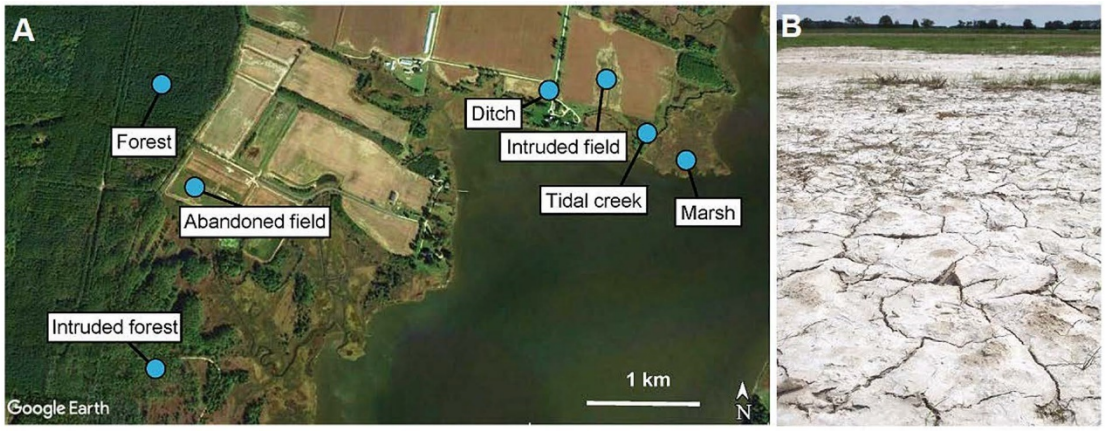

Figure 1-3

Soil porewater and surface water conductivity (EC) by habitat for each year of the study. “All years” indicates average values taken across all three years. Statistically significant differences in means are indicated by different letters at $P < 0.01$. Error bars represent standard error of the mean. Tidal creeks were not monitored in 2016 but were added as a habitat in 2017 and 2018.

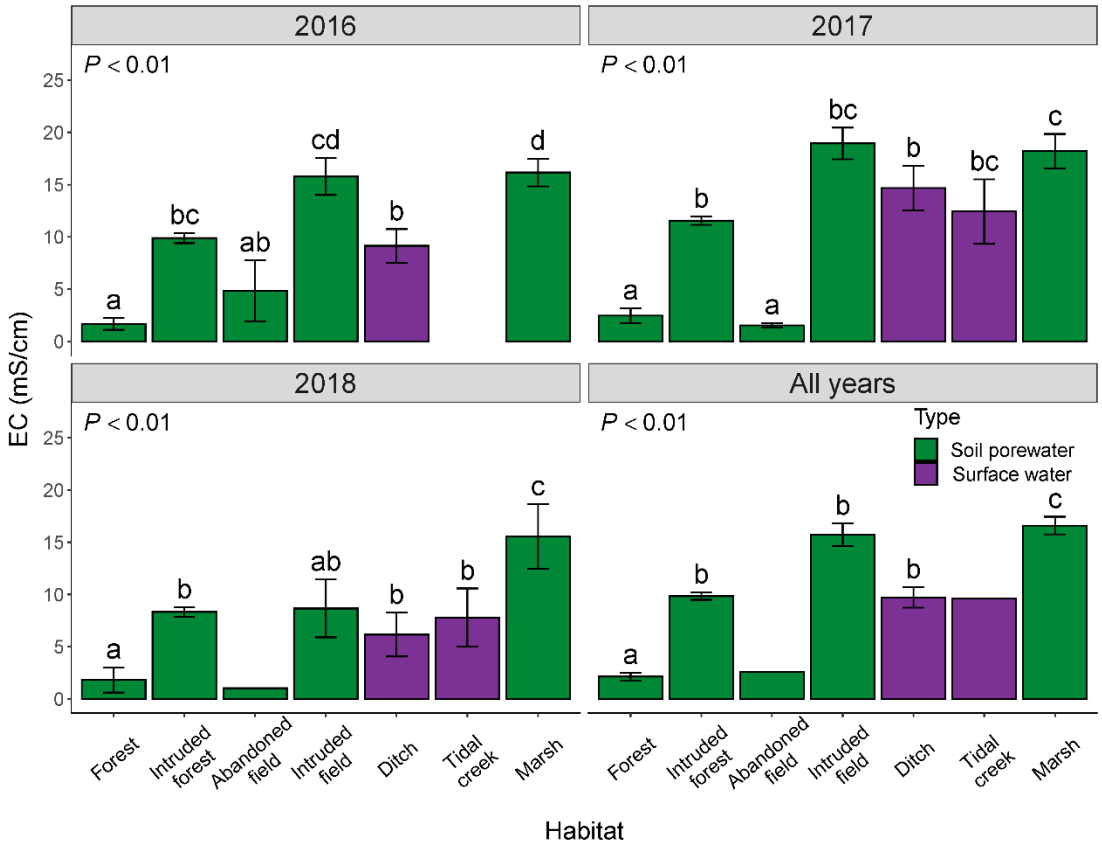

Figure 1-4

Soil porewater and surface water pH by habitat for each year of the study. "All years" indicates average values taken across all three years. Statistically significant differences in means are indicated by different letters at $P < 0.01$. Error bars represent standard error of the mean. Tidal creeks were not monitored in 2016 but were added as a habitat in 2017 and 2018.

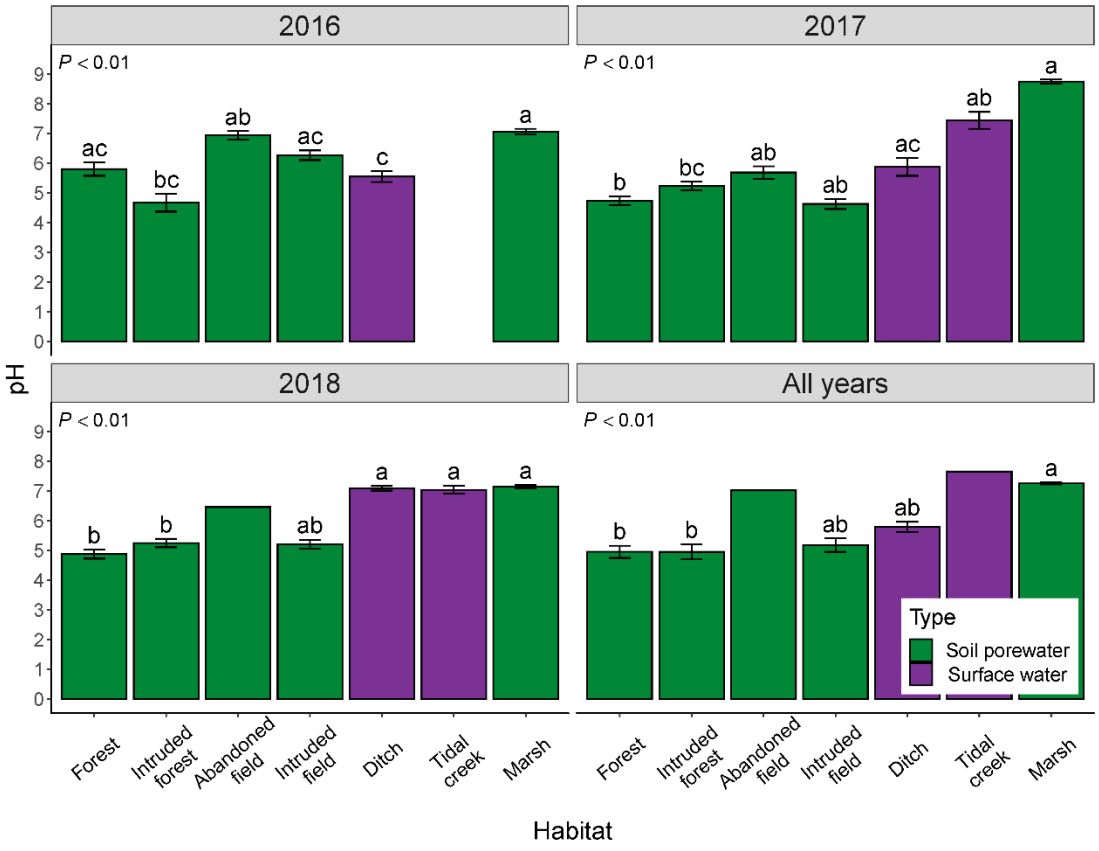

Figure 1-5

Soil porewater and surface water ammonium-nitrogen (NH_4-N) concentrations by habitat for each year of the study. "All years" indicates average values taken across all three years. Statistically significant differences in means are indicated by different letters at $P < 0.01$. Error bars represent standard error of the mean. Tidal creeks were not monitored in 2016 but were added as a habitat in 2017 and 2018.

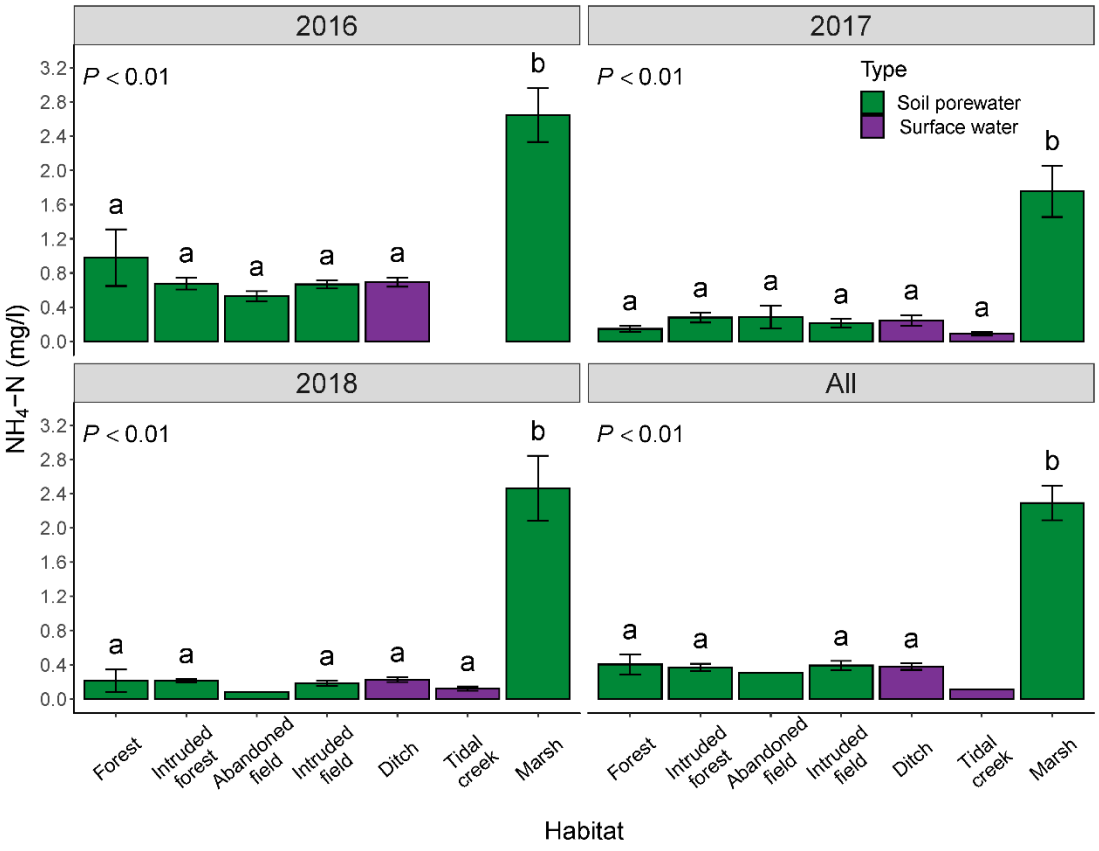

Figure 1-6

Soil porewater and surface water soluble reactive phosphorus (SRP) concentrations by habitat for each year of the study. “All years” indicates average values taken across all three years. Error bars represent standard error of the mean. Statistically significant differences in means are indicated by different letters at $P < 0.01$. Dashed line shows EPA designated total phosphorus concentration threshold of 0.03 mg P/l for eutrophication of rivers, streams, and creeks of the Atlantic Coastal Plain (USEPA 2000). Tidal creeks were not monitored in 2016 but were added as a habitat in 2017 and 2018.

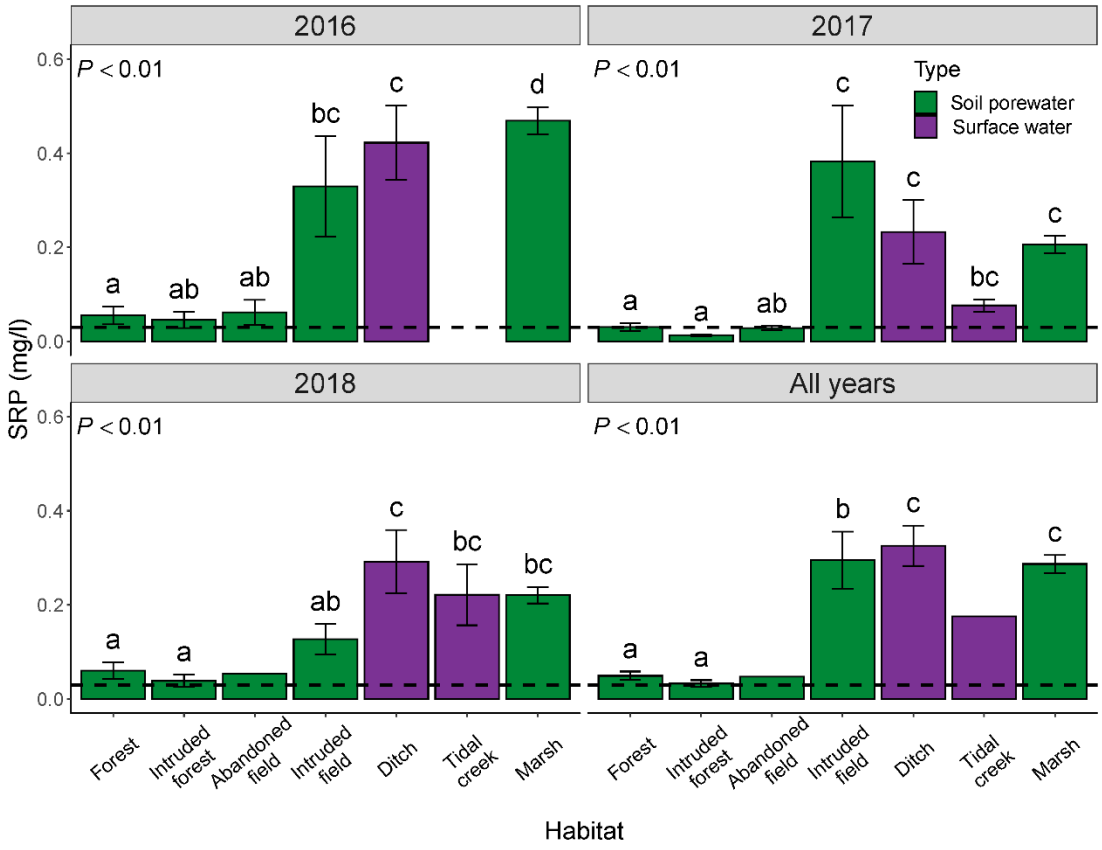

Figure 1-7

A: Soil porewater and surface water dissolved organic phosphorus (DOP) and soluble reactive phosphorus (SRP) concentrations in mg P/l by habitat in 2017. The sum of the means of the stacked bars equals the mean total dissolved phosphorus (TDP) for each habitat type. Error bars represent standard error of the mean. B: Soil porewater total dissolved iron (TDFe) concentrations across habitats for the July 5, 2017 sampling date. Statistically significant differences in TDFe means are indicated by different letters at $P < 0.01$. Error bars represent standard error of the mean. C: Surface water total dissolved iron (TDFe) concentrations across habitats for the July 5, 2017 sampling date. Statistically significant differences in TDFe means are indicated by different letters at $P < 0.01$ and are comparable across Figure 1-7B and 1-7C. Error bars represent standard error of the mean.

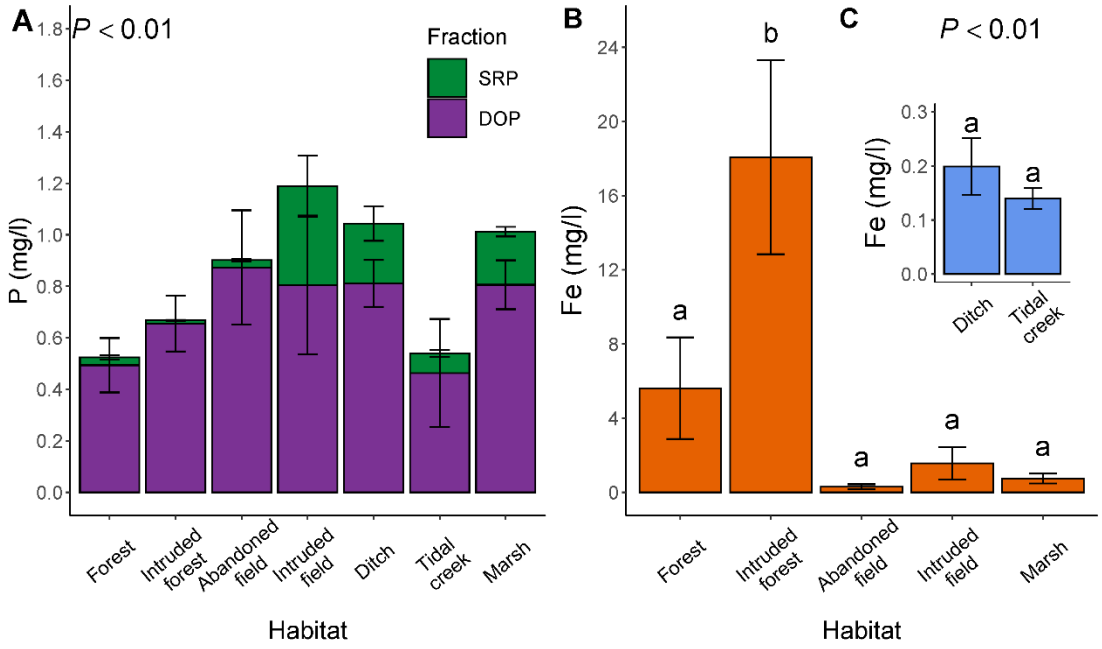

Works cited

Allison, L. E., L. Bernstein, J. W. Brown, M. Fireman, L. A. Richards, H. E. Hayward, G. A. Pearson, L. v Wilcox, R. C. Reeve, C. A. Bower, and J. T. Hatcher. 1954. Diagnosis and Improvement of Saline and Alkaline Soils. Washington D.C.

Ardón, M., A. M. Helton, M. D. Scheuerell, and E. S. Bernhardt. 2017. Fertilizer legacies meet saltwater incursion : challenges and constraints for coastal plain wetland restoration. Elementa: Science of the Anthropocene 5:41.

Ardón, M., J. L. Morse, B. P. Colman, and E. S. Bernhardt. 2013. Drought-induced saltwater incursion leads to increased wetland nitrogen export. Global Change Biology 19:2976–2985.

Bates, D., M. Maechler, B. Bolker, S. Walker, R. Haubo, B. Christensen, H. Singmann, B. Dai, F. Scheipl, and G. Grothendieck. 2018. lme4 Linear Mixed-Effects Models using "Eigen" and S4. https://cran.r-project.org/web/packages/lme4/lme4.pdf.

Bhattachan, A., R. E. Emanuel, M. Ardon, E. S. Bernhardt, S. M. Anderson, M. G. Stillwagon, E. A. Ury, T. K. Bendor, and J. P. Wright. 2018. Evaluating the effects of land-use change and future climate change on vulnerability of coastal landscapes to saltwater intrusion. Elem Sci Anth 6:62.

Boesch, D. F. 2006. Scientific requirements for ecosystem-based management in the restoration of Chesapeake Bay and Coastal Louisiana. Ecological Engineering 26:6–26.

Boesch, D. F., R. B. Brinsfield, and R. E. Magnien. 2001. Chesapeake Bay

Eutrophication. Journal of Environmental Quality 30:303–320.

Box, G. E. P., and D. R. Cox. 1964. An analysis of transformations. Journal of the Royal Statistical Society. Series B (Methodological) 26:190–197.

Brady, N. C., and R. R. Weil. 2016. The Nature and Properties of Soils. 15th edition. Pearson, Columbus.

Brand-Klibanski, S., M. I. Litaor, and M. Shenker. 2007. Overestimation of Phosphorus Adsorption Capacity in Reduced Soils: An Artifact of Typical Batch Adsorption Experiments. Soil Science Society of America Journal 71:1128.

Burgin, A. J., and S. K. Hamilton. 2007. Have we overemphasized the role of denitrification in aquatic ecosystems? A review of nitrate removal pathways. Frontiers in Ecology and the Environment 5:89–96.

Chambers, R. M., and W. E. Odum. 1990. Porewater oxidation, dissolved phosphate and the iron curtain - Iron-phosphorus relations in tidal freshwater marshes. Biogeochemistry 10:37–52.

Chesapeake Bay Program. 2018. 2017 and 2025 Watershed Implementation Plans (WIPs). https://www.chesapeakeprogress.com/clean-water/watershed-implementation-plans.

Chesapeake Bay Program. 2019. Chesapeake Bay Program: Water Quality Database. https://www.chesapeakebay.net/what/downloads/cbp_water_quality_database_1984_present.

Clarke, R. A., C. D. Stanley, B. L. McNeal, and B. W. MacLeod. 2002. Impact of agricultural land use on nitrate levels in Lake Manatee, Florida. Journal of Soil and Water Conservation 57:106–111.

Condron, L. M., B. L. Turner, and B. J. Cade-Menun. 2005. 04 Chemistry and dynamics of soil organic phosphorus. Agronomy Monographs: Phosphorus: Agriculture and the Environment 46:87–120.

Dierberg, F. E., T. A. DeBusk, N. R. Larson, M. D. Kharbanda, N. Chan, and M. C. Gabriel. 2011. Effects of sulfate amendments on mineralization and phosphorus release from South Florida (USA) wetland soils under anaerobic conditions. Soil Biology and Biochemistry 43:31–45.

Ezer, T., and W. B. Corlett. 2012. Is sea level rise accelerating in the Chesapeake Bay? A demonstration of a novel new approach for analyzing sea level data. Geophysical Research Letters 39:1–6.

Fowler, D. N., S. L. King, and D. C. Weindorf. 2014. Evaluating Abiotic Influences on Soil Salinity of Inland Managed Wetlands and Agricultural Croplands in a Semi-Arid Environment. Wetlands 34:1229–1239.

Gächter, R., and B. Müller. 2003. Why the phosphorus retention of lakes does not necessarily depend on the oxygen supply to their sediment surface. Limnology and Oceanography 48:929–933.

Gascho, G. J., and M. B. Parker. 2001. Long-term liming effects on Coastal Plain soils and crops. Agronomy Journal 93:1305–1315.

Gburek, W. J., E. Barberis, P. M. Haygarth, B. Kronvang, and C. Stamm. 2005. Phosphorus Mobility in the Landscape. Phosphorus: Agriculture and the Environment:941–979.

Gedan, K. B., and E. Fernández-Pascual. 2019. Salt marsh migration into salinized agricultural fields: A novel assembly of plant communities. Journal of

Vegetation Science 30:1007–1016.

Giblin, A. E., C. R. Tobias, B. Song, N. Weston, G. T. Banta, and V. H. Rivera-Monroy. 2013. The importance of dissimilatory nitrate reduction to ammonium (DNRA) in the nitrogen cycle of coastal ecosystems. Oceanography 26:124–131.

Giesler, R., T. Andersson, L. Lövgren, and P. Persson. 2005. Phosphate Sorption in Aluminum-and Iron-Rich Humus Soils. Soil Science Society of America Journal 69:77–86.

Glick, P., J. Clough, and B. Nunley. 2008. Sea-Level Rise and Coastal Habitats in the Chesapeake Bay Region Technical Report:1–121.

Google Earth. 2019. Google Earth imagery. Google. http://www.earth.google.com.

Hanin, M., C. Ebel, M. Ngom, L. Laplaze, and K. Masmoudi. 2016. New Insights on Plant Salt Tolerance Mechanisms and Their Potential Use for Breeding. Frontiers in Plant Science 7:1–17.

Hartzell, J. L., and T. E. Jordan. 2012. Shifts in the relative availability of phosphorus and nitrogen along estuarine salinity gradients. Biogeochemistry 107:489–500.

Hartzell, J. L., T. E. Jordan, and J. C. Cornwell. 2017. Phosphorus Sequestration in Sediments Along the Salinity Gradients of Chesapeake Bay Subestuaries. Estuaries and Coasts 40:1607–1625.

Harvey, J. W., and C. Hall. 1992. Ammonium and Phosphate Dynamics in a Virginia Salt Marsh. Estuaries 15:349–359.

Helton, A. M., M. Ardón, and E. S. Bernhardt. 2015. Thermodynamic constraints on the utility of ecological stoichiometry for explaining global biogeochemical patterns. Ecology Letters 18:1049–1056.

Helton, A. M., E. S. Bernhardt, and A. Fedders. 2014. Biogeochemical regime shifts in coastal landscapes: The contrasting effects of saltwater incursion and agricultural pollution on greenhouse gas emissions from a freshwater wetland. Biogeochemistry 120:133–147.

Hothorn, T., F. Bretz, P. Westfall, R. M. Heiberger, A. Schuetzenmeister, and S. Scheibe. 2017. Simultaneous Inference in General Parametric Models. https://cran.r-project.org/web/packages/multcomp/.

Hussein, A. H., and M. C. Rabenhorst. 2010. Tidal Inundation of Transgressive Coastal Areas. Soil Science Society of America Journal 65:536.

Islam, A. K. M. S., D. G. Edwards, and C. J. Asher. 1980. pH optima for crop growth. Plant and Soil 54:339–357.

Jessen, S., D. Postma, L. Thorling, S. Müller, J. Leskelä, and P. Engesgaard. 2017. Decadal variations in groundwater quality: A legacy from nitrate leaching and denitrification by pyrite in a sandy aquifer. Water Resources Research 53:184–198.

Jia, J., J. Bai, H. Gao, X. Wen, G. Zhang, B. Cui, and X. Liu. 2017. In situ soil net nitrogen mineralization in coastal salt marshes (Suaeda salsa) with different flooding periods in a Chinese estuary. Ecological Indicators 73:559–565.

Johnson, S. E., and R. H. Loeppert. 2006. Role of Organic Acids in Phosphate Mobilization from Iron Oxide. Soil Science Society of America Journal 70:222.

Jordan, T. E., J. C. Cornwell, W. R. Boynton, J. T. Anderson, and C. Cornwell. 2008. Changes in phosphorus biogeochemistry along an estuarine salinity gradient: The iron conveyer belt. Limnology and Oceanography 53:172–184.

Kemp, W. M., W. R. Boynton, J. E. Adolf, D. F. Boesch, W. C. Boicourt, G. Brush, J. C. Cornwell, T. R. Fisher, P. M. Glibert, J. D. Hagy, L. W. Harding, E. D. Houde, D. G. Kimmel, W. D. Miller, R. I. E. Newell, M. R. Roman, E. M. Smith, and J. C. Stevenson. 2005. Eutrophication of Chesapeake Bay: historical trends and ecological interactions. Marine Ecology Progress Series 303:1–29.

King, K. W., M. R. Williams, M. L. Macrae, N. R. Fausey, J. Frankenberger, D. R. Smith, P. J. A. Kleinman, and L. C. Brown. 2015. Phosphorus Transport in Agricultural Subsurface Drainage: A Review. Journal of Environmental Quality 44:467–485.

Kirwan, M. L., and K. B. Gedan. 2019. Sea-level driven land conversion and the formation of ghost forests. Nature Climate Change 9:450–457.

Kirwan, M. L., J. L. Kirwan, and C. A. Copenheaver. 2007. Dynamics of an Estuarine Forest and its Response to Rising Sea Level. Journal of Coastal Research 232:457–463.

Kleinman, P. J. A., A. N. Sharpley, A. R. Buda, R. W. McDowell, and A. L. Allen. 2011. Soil controls of phosphorus in runoff: Management barriers and opportunities. Canadian Journal of Soil Science 91:329–338.

Koop-jakobsen, K., and A. E. Giblin. 2010. The effect of increased nitrate loading on nitrate reduction via denitrification and DNRA in salt marsh sediments. Limnology and Oceanography 55:789–802.

Koretsky, C. M., P. Van Cappellen, T. J. Dichristina, J. E. Kostka, K. L. Lowe, C. M. Moore, A. N. Roychoudhury, and E. Viollier. 2005. Salt marsh pore water geochemistry does not correlate with microbial community structure. Estuarine,

Coastal and Shelf Science 62:233–251.

Kraal, P., E. D. Burton, and R. T. Bush. 2013. Iron monosulfide accumulation and pyrite formation in eutrophic estuarine sediments. Geochimica et Cosmochimica Acta 122:75–88.

Lilienfein, J., R. G. Qualls, S. M. Uselman, and S. D. Bridgham. 2004. Adsorption of Dissolved Organic and Inorganic Phosphorus in Soils of a Weathering Chronosequence. Soil Science Society of America Journal 68:620–628.

Lister, T. W., J. L. Perdue, C. J. Barnett, B. J. Butler, S. J. Crocker, G. M. Domke, D. Griffith, M. A. Hatfield, C. M. Kurtz, A. J. Lister, R. S. Morin, W. K. Moser, M. D. Nelson, C. H. Perry, R. J. Piva, R. Riemann, R. Widmann, and C. W. Woodall. 2011. Maryland's forests 2008. Newtown Square, PA. https://www.nrs.fs.fed.us/pubs/rb/rb_nrs58.pdf.

Markewich, H. W., M. J. Pavich, and G. R. Buell. 1990. Contrasting soils and landscapes of the Piedmont and Coastal Plain, eastern United States. Geomorphology 3:417–447.

Marton, J. M., E. R. Herbert, and C. B. Craft. 2012. Effects of salinity on denitrification and greenhouse gas production from laboratory-incubated tidal forest soils. Wetlands 32:347–357.

Maryland Department of Natural Resources, and NOAA [National Oceanic and Atmospheric Administration]. 2008. Somerset County, Maryland: Rising Sea Level Guidance. https://dnr.maryland.gov/ccs/Publication/SeaLevel_Somerset.pdf.

Maryland Department of the Environment. 2018. Maryland's Integrated Report of

Surface Water Quality. Baltimore, MD. https://mde.maryland.gov/programs/Water/TMDL/Integrated303dReports/Pages/2018IR.aspx.

Miller, K. G., R. E. Kopp, B. P. Horton, J. V. Browning, and A. C. Kemp. 2013. A geological perspective on sea-level rise and its impacts along the U.S. mid-Atlantic coast. Earth's Future 1:3–18.

Moomaw, W. R., G. L. Chmura, G. T. Davies, C. M. Finlayson, B. A. Middleton, S. M. Natali, J. E. Perry, N. Roulet, and A. E. Sutton-Grier. 2018. Wetlands In a Changing Climate: Science, Policy and Management. Wetlands:1–23.

Moyer, D. L., and J. D. Blomquist. 2018. Summary of Nitrogen, Phosphorus, and Suspended-Sediment Loads and Trends Measured at the Nine Chesapeake Bay River Input Monitoring Stations: Water Year 2017 Update. https://cbrim.er.usgs.gov/data/RIM Load and Trend Summary 2017_Combined.pdf.

Musolff, A., B. Selle, O. Büttner, M. Opitz, K. Knorr, J. H. Fleckenstein, T. Reemtsma, and J. Tittel. 2017. Does iron reduction control the release of dissolved organic carbon and phosphate at catchment scales? Need for a joint research effort. Global Change Biology 23:e5–e6.

Nair, V. D., K. R. Reddy, R. D. DeLaune, K. R. Reddy, C. J. Richardson, and J. P. Megonigal. 2013. Phosphorus Sorption and Desorption in Wetland Soils. Pages 667–681 Methods in Biogeochemistry of Wetlands. Madison, WI.

National Oceanic and Atmospheric Administration - National Centers for Environmental Information [NOAA-NCEI]. 2018. Climate Data Online.

https://www.ncdc.noaa.gov/cdo-web/.

Paerl, H. W., N. S. Hall, B. L. Peierls, and K. L. Rossignol. 2014. Evolving Paradigms and Challenges in Estuarine and Coastal Eutrophication Dynamics in a Culturally and Climatically Stressed World. Estuaries and Coasts 37:243–258.

Perez, M. R. 2015. Regulating Farmer Nutrient Management: A Three-State Case Study on the Delmarva Peninsula. Journal of Environmental Quality 44:402.

Qualls, R. G., and B. L. Haines. 1991. Geochemistry of Dissolved Organic Nutrients in Water Percolating through a Forest Ecosystem. Soil Science Society of America Journal 55:1112–1123.

Qualls, R. G., B. L. Haines, W. T. Swank, and S. W. Tyler. 2000. Soluble Organic and Inorganic Nutrient Fluxes in Clearcut and Mature Deciduous Forests. Soil Science Society of America Journal 64:1068–1077.

R Studio Team. 2019. RStudio: Integrated Development for R. R Studio Incorporated, Boston, MA.

Reddy, K. R., and R. D. DeLaune. 2008. Biogeochemistry of Wetlands. First edition. CRC Press, Boca Raton, Florida.

Roman, C. T., and D. M. Burdick. 2012. Tidal Marsh Restoration. Page (C. T. Roman and D. M. Burdick, Eds.) Tidal Marsh Restoration: A Synthesis of Science and Management. Island Press/Center for Resource Economics, Washington, DC.

Rütting, T., P. Boeckx, C. Müller, and L. Klemedtsson. 2011. Assessment of the importance of dissimilatory nitrate reduction to ammonium for the terrestrial nitrogen cycle. Biogeosciences 8:1779–1791.

Sharpley, A. N., H. P. Jarvie, A. R. Buda, L. May, B. Spears, and P. J. A. Kleinman.

2014. Phosphorus Legacy: Overcoming the Effects of Past Management Practices to Mitigate Future Water Quality Impairment. Journal of Environmental Quality 42:1308–1326.

Sharpley, A. N., P. J. A. Kleinman, P. Jordan, L. Bergström, and A. L. Allen. 2006. Evaluating the success of phosphorus management from field to watershed. Journal of Environmental Quality 38:1981–1988.

Shepard, A., D. Curson, K. Patton, and N. Dubois. 2013. Sea-level Rise Is for the Birds: Landscape-level Conservation Planning to Protect Communities, Coastal Wetlands and Salt Marsh Birds. https://defenders.org/sites/default/files/publications/Lower-Shore-Tidal-Marsh-Climate-Adaptation-Project.pdf.

Smith, J. A. M. 2013. The Role of Phragmites australis in Mediating Inland Salt Marsh Migration in a Mid-Atlantic Estuary. PLoS ONE 8:e65091.

Soil Survey Staff. 2018. Web Soil Survey. https://websoilsurvey.sc.egov.usda.gov/.

Tanner, C. C., and J. P. S. Sukias. 2011. Multiyear Nutrient Removal Performance of Three Constructed Wetlands Intercepting Tile Drain Flows from Grazed Pastures. Journal of Environmental Quality 40:620.

Tobias, C. R., S. A. Macko, I. C. Anderson, E. A. Canuel, and J. W. Harvey. 2001. Tracking the fate of a high concentration groundwater nitrate plume through a fringing marsh: A combined groundwater tracer and in situ isotope enrichment study. Limnology and Oceanography 46:1977–1989.

Trimble, S. W. 2008. Man-induced soil erosion on the Southern Piedmont, 1700-1970. (S. W. Trimble, Ed.). Second edition. Soil and Water Conservation

Society, Ankeny, IA.

Tully, K., K. Gedan, R. Epanchin-Niell, A. Strong, E. S. Bernhardt, T. BenDor, M. Mitchell, J. Kominoski, T. E. Jordan, S. C. Neubauer, and N. B. Weston. 2019a. The Invisible Flood: The Chemistry, Ecology, and Social Implications of Coastal Saltwater Intrusion. BioScience 69:368–378.

Tully, K. L., D. Weissman, W. J. Wyner, J. Miller, and T. Jordan. 2019b. Soils in transition: saltwater intrusion alters soil chemistry in agricultural fields. Biogeochemistry 142:339–356.

United States Department of Agriculture - National Agricultural Statistics Service [USDA-NASS]. 2012. 2012 Census of Agriculture County Profile: Somerset County, Maryland. Washington, DC. https://www.nass.usda.gov/Publications/.

United States Environmental Protection Agency [USEPA]. 2000. Ambient Water Quality Criteria Recommendations of State and Tribal Nutrient Criteria Lakes and Reservoirs in Nutrient Ecoregion II. https://www.epa.gov/sites/production/files/documents/rivers14.pdf.

Viollier, E., P. . Inglett, K. Hunter, A. . Roychoudhury, and P. Van Cappellen. 2000. The ferrozine method revisited: Fe(II)/Fe(III) determination in natural waters. Applied Geochemistry 15:785–790.

Waldrip, H. M., P. H. Pagliari, Z. He, R. D. Harmel, N. A. Cole, and M. Zhang. 2015. Legacy Phosphorus in Calcareous Soils: Effects of Long-Term Poultry Litter Application. Soil Science Society of America Journal 79:1601.

Walsh, S., and R. Miskewitz. 2013. Impact of sea level rise on tide gate function. Journal of Environmental Science and Health, Part A 48:453–463.

Wasson, K., A. Woolfolk, and C. Fresquez. 2013. Ecotones as Indicators of Changing Environmental Conditions: Rapid Migration of Salt Marsh-Upland Boundaries. Estuaries and Coasts 36:654–664.

Weinberg, H. 2008. Chesapeake Bay Salinity Maps. https://www.chesapeakebay.net/what/maps/keyword/salinity.

Weston, N. B., R. E. Dixon, and S. B. Joye. 2006. Ramifications of increased salinity in tidal freshwater sediments: Geochemistry and microbial pathways of organic matter mineralization. Journal of Geophysical Research: Biogeosciences 111:1–14.

Weston, N. B., M. A. Vile, S. C. Neubauer, and D. J. Velinsky. 2011. Accelerated microbial organic matter mineralization following salt-water intrusion into tidal freshwater marsh soils. Biogeochemistry 102:135–151.

White, E., and D. Kaplan. 2017. Restore or retreat? Saltwater intrusion and water management in coastal wetlands. Ecosystem Health and Sustainability 3:e01258.

Williams, A. A., N. T. Lauer, and C. T. Hackney. 2014. Soil phosphorus dynamics and saltwater intrusion in a florida estuary. Wetlands 34:535–544.

Wilson, A. M., and J. T. Morris. 2012. The influence of tidal forcing on groundwater flow and nutrient exchange in a salt marsh-dominated estuary. Biogeochemistry 108:27–38.

Zhang, Q., R. R. Murphy, R. Tian, M. K. Forsyth, E. M. Trentacoste, J. Keisman, and P. J. Tango. 2018. Chesapeake Bay's water quality condition has been recovering: Insights from a multimetric indicator assessment of thirty years of tidal monitoring data. Science of the Total Environment 637–638:1617–1625.

Chapter 2: Saltwater intrusion affects nitrogen, phosphorus and iron transformations under aerobic and anaerobic conditions: An incubation experiment

Abstract

Low-lying coastal ecosystems are rapidly salinizing due to sea level rise and associated saltwater intrusion (SWI). In agricultural soils, SWI can alter biogeochemical cycling of key nutrients such as nitrogen (N), phosphorus (P), and iron (Fe). The main objective of this study was to quantify the amount of nitrate-N (NO_3-N), ammonium-N (NH_4-N), soluble reactive P (SRP), and total dissolved iron (TDFe) released from agricultural soils undergoing SWI to determine their potential loss to downstream waterways. Agricultural soils were incubated for 0, 15, and 30 days (under aerobic and anaerobic conditions) with various salt solution combinations of sodium chloride, sodium sulfate (Na_2SO_4), and calcium sulfate with high (15 parts per thousand), low (~1.5 ppt), or no (0 ppt) ionic strength to mimic (1) different ionic constituents of saltwater and (2) different soil amendments. At day 30, anaerobic soils released significantly more NH_4-N (by 134 times), SRP (by 5.1 times), and TDFe (by 206 times) to the soil solution than aerobic soils ($P < 0.05$) likely due to enhanced rates of dissimilatory NO_3 reduction to NH_4 and the reductive dissolution of Fe, which releases Fe(II) and SRP into solution. Concentrations of SRP were moderately and significantly positively correlated with TDFe concentrations ($R^2 = 0.49$, $P < 0.0001$), suggesting that Fe reduction is likely the driver of SRP release from inundated soils. NH_4-N concentrations were near zero under aerobic conditions.

Regardless of oxygen level, soils exposed to high ionic strength solutions released significantly more NH_4-N into overlying water than soils exposed to low ionic strength solutions ($P < 0.05$) due to increased soil cation exchange. After 30 days of inundation with saltwater, as much as 21% of bioavailable soil P (as SRP) and as much as 41% of total inorganic N could be released to overlying water (as NH_4-N) if soils were under anaerobic conditions. Our work indicates that the influx and inundation of salts to SWI-affected farm fields could lead to a large export of N and P from agricultural soils and potentially affect downstream water quality.

Introduction

Saltwater intrusion (SWI) into freshwater systems is a growing problem in coastal regions worldwide (White and Kaplan 2017; Tully et al. 2019a). Driven by sea level rise, the frequency and intensity of storms and droughts, water extraction for human use, and the connectivity of the landscape to sources of saltwater (e.g. canals, ditches, etc.), SWI can push sea salts inland far beyond the high tide line (Schoepfer et al. 2014; Bhattachan et al. 2018; Tully et al. 2019b). By 2050, global sea levels are expected to rise by 20 to 30 cm (IPCC 2013). The effects of SWI include, but are not limited to, marsh migration, forest die-off, the spread of invasive species, crop yield declines, and nutrient pollution through changes in biogeochemical cycles in soils (Tully et al. 2019a). In this study, we focus on biogeochemical effects of SWI that alter nitrogen (N) and phosphorus (P) cycling in agricultural soils and can lead to pollution in coastal waterways downstream of SWI-affected farm fields (Ardón et al. 2013; Williams et al. 2014).

Many coastal farms are located on former wetlands that were drained for agricultural use (Moomaw et al. 2018). In areas very close to saline water bodies, such as tidal creeks and salt marshes, ditches can regularly flood with saltwater, even during baseline hydrologic flow conditions (Bhattachan et al. 2018). In coastal regions with low elevations, extensive ditch networks were historically carved into the landscape to allow excess water to flow off farm fields (Reddy and DeLaune 2008). However, as SWI moves inland, ditches serve the reverse purpose and frequently act as conduits that allow saltwater to concentrate on fields during high tides, storms, and droughts (Tully et al. 2019a). Saltwater can remain on these fields for days or even weeks and spur major changes in soil chemistry and nutrient release (Weissman and Tully 2020).

Though the theoretical understanding of the biogeochemical processes that lead to nutrient release in soils exposed to inundation and saltwater has been well established, the rate and extent of their occurrence vary greatly from site to site depending on prevailing environmental conditions (Roman and Burdick 2012). Further, most studies on SWI have been conducted on freshwater wetlands that are becoming salinized (Neubauer et al. 2013; Helton et al. 2014; White and Kaplan 2017). Agricultural soils have distinct properties from freshwater wetland soils, which causes nutrient cycles to behave differently in each of these environments. For example, since wetlands are frequently inundated, nitrate (NO_3^-) and sulfate (SO_4^{2-}) tend to leach quickly from their soils, while well-drained agricultural soils better retain these nutrients (Megonigal and Neubauer 2009). Because wetland soils usually contain a thicker horizon of carbon (C)-rich organic material than agricultural soils,

biological activity is often more C-limited in the latter (Roman and Burdick 2012). Finally, wetland soils tend to be anaerobic and release soluble reactive P (SRP) into solution more readily than well-drained agricultural soils (Nair et al. 2015). Thus, in order to better understand the potential consequences of large-scale SWI in coastal farmlands, we conducted a detailed incubation study with agricultural soil to mimic different aspects of SWI (e.g. ionic strength, SO_4^{2-} reduction, oxygen levels, and soil amendments) and assess their impacts on N and P release to overlying waters.

To achieve our study objective, we simulated four moderators of nutrient release: (1) change in ionic strength (Ardón et al. 2013); (2) enhanced SO_4^{2-} reduction (Williams et al. 2014); (3) decreased oxygen levels (Nair et al. 2013); and (4) soil amendments (Grubb et al. 2012). Saltwater is comprised of a variety of ions that can affect biogeochemical cycling in soils such as base cations like sodium (Na^+), calcium (Ca^{2+}), magnesium, and potassium, and the anion SO_4^{2-}. Combined with lowered oxygen levels in soils that result from inundation, ions have synergistic effects on nutrient release.

In SWI-affected areas, N pollution increases with inundation and ionic strength (Schoepfer et al. 2014; Tully et al. 2019a). Because of its negative charge, NO_3^- is repelled by negatively charged soil particles and hence tends to leach quickly from saturated soils (Goyne et al. 2008). On the other hand, ammonium (NH_4^+) ions tend to readily sorb to exchange sites on agricultural soil but are easily displaced by cations found in saltwater, such as Na^+. Both of these processes can lead to a large export of N into local waterways (Ardón et al. 2013).

Interactions between SO_4^{2-} and iron (Fe) can enhance P release in SWI-affected soils (Williams et al. 2014). In aerobic soils, Fe is found in its oxidized form (Fe(III)) and tends to bind tightly to phosphate (PO_4^{3-}), the bioavailable form of P in poorly-crystalline organic matter complexes (McDowell and Sharpley 2001). However, Fe(III) is biotically and abiotically reduced to Fe(II) under low oxygen conditions, such as in a field that has been inundated, and releases PO_4^{3-} into the soil porewater (Nair et al. 2013). Unlike freshwater, saltwater is rich in SO_4^{2-} and provides another terminal electron acceptor in saturated soils. Microbial populations reduce SO_4^{2-} to sulfide (a compound containing one or more S^{2-} ions), which can bind to Fe(II), forming Fe sulfides (FeS_x) in reducing environments (Schoepfer et al. 2014). This process immobilizes Fe and makes it unavailable to rebind P even when soils become aerobic (Jordan et al. 2008).

Other transformations of N and P are also greatly affected by changing soil redox conditions that co-occur with SWI. Aerobic microbial respiration pathways (where oxygen is reduced) are the most thermodynamically favorable, and thus are the dominant form of respiration in well-aerated (aerobic) soil. However, soils are depleted in oxygen as they become saturated, and other respiration pathways begin to dominate. The next most widespread and energetically favorable pathways are NO_3^- reduction, followed by Fe reduction, and SO_4^{2-} reduction (Schoepfer et al. 2014). In saturated soils, much of the NO_3^- present is rapidly reduced to N_2 gas through the process of denitrification. However, many studies have shown that a large portion of NO_3^- can also be reduced to NH_4^+ through dissimilatory reduction pathways (DNRA),

particularly in saline soils (Tobias et al. 2001, Burgin and Hamilton 2007, Giblin et al. 2013).

Finally, soil amendments can also affect soluble reactive P (SRP; a form of phosphate) concentrations in soil porewater (Grubb et al. 2012). Calcium is often added to fields as gypsum ($CaSO_4$) to remediate sodic soils (Fowler et al. 2014) and as agricultural lime ($Ca(OH)_2$) to raise soil pH (Brady and Weil 2016). Because Ca also binds and sequesters SRP in soils, it has been studied for its potential to reduce P pollution in agricultural ditches (Moore and Miller 1994; Grubb et al. 2012). Thus, we chose to explore the effects of the addition of $CaSO_4$ to soil because it is a management response to SWI.

The main objective of this study was to quantify the effect of different ionic constituents of saltwater and $CaSO_4$ on the release of dissolved inorganic N (DIN), SRP, and total dissolved Fe (TDFe) release from an agricultural soil under aerobic and anaerobic conditions. We also measured total and poorly-crystalline Fe to determine if the amount of Fe dissolved into soil solution caused a significant change in overall pools of soil Fe after 30 days. Because of DNRA and cation exchange on soil particle surfaces, we hypothesized that anaerobic high ionic strength treatments would enhance NH_4-N release to the soil solution while driving NO_3-N concentrations to near-zero levels. Additionally, we expected to observe increased SRP release under anaerobic conditions due to Fe and SO_4^{2-} reduction. Finally, because Ca^{2+} readily binds to SRP, we expected that calcium sulfate (+$CaSO_4$) treatments would suppress SRP release from both aerobic and anaerobic soils. Although there is a growing body of literature using incubation studies to assess the

effects of SWI on wetland soils (Williams et al. 2014; Steinmuller and Chambers 2018), no prior laboratory studies have examined how incoming saltwater affects nutrient release from agricultural soils undergoing SWI. Therefore, our controlled incubation study represents a novel effort to quantify N and P release from coastal agricultural soils into downstream waterways. Our study results can be used to develop improved nutrient reduction targets for ecologically-sensitive coastal areas.

Methods

Study site

In Maryland, the Chesapeake Bay surrounds the western shores of Dorchester, Wicomico, and Somerset counties (Figure 2-1A). We collected soils on a farm field near Princess Anne, in Somerset County, the southernmost county in Maryland (38.2° N, 75.7° W; Figure 2-1B). The soil was comprised of a mesic Aquic Hapludult loam mainly from the Manokin soil series (Soil Survey Staff 2018). Additional physical and chemical characteristics of the soil are described in Table 2-1. We collected soils from the top 10 cm of the agricultural field in April 2019 and stored the field-moist soils at 4°C. The sampling point was 500 meters from the closest salt marsh (Figure 2-1B), and while neighboring fields had been affected, the focal field did not yet show signs of SWI. The nearby marsh soils were comprised of a combination of Transquaking and Mispillion soil series and had an average salinity of 22 parts per thousand (ppt) in the top 50 cm of the soil porewater (Soil Survey Staff 2018). Most of the county is expected to undergo regular tidal flooding by 2050 (Maryland Department of Natural Resources and NOAA 2008). The area receives an average of

1040 mm of precipitation annually. The mean annual maximum temperature is 21°C and the mean annual minimum temperature is 6°C (NOAA-NCEI 2018).

Soil solution sample collection and analysis

In order to examine the effect of SWI on soil N, P, and Fe dynamics, we created a suite of salt solution treatments to determine the relative effect of different ionic constituents and ionic strength on N, P, and Fe release from soils (Table 2-2). Throughout this paper, we refer to "release" as the sum of biotic and abiotic processes that spur the movement of ions out of the soil and into the soil solution. Treatments containing calcium sulfate (+$CaSO_4$ treatments) were designed to simulate gypsum additions to SWI-affected fields. Treatments containing sodium sulfate (+Na_2SO_4 treatments) were intended to simulate SO_4^{2-} addition from saltwater without including the suppressive effects of Ca on SRP release. Treatments containing sodium chloride (+NaCl treatments) were designed to determine the effects of high ionic strength on nutrient release to soil porewater, and the Na_2SO_4 and $CaSO_4$ treatments mimicked low ionic strength. We also included deionized water (DIW) and Instant Ocean® Sea Salt (Spectrum Brands, VA, USA) as freshwater and saltwater controls, respectively.

In total, we created eight salt treatment solutions: (1) DIW; (2) Na_2SO_4 (~1.5 ppt); (3) $CaSO_4$ (~ 1.5 ppt); (4) NaCl + $CaSO_4$ (15 ppt); (5) NaCl + Na_2SO_4 (15 ppt); (6) NaCl (15 ppt; (7) NaCl + Na_2SO_4 + $CaSO_4$ (15 ppt); and (8) Instant Ocean® Sea Salt (15 ppt; Table 2-2). The Na_2SO_4, $CaSO_4$, NaCl + Na_2SO_4, and NaCl + $CaSO_4$ treatments contained SO_4^{2-} at the same ratio found in 15 ppt (brackish) saltwater (1.14 g SO_4^{2-}/l) and the addition of NaCl brought those treatments up to 15 ppt total. Exact stock solution mixtures are detailed in Table 2-2. We selected 15 ppt as the high ionic

strength salt treatments for this experiment based on the results of a previous field study we conducted on actively farmed fields undergoing SWI in Somerset County where soil porewater salinity in the top 25 cm of SWI-affected parts of these fields ranged from approximately 5-25 ppt throughout the data collection period (Tully et al. 2019b).

Each microcosm consisted of a slurry of 120 ml of treatment water added to 20 g field-moist soil and incubated at 25 °C. Slurries were made in duplicate and one was maintained aerated and the other, anaerobic, to simulate high and low redox potential saturated environments. Though aerated slurries were also saturated with solution, we herein will refer to them as "aerobic" for consistency. Aerobic slurries were created in 250 ml beakers, sealed with gas-permeable membranes and stirred daily, to maintain aeration and prevent SRP from being released due to Fe reduction from $FePO_4$ complexes under lower redox conditions. Anaerobic slurries were placed into 125 ml Erlenmeyer flasks and sealed with airtight rubber septa. These slurries were purged for ten minutes with purified N_2 gas. Each oxygen level by salt solution combination was replicated four times for each sampling date (day 0, 15, and 30; n_{total} = 192). Microcosms were destructively sampled to avoid changing the total soil solution volume throughout the experiment. To limit the introduction of air to the water sample, anaerobic microcosms were sampled via a syringe through the rubber septa. Aerobic microcosms were sampled by syringes placed directly into the soil solution.

All soil solution samples were immediately filtered through 0.45 μm glass fiber filters, and frozen until analysis. A subsample of each sample to be analyzed for

dissolved inorganic phosphorus (measured as SRP) was acidified to pH ~ < 2 with hydrochloric acid to prevent PO_4^{3-} coprecipitation with Fe upon sample exposure to oxygen. Samples were analyzed colorimetrically on a LACHAT QuikChem (LACHAT Instruments Loveland, CO) using the sulfanilamide method for NO_3-N, the salicylate-nitroprusside method for NH_4-N, and the molybdate-blue method for SRP.

All soil solutions were analyzed for total dissolved Fe (TDFe) using the modified ferrozine method to reduce all dissolved Fe(III) to Fe(II) (Viollier et al. 2000). A reducing agent, 1.4*M* hydroxylamine hydrochloride ($H_2NOH.HCl$), was prepared in 2*M* hydrochloric acid. A 10*M* ammonium acetate ($C_2H_7NO_2$) buffer was prepared and adjusted to pH 9.5 with a solution of ammonium hydroxide (NH_4OH). Then, 2 ml of the reducing agent and 1.67 ml of the buffer was added to 10 ml of the water sample. All soil solutions were analyzed for Fe, which represents the total dissolved Fe(II) and Fe(III) oxyhydroxides present in the water samples, on an atomic adsorption spectrometer (PinAAcle 900; Perkin Elmer; CT, USA) using an air-acetlyene flame.

Soil analyses

At each sampling point in the experiment (day 0, 15, and 30), we determined total and poorly-crystalline forms of Fe in all of the microcosm soils in order to determine whether measurable iron transformations occurred in these major pools of soil Fe over time. Soils from each microcosm were air-dried, ground, and passed through a 2mm sieve. They were then extracted for total (crystalline + poorly-crystalline) Fe via the dithionite citrate bicarbonate (DCB) extraction method (Darke

and Walbridge 1994), which uses a powerful reductant, dithionite, to reduce Fe(III) oxides to Fe(II). The oxalate extraction method (Darke and Walbridge 1994) dissolved the poorly-crystalline forms of Fe in soils, which are more labile than crystalline Fe. The supernatant for both extractions was decanted, filtered through Whatman 42 filter paper (2.5 μm) and analyzed for Fe on an atomic absorption spectrometer (PinAAcle 900; Perkin Elmer; CT, USA) using an air-acetylene flame.

Statistical approach

To examine differences in NO_3-N, NH_4-N, SRP, and TDFe in soil solutions and poorly-crystalline and total Fe in soils, we used a linear fixed-effects (LM) model *lme4* package for R (Bates et al. 2018). Salt treatment, oxygen level, and day (0, 15, and 30) were included as fixed effects. We examined the main effect of salt treatment, oxygen level, and day and interactive effects for each variable. For each day sampled, we used *Tukey post-hoc* tests to examine pairwise differences in water chemistry among treatment combinations (*multcomp* package; Hothorn et al. 2017). We used the Box-Cox method (Box and Cox 1964) for log transformations prior to analysis to meet the assumptions of the statistical model when needed. All statistics were computed in R Studio (R Studio Team 2019).

To increase statistical power, and thus the ability to detect significant differences among pairwise comparisons at day 30, we grouped NH_4-N and SRP data into broader salt treatment groups based on our hypotheses. Because we hypothesized that higher ionic strength treatments would result in greater NH_4-N release to soil solution, we grouped salt treatments into two categories: high ionic strength (15 ppt: NaCl, NaCl + Na_2SO_4, NaCl + $CaSO_4$, NaCl + Na_2SO_4 + $CaSO_4$, and Instant

Ocean®) and low ionic strength (~ 1.5 ppt: Na_2SO_4 and $CaSO_4$). The DIW treatment (no ionic strength) was not included because it was only comprised of one salt treatment and did not allow for adequate statistical power to detect significance between this treatment and the other treatment groups. Since we hypothesized that the form of SO_4^{2-} was the main driver of SRP release from soils, we grouped data from the salt treatments based on whether they contained added Na_2SO_4, $CaSO_4$, neither constituent, or a combination of both. These treatments are referred to as: (1) $+Na_2SO_4$ treatments; (2) $+CaSO_4$ treatments; (3) $-SO_4^{2-}$ treatments; (4) or $+Na_2SO_4$ and $CaSO_4$ treatments. We conducted a Pearson correlation to determine the linear relationship between TDFe and SRP concentrations but omitted data from day 0 as this was our baseline before there was adequate time for chemical transformations to take place in the soil.

We calculated potential nutrient release from the aerobic and anaerobic soils used for this experiment (top 10 cm of topsoil from the field) based on a bulk density of 1.55 g/cm^3 from Web Soil Survey (Soil Survey Staff 2018) and results from the Instant Ocean® treatment at day 30 of the experiment. This salt treatment reflects soils inundated with 15 ppt saltwater without any soil amendments. To estimate the suppression of SRP release from $+CaSO_4$ treatments, we also calculated these values for the NaCl + Na_2SO_4 + $CaSO_4$ salt treatment as it was our closest analog to 15 ppt saltwater with a Ca soil amendment.

Results

Overall, we found that oxygen levels and salt treatments had major effects on N, P, and TDFe release into the soil solution. Anaerobic soils released more NH_4-N,

SRP, and TDFe to the overlying water than aerobic soils after 15 and 30 days (Tables 2-3 and 2-4; Figures 2-2A, 2-3B, 2-4B, and 2-6; $P < 0.05$). Concentrations of NH_4-N, SRP, and TDFe were lowest in anaerobic soil solutions at day 0 (0.28 mg N/l, 0.30 mg P/l, and 0.99 mg Fe/l, respectively), intermediate at day 15 (4.13 mg N/l, 5.67 mg P/l, and 7.61 mg Fe/l, respectively), and highest at day 30 (5.19 mg N/l, 9.31 mg P/l, and 16.74 mg Fe/l, respectively; Figures 2-3A, 2-4A, and 2-6), while NO_3-N concentrations decreased from around 8 mg N/l at day 0 to near zero levels by day 15 (Figure 2-2A). Nitrate-N release from aerobic soils was lowest at day 0 (7.68 mg N/l), intermediate at day 15 (8.87 mg N/l), and highest at day 30 (10.04 mg N/l) while NH_4-N and TDFe concentrations remained near zero throughout the incubation period (Figures 2-2A, 2-3A, and 2-6). In aerobic soils, SRP release was lowest at day 0, but similar between day 15 and day 30 (0.29 mg P/l, 2.21 mg P/l, and 2.57 mg P/l, respectively; Figure 2-4A). As we were mainly interested in the results at the end of the incubation period (day 30), we further explored the effects of salt treatment and oxygen level at day 30.

At day 30, significantly more NO_3-N was released to the overlying solution under aerobic conditions (3.89 to 13.48 mg NO_3-N/l) as compared to anaerobic conditions (0.01 to 0.21 mg NO_3-N/L; $P < 0.05$). However, there was no effect of salt treatment on NO_3-N release regardless of oxygen level (Table 2-4 and Figure 2-2A). By day 30, NH_4-N concentrations were much higher under anaerobic conditions (3.06 to 7.23 mg NH_4-N/l) than under aerobic conditions (0.02 to 0.26 mg NH_4-N/l; $P < 0.0001$; Table 2-4 and Figure 2-3A). Because there were no significant differences in NH_4-N concentrations among +Na_2SO_4 treatments versus +$CaSO_4$ treatments, we

grouped data from the treatments based on their overall ionic strength (total salts g/l). These treatments were either high ionic strength (15 ppt: NaCl, NaCl + Na_2SO_4, NaCl + $CaSO_4$, NaCl + Na_2SO_4 + $CaSO_4$, and Instant Ocean®) or low ionic strength (~ 1.5 ppt: Na_2SO_4 and $CaSO_4$) treatments. By day 30, twice as much NH_4-N was released to overlying waters in high ionic strength solution than in the low ionic strength solution, under both aerobic and anaerobic conditions ($P < 0.05$; Figure 2-3B).

At day 30, SRP release was significantly lower under aerobic conditions (1.49-3.78 mg SRP/l) than under anerobic conditions (6.10-12.96 mg SRP/l; $P < 0.05$; Figure 2-4A). As PO_4^{3-} binding in soils is controlled by SO_4^{2-} reduction and the presence of Ca, we grouped data from the treatments based on whether they contained only Na_2SO_4, only $CaSO_4$, neither constituent, or a combination of both. Concentrations of SRP were significantly lower in $CaSO_4$-only (gypsum soil amendment) treatments than in Na_2SO_4-only treatments with other treatments releasing intermediate amounts of SRP to soil solution (Figure 2-4B; $P < 0.05$).

There was a moderate and significant correlation between TDFe and SRP concentrations in soil solution (Figure 2-5; $R^2 = 0.49$, $P < 0.0001$). Concentrations of TDFe were significantly higher under anaerobic conditions (6.90-26.57 mg Fe/l) than under aerobic conditions (0.07-1.45 mg Fe/l; $P < 0.05$). We observed no effect of salt treatment on the release of total Fe to solution (Table 2-4 and Figure 2-6).

Finally, there was no significant difference between poorly-crystalline Fe and total Fe concentrations in the post-incubation soils across oxygen levels, salt treatments, or days (Table 2-3). On average, throughout the incubation, soils contained 2.05 mg poorly-crystalline Fe/g of dry soil and 6.48 mg total Fe/g of dry

soil. Thus, about one-third of the total soil Fe was in the poorly-crystalline form (Figure 2-7A and 2-7B).

When scaled to kg/ha, N release was similar between the Instant Ocean® and NaCl + Na_2SO_4 + $CaSO_4$ (representing a field with added gypsum amendments) salt treatments. Under anaerobic conditions, soils released a negligible amount (0.1 kg of NO_3-N/ha) to overlying solution in both Instant Ocean® and NaCl + Na_2SO_4 + $CaSO_4$ treatments, and they released about 76 kg NH_4-N/ha to solution in the two salt treatments (Table 2-5). On the other hand, SRP and TDFe release was much lower in the soils treated with NaCl + Na_2SO_4 + $CaSO_4$ than when exposed to Instant Ocean (90.4 and 119.7 kg P/ha, respectively), illustrating the suppressive effects of Ca on nutrient release. Under aerobic conditions, NO_3-N, NH_4-N, SRP, and TDFe release was similar between the Instant Ocean® and NaCl + Na_2SO_4 + $CaSO_4$ salt treatments.

In the Instant Ocean® treatment, NO_3-N release was almost 1450 times greater under aerobic than anaerobic conditions (143.3 kg N/ha and 0.1 kg N/ha, respectively) while NH_4-N release was nearly 135 times greater under anaerobic versus aerobic conditions (80.3 kg N/ha and 0.6 kg N/ha, respectively; Table 2-5). Finally, SRP was over 6 times greater under anaerobic versus aerobic conditions (119.7 kg P/ha and 19.8 kg P/ha, respectively). TDFe was almost 200 times greater under anaerobic versus aerobic conditions (295.2 kg Fe/ha and kg 1.5 Fe/ha, respectively; Table 2-5).

Discussion

Overall, our results have major implications for how N, P, and Fe may be transformed and released from agricultural soils undergoing SWI. The soil used for this study was

from a farm field that is at risk for SWI in the coming years as it is located only 500 m from a tidal salt marsh and hydrologically connected to the marsh through agricultural ditches. This farm soil shows a high potential for N and P release when exposed to saltwater. For example, when the soil becomes anaerobic due to inundation, concentrations of NH_4-N, SRP, and TDFe may increase in overlying waters. Although release of NH_4-N, SRP, and TDFe was lower under aerobic soil conditions, NO_3-N release was greatly increased. Ionic strength was a strong driver of NH_4-N release from anaerobic soils while the addition of Ca suppressed SRP release from both aerobic and anaerobic soils.

Nitrogen

The main form of DIN release differed between aerobic and anaerobic soil solution due to divergent redox pathways for N. By day 15, NO_3-N concentrations were near zero under anaerobic conditions (Figure 2-2A), which indicates that NO_3-N was either denitrified or converted to NH_4-N via DNRA, as has been observed in previous studies of anaerobic soils (Tobias et al. 2001; Koop-jakobsen and Giblin 2010; Giblin et al. 2013). Research has shown that DNRA rates tend to be higher in saline soils because bisulfide (HS^-) produced from anaerobic SO_4^{2-} reduction is utilized as a reactant and oxidized back to SO_4^{2-} through one of the major DNRA pathways (Giblin et al. 2013).

High ionic strength treatments resulted in a greater NH_4-N release to overlying water than low ionic strength treatments (Figure 2-3B) likely due to cations in saltwater replacing NH_4^+ ions on soil exchange sites (Ardón et al. 2013). This effect was more pronounced under anaerobic conditions where concentrations of

NH_4-N in solution were higher than under aerobic conditions. Of note, high ionic strength treatments contained 10 times the salts of low ionic strength treatments, but NH_4-N release was only two times as much in the former, which suggests a non-linear relationship between ionic strength and NH_4-N release (Figure 2-3B). Thus, when fields undergo SWI, even low levels of salinity exposure (~ 1.5 ppt) may spur the release of large quantities of NH_4-N from soils. Future research could quantify NH_4-N release from soils under incremental increases in ionic strength by modelling response curves.

As expected, NO_3-N was the dominant form of DIN in aerobic soil solutions and NH_4-N concentrations were close to zero. Nitrate-N concentrations remained relatively constant under aerobic conditions throughout the incubation period as most of the NO_3-N was immediately released into solution (Figure 2-2A). Because NO_3-N is prone to rapid leaching from soils (Jessen et al. 2017), SWI may spur a large amount of N loss to downstream waterways through inundation, before soils even become anaerobic. Since there are no studies that have attempted to quantify NO_3-N losses from a field initially undergoing SWI, this hypothesis should be tested through future research.

Phosphorus

Overall, the soil used in this study had a very high level of bioavailable P (363 mg P/kg dry soil), which was over three times higher than bioavailable N concentrations (120 mg N/kg dry soil; Table 2-1). Due to the historic over-application of poultry manure, a fertilizer with a low N to P ratio (Waldrip et al. 2015), these P concentrations are more than four times what is needed for optimal crop growth in the

study region (Sharpley et al. 2003). Therefore, this soil has the potential to release a large amount of P pollution downstream through runoff and with exposure to SWI.

Calcium played an important role in P dynamics under both aerobic and anaerobic conditions while SO_4^{2-} played an additional important role in anaerobic systems. By day 30, we observed a significant suppression of SRP release in +$CaSO_4$ treatments versus +Na_2SO_4 treatments under both oxygen levels (Figure 2-4B) because Ca ions tend to bind to SRP and form insoluble apatite minerals ($Ca_{10}(PO_4)_6(OH,F,Cl)_2$; Zak et al. 2009), thus removing this form of P from the soil solution (Grubb et al. 2011). Additionally, by day 30, +$CaSO_4$ aerobic treatments released significantly less SRP concentrations than the aerobic -SO_4 treatments (Figure 2-4B). However, this was not the case for the corresponding anaerobic treatments, likely due to differences in redox pathways under aerobic and anaerobic conditions.

We found that the ability of Ca to suppress SRP release differed between the +$CaSO_4$ and -SO_4 treatments under aerobic versus anaerobic conditions because of interacting relationships between Fe, sulfur (S), and P cycling. Field observations show that sulfide (reduced S) tends to bind reduced Fe in solution in anaerobic sediments and form insoluble FeS_x complexes that prevent Fe from sequestering SRP (Jordan et al. 2008). The soil used for the incubations already contained a high background level of SO_4-S and salt treatments with SO_4^{2-} increased SO_4^{2-} in the microcosm by only 11%. Therefore, under anaerobic conditions, the suppressive effects of Ca on SRP release could have been muted by high rates of SO_4^{2-} reduction in the soil and soil solution, which spurred SRP release from the soils and

counteracted the effects of Ca. Consequently, as an agricultural field is initially undergoing SWI, Ca amendments may provide a moderate ability to prevent SRP loss downstream but as the field becomes anaerobic, this ability is reduced.

Iron

Over the course of our incubations, we observed significantly greater TDFe concentrations in solution in the anaerobic microcosms than in the aerobic microcosms (Figure 2-6). Therefore, it is clear that anaerobic conditions spurred the reductive dissolution of Fe (Hartzell et al. 2017). Under aerobic conditions, Fe oxyhydroxides tend to coprecipitate with SRP, thus removing it from solution (Weston et al. 2006), which is why we observed near zero concentrations of TDFe in the aerobic microcosms (Figure 2-6). In contrast to TDFe concentrations, poorly-crystalline and total Fe concentrations remained constant throughout the entire incubation period (Figures 2-7A and 2-7B). Crystalline Fe has low solubility in water with circumneutral pH, and it can take years for a significant proportion of the Fe to undergo dissolution to poorly-crystalline or dissolved forms as a soil undergoes SWI (Weston et al. 2006). In a previous study, we showed that the major pool of Fe in the soil shifted from crystalline to poorly-crystalline near field edges, which have been exposed to SWI for years (Tully et al. 2019b). In contrast, our incubations were only measured over 30 days, an insufficient time for dissolution to occur. In the anaerobic treatments, TDFe concentrations were approximately 10% of poorly-crystalline Fe concentrations and less than 3% of total Fe concentrations (Figures 2-6, 2-7A, and 2-7B), which illustrates that TDFe constitutes a small but chemically important pool of Fe in SWI-affected systems. The fact that we observed a moderate and significant

positive correlation between TDFe and SRP concentrations (Figure 2-5) suggests that TDFe plays an important role in sequestering and releasing SRP from inundated soils, as is supported by studies conducted in wetland ecosystems (Chambers and Odum 1990; Hartzell and Jordan 2012).

Additionally, S plays an important role in preventing Fe from re-binding SRP under changing oxygen conditions. As previously mentioned, SO_4^{2-} in soil and soil amendments is reduced to sulfide under anaerobic conditions and tends to bind Fe in FeS_x complexes (Schoepfer et al. 2014). The fact that we still observed high levels of TDFe in solution under anaerobic conditions suggests that the rate of Fe dissolution is faster than its precipitation with sulfide. Therefore, Fe reduction is likely the driver of SRP release from inundated soils while FeS_x formation prevents Fe from sequestering SRP if soil conditions become aerobic again. Fields affected by SWI are subject to these interacting processes because they undergo wetting and drying cycles, which cause them to fluctuate between aerobic and anaerobic redox states (Tully et al. 2019b).

Potential soil nutrient release

Because we generated constant oxygen levels and salinity exposure it is important to note that our estimates reflect a potential for nutrient release from soils over time. Unlike in a controlled laboratory setting, soil conditions in agricultural fields are dynamic. For example, the level of salinity exposure in an SWI-affected can change spatially and temporally, depending on factors such as tidal inundation, and precipitation and evapotranspiration rates (Weissman and Tully 2020). Consequently, the quantity and form of nutrients released from SWI-affected soils is highly

dependent on the timing and magnitude of environmental variables. For example, it is possible that much of the NO_3-N in the soil would rapidly be lost to leaching with saltwater inundation, before the soils could become oxygen-depleted. In turn, less NO_3-N would be present in the soil to undergo DNRA, thus releasing less NH_4-N to porewater when soils finally became anaerobic. Therefore, the total proportion of inorganic N released as NO_3-N versus NH_4-N over time would vary depending on field conditions.

Overall, our results show that large quantities of N and P are poised for loss from agricultural fields undergoing SWI. Soils were collected in April 2019, when precipitation rates in our study region are high, spring tides frequently flood coastal areas, and about a month before farmers tend to plant cash crops (Tully et al. 2019b). Consequently, nutrient export is likely highest during the spring, when there is less plant nutrient uptake because fields are planted in cover crops, conditions are prime for saltwater to move onto fields, and soils tend to remain saturated, sometimes for weeks. After 30 days of inundation with saltwater (e.g. Instant Ocean® treatment), as much as 41% of the total inorganic N could be released (as NH_4-N) if soils were under anaerobic conditions. As much as 21% of the bioavailable soil P could be released as SRP to overlying water after a month of inundation with saltwater. As mentioned previously, bioavailable P levels in the soil were over four times the maximum recommended level to optimize crop yield while minimizing P runoff losses (Sharpley et al. 2003). Thus, SRP release from SWI-affected fields could be a major source of nutrient pollution to nearby waterways. In order to better understand rates of nutrient loss, future research could be focused on determining how conditions

such as soil porewater salinity and redox potential change with nutrient concentrations in SWI-affected fields over time.

Conclusion

As sea levels rise, SWI will cause extended periods of soil inundation in coastal agroecosystems. Here we simulated this effect on an agricultural soil collected from a farm field vulnerable to SWI. Overall, we found that oxygen depletion in inundated soils contributes to SRP release from soils and shifts N cycling so that the DIN pool is dominated by NH_4-N. Higher ionic strength, in turn, enhances NH_4-N release from both aerobic and anaerobic soils. Additionally, even without the addition of added salts, high levels of Fe in agricultural soils can cause a large release of SRP from anaerobic soils as a result of reductive dissolution. However, Ca addition from soil amendments such as agricultural lime or gypsum can bind to P and suppress its release into water overlying inundated soil. These findings imply that SWI-affected fields may be hotspots of nutrient pollution, particularly during the spring, when they have the potential to release a large proportion of inorganic soil N and P to downstream waterways. Therefore, defining mechanisms through which ions interact in solution is critical for quantifying N and P export in coastal agricultural soils affected by SWI.

Tables and figures

Table 2-1

Soil physical and chemical properties

CEC (meq/100g)	**pH**	**OM (%)**	**Total C (%)**	**EC (mS/cm)**	**% Sand**	**% Silt**	**% Clay**	**mg/kg**			
								Total N	**NO_3-N**	**NH_4-N**	**P***
11.29	5.9	2.74	1.9	0.41	43.4	42.6	14.0	1670	117.8	1.5	363
mg/kg											
Ca*	**Mg***	**K***	**Na***	**B***	**Fe***	**Mn***	**Cu***	**Zn***	**Al***	**Cl-**	**SO_4^{2-}**
1271	176	287	15	0.67	374	38	13.64	32.67	663	5.32	23.32

* Mehlich III extractable

Table 2-2

Microcosm salt treatments. Deionized water (DIW) is the no salt control and Instant Instant Ocean® is the 15 parts per thousand (ppt) salinity control designed to mimic the full suite of ions in saltwater. Treatments containing sodium chloride (NaCl) are high ionic strength treatments (15 ppt total salts). Treatments without NaCl are low ionic strength treatments (~1.5 ppt). Treatments containing gypsum ($CaSO_4$) are designed to simulate soil amendments used to reclaim sodic soils. Treatments containing sodium sulfate (Na_2SO_4) are designed to simulate the sulfate component of saltwater.

Treatment	Salt added (g/l)				Total salinity (ppt)
	NaCl	$CaSO_4$	Na_2SO_4	Instant Ocean®	
Deionized water (DIW)	0	0	0	0	0
$CaSO_4$	0	1.47	0	0	1.47
Na_2SO_4	0	0	1.53	0	1.53
NaCl	15	0	0	0	15
NaCl + $CaSO_4$	13.53	1.47	0	0	15
NaCl + Na_2SO_4	13.47	0	1.53	0	15
NaCl + Na_2SO_4 + $CaSO_4$	12.00	1.47	1.53	0	15
Instant Ocean®	0	0	0	15	15

Table 2-3

Results of ANOVA for the effect of oxygen level (O2.level), salt treatment (Trt.), and day (Day) on each variable and all interactive effects. Variables are nitrate-nitrogen (NO_3-N), ammonium-nitrogen (NH_4-N), soluble reactive phosphorus (SRP), total dissolved iron (TDFe), poorly-crystalline Fe, and total Fe.

Variable	Factor	num df	den df	Sum of squares	*F* value	*P* value
NO_3-N	O2.level	1	14	578.25	271.94	< 0.0001***
NO_3-N	Trt.	7	14	9.27	0.62	0.7368
NO_3-N	Day	1	14	220.87	103.87	< 0.0001***
NO_3-N	O2.level:Trt.	7	14	10.26	0.69	0.6810
NO_3-N	O2.level:Day	1	14	212.33	99.86	< 0.0001***
NO_3-N	Trt.:Day	7	14	4.94	0.33	0.9384
NO_3-N	O2.level:Trt.:Day	7	14	7.22	0.49	0.8444
NH_4-N	O2.level	1	14	425.54	273.37	< 0.0001***
NH_4-N	Trt.	7	14	81.20	7.45	< 0.0001***
NH_4-N	Day	1	14	79.47	51.06	< 0.0001***
NH_4-N	O2.level:Trt.	7	14	14.84	1.36	0.2249
NH_4-N	O2.level:Day	1	14	157.84	101.40	< 0.0001***
NH_4-N	Trt.:Day	7	14	1.21	0.11	0.9975
NH_4-N	O2.level:Trt.:Day	7	14	7.21	0.66	0.7043
SRP	O2.level	1	14	32.12	66.17	< 0.0001***
SRP	Trt.	7	14	23.11	6.80	< 0.0001***
SRP	Day	1	14	256.30	527.92	< 0.0001***
SRP	O2.level:Trt.	7	14	0.56	0.16	0.9919
SRP	O2.level:Day	1	14	16.21	33.39	< 0.0001***
SRP	Trt.:Day	7	14	2.40	0.71	0.6660
SRP	O2.level:Trt.:Day	7	14	0.91	0.27	0.9652
TDFe	O2.level	1	14	255.75	184.07	< 0.0001***
TDFe	Trt.	7	14	20.27	2.08	0.1153
TDFe	Day	1	14	75.79	54.55	< 0.0001***
TDFe	O2.level:Trt.	7	14	34.47	3.54	0.0210*
TDFe	O2.level:Day	1	14	128.91	92.78	< 0.0001***
TDFe	Trt.:Day	7	14	5.07	0.52	0.8173
TDFe	O2.level:Trt.:Day	7	14	20.60	2.12	0.1097
Poorly-cryst. Fe	O2.level	1	14	578.25	271.94	0.7564
Poorly-cryst. Fe	Trt.	7	14	0.02	0.70	0.6752
Poorly-cryst. Fe	Day	1	14	0.07	14.85	0.0573

Poorly-cryst. Fe	O2.level:Trt.	7	14	0.01	0.29	0.9577
Poorly-cryst. Fe	O2.level:Day	1	14	0.00	0.02	0.8883
Poorly-cryst. Fe	Trt.:Day	7	14	0.06	1.68	0.1185
Poorly-cryst. Fe	O2.level:Trt.:Day	7	14	0.02	0.64	0.7223
Total Fe	O2.level	1	14	0.00	0.23	0.6352
Total Fe	Trt.	7	14	0.06	0.50	0.8345
Total Fe	Day	1	14	0.01	0.65	0.4222
Total Fe	O2.level:Trt.	7	14	0.11	0.85	0.5480
Total Fe	O2.level:Day	1	14	0.01	0.50	0.4795
Total Fe	Trt.:Day	7	14	0.11	0.86	0.5391
Total Fe	O2.level:Trt.:Day	7	14	0.11	0.89	0.5155

* $P < 0.05$, ** = $P < 0.01$, *** = $P < 0.001$

Table 2-4

Results of ANOVA for the effect of oxygen level (O2.level) and salt treatment (Trt.) on each variable and all interactive effects on day 30 of the experiment. Variables are nitrate-nitrogen (NO_3-N), ammonium-nitrogen (NH_4-N), soluble reactive phosphorus (SRP), total dissolved iron (TDFe), poorly-crystalline iron (Fe), and total Fe.

Variable	Factor	num df	den df	Sum of squares	*F* value	*P* value
NO_3-N	Trt.	7	7	10.53	0.69	0.6791
NO_3-N	O2.level	1	7	758.52	348.37	< 0.0001***
NO_3-N	Trt.:O2.level	7	7	14.10	0.93	0.4958
NH_4-N	Trt.	7	7	10.51	3.69	0.0532
NH_4-N	O2.level	1	7	251.67	618.45	< 0.0001***
NH_4-N	Trt.:O2.level	7	7	3.49	1.23	0.3076
SRP	Trt.	7	7	11.87	4.65	0.0301*
SRP	O2.level	1	7	36.75	86.37	< 0.0001***
SRP	Trt.:O2.level	7	7	0.77	0.30	0.9316
TDFe	Trt.	7	7	6.55	0.75	0.6344
TDFe	O2.level	1	7	352.74	281.19	< 0.0001***
TDFe	Trt.:O2.level	7	7	33.12	3.77	0.0505
Poorly-cryst. Fe	Trt.	7	7	0.16	0.80	0.5937
Poorly-cryst. Fe	O2.level	1	7	0.01	0.43	0.5135
Poorly-cryst. Fe	Trt.:O2.level	7	7	0.19	0.93	0.4951
Total Fe	Trt.	7	7	0.07	0.61	0.7419
Total Fe	O2.level	1	7	0.03	1.84	0.1812
Total Fe	Trt.:O2.level	7	7	0.13	1.22	0.3141

Note: * $P < 0.05$, ** = $P < 0.01$, *** = $P < 0.001$

Table 2-5

Potential nitrate-nitrogen (NO_3-N), ammonium-N (NH_4-N), soluble reactive phosphorus (SRP), and total dissolved iron (TDFe) release from soils exposed to the Instant Ocean® salt treatment and the NaCl + Na_2SO_4 + $CaSO_4$ treatment in kg/ha based on data from day 30 of the experiment.

	Nutrient release (kg/ha)			
Variable	aerobic		anaerobic	
	Instant Ocean®	NaCl + Na_2SO_4 + $CaSO_4$	Instant Ocean®	NaCl + Na_2SO_4 + $CaSO_4$
NO_3-N	143.3	149.7	0.1	0.1
NH_4-N	0.6	1.8	80.3	72.5
SRP	19.8	20.9	119.7	90.4
TDFe	1.5	1.1	295.2	240.7

Figure 2-1

A: Map of the Chesapeake Bay region, United States. Somerset County is outlined by the dotted rectangle. Blue dot is location of soil collection site B: Satellite imagery of the soil collection site (Google Earth 2019).

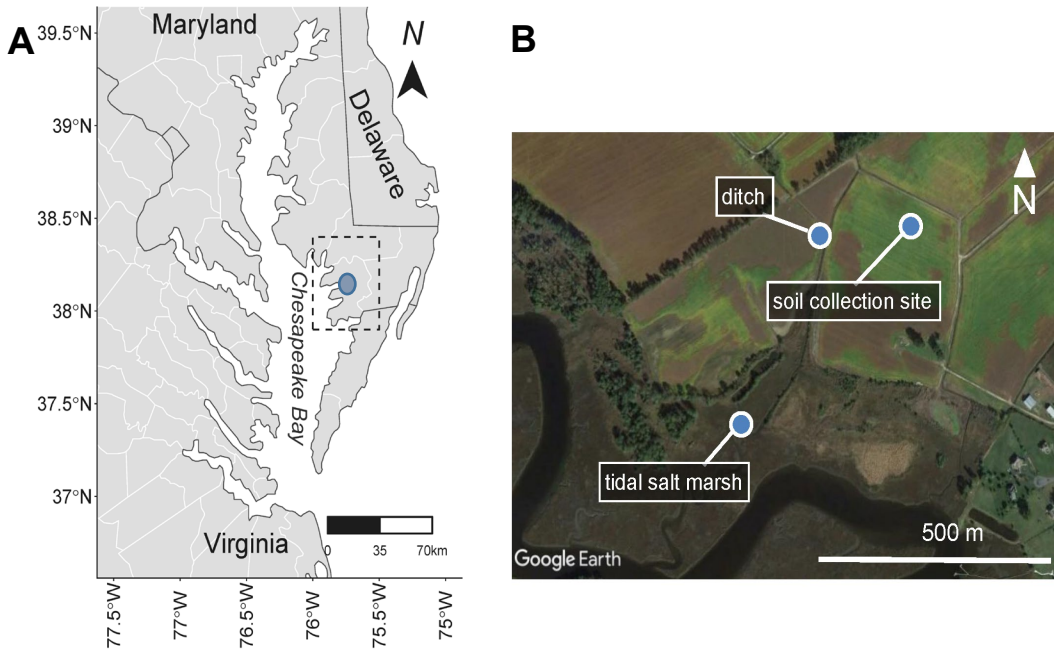

Figure 2-2

A: Microcosm soil solution nitrate-nitrogen (NO_3-N) concentrations in mg NO_3-N/l at days 0, 15, and 30 of the experiment under aerobic and anaerobic conditions (oxygen level). Error bars represent standard error of the mean. Statistically significant differences within each day are indicated by different letters at $P < 0.05$. B: Microcosm soil solution nitrate-nitrogen (NO_3-N) concentrations in mg NO_3-N/l at day 30 of the experiment grouped by low ionic strength (Na_2SO_4, $CaSO_4$; both ~ 1.5 ppt) and high ionic strength (NaCl, NaCl + Na_2SO_4, NaCl + $CaSO_4$, NaCl + Na_2SO_4 + $CaSO_4$, and Instant Ocean®; all 15 ppt) treatments. Statistically significant differences in means are indicated by different letters at $P < 0.05$.

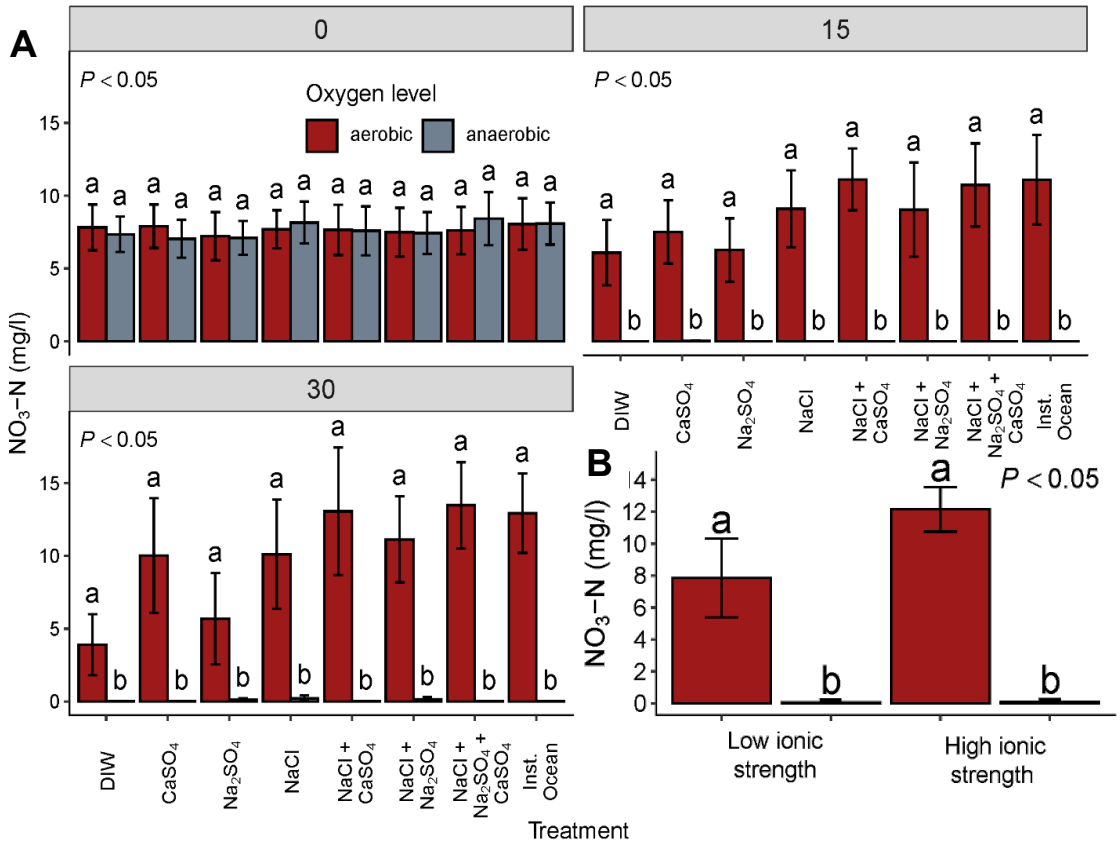

Figure 2-3

A: Microcosm soil solution ammonium-nitrogen (NH_4-N) concentrations in mg NH_4-N/l at days 0, 15, and 30 of the experiment under aerobic and anaerobic conditions (oxygen level). Error bars represent standard error of the mean. Statistically significant differences within each day are indicated by different letters at $P < 0.05$. B: Microcosm soil solution ammonium-nitrogen (NH_4-N) concentrations in mg NH_4-N/l at day 30 of the experiment grouped by low ionic strength (Na_2SO_4, $CaSO_4$; both ~ 1.5 ppt) and high ionic strength (NaCl, NaCl + Na_2SO_4, NaCl + $CaSO_4$, NaCl + Na_2SO_4 + $CaSO_4$, and Instant Ocean®; all 15 ppt) treatments. Statistically significant differences in means are indicated by different letters at $P < 0.05$.

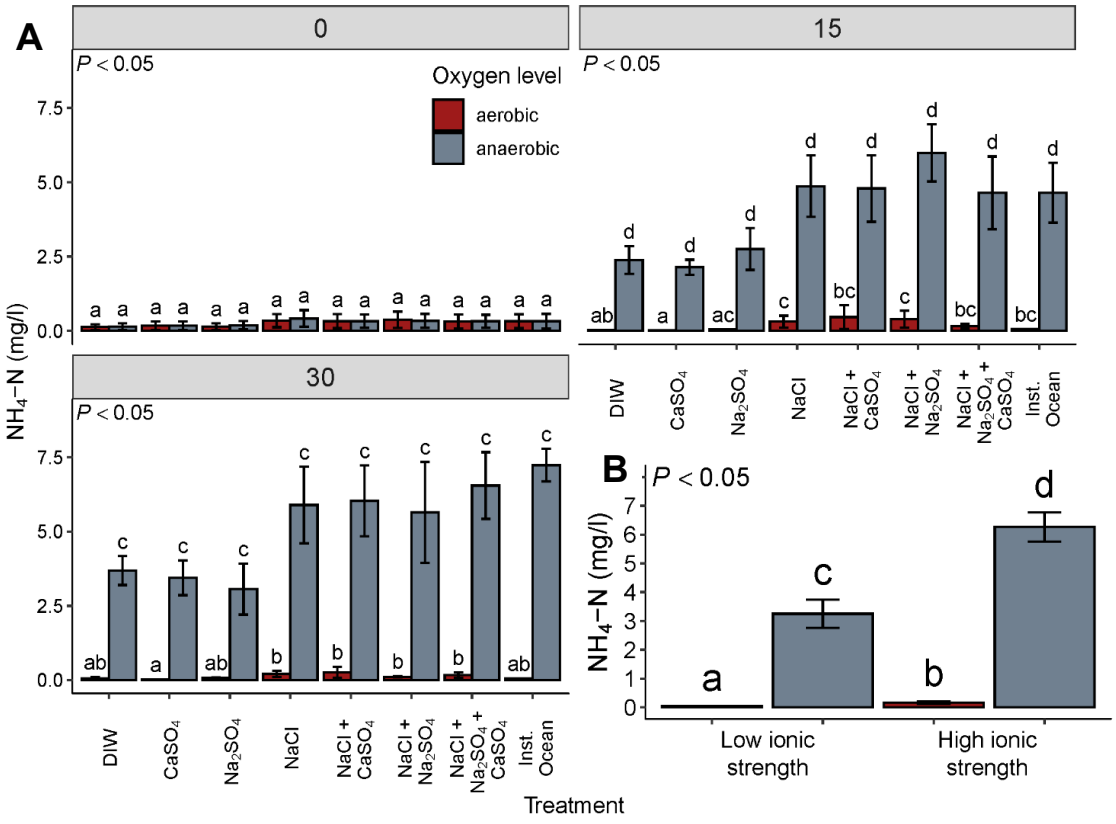

Figure 2-4

A: Microcosm soil solution soluble reactive phosphorus (SRP) concentrations in mg P/l at days 0, 15, and 30 of the experiment under aerobic and anaerobic conditions (oxygen level). Error bars represent standard error of the mean. Statistically significant differences within each day are indicated by different letters at $P < 0.05$. B: Microcosm soil solution soluble reactive phosphorus (SRP) concentrations in mg P/l at day 30. Treatments are grouped by the form of sulfate (SO_4^{2-}) they contained: Na_2SO_4, $CaSO_4$, neither constituent, or a combination of both (Na_2SO_4 and $CaSO_4$). Treatments containing gypsum ($CaSO_4$) are designed to simulate soil amendments used to reclaim sodic soils. Treatments containing sodium sulfate (Na_2SO_4) are designed to simulate the sulfate component of saltwater. Statistically significant differences in means are indicated by different letters at $P < 0.05$.

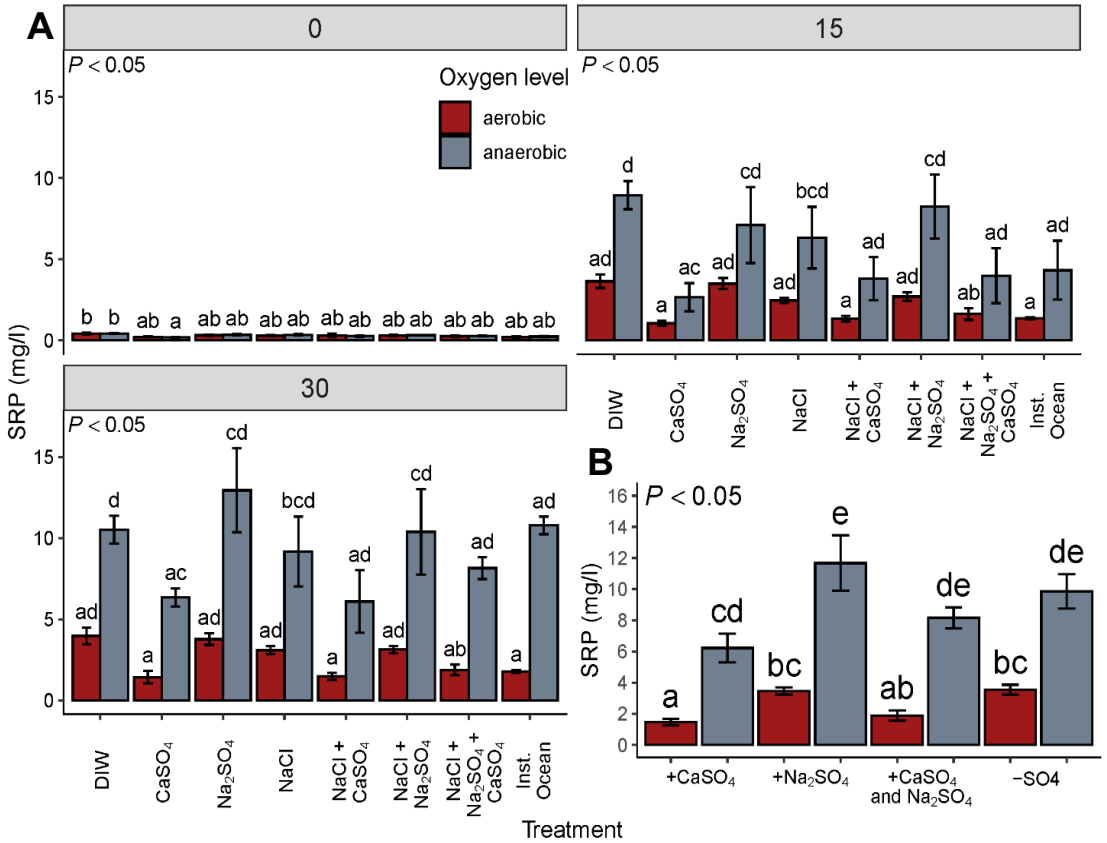

Figure 2-5

Total dissolved iron (TDFe) concentrations in mg Fe/l versus soluble reactive phosphorus (SRP) concentrations in mg SRP/l for days 15 and 30 of the experiment. Dotted red line is the line of best fit based on Pearson correlation.

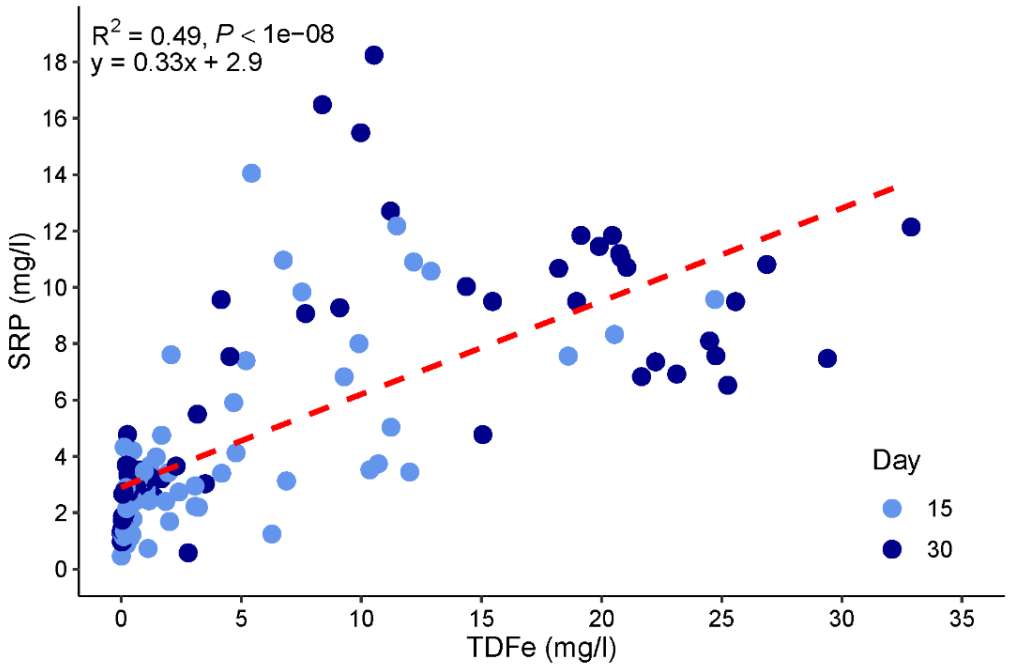

Figure 2-6

Total dissolved iron (TDFe) concentrations in microcosm soil solution in mg Fe/l at days 0, 15, and 30 of the experiment under aerobic and anaerobic conditions (oxygen level). Error bars represent standard error of the mean. Statistically significant differences in means are indicated by different letters at $P < 0.05$.

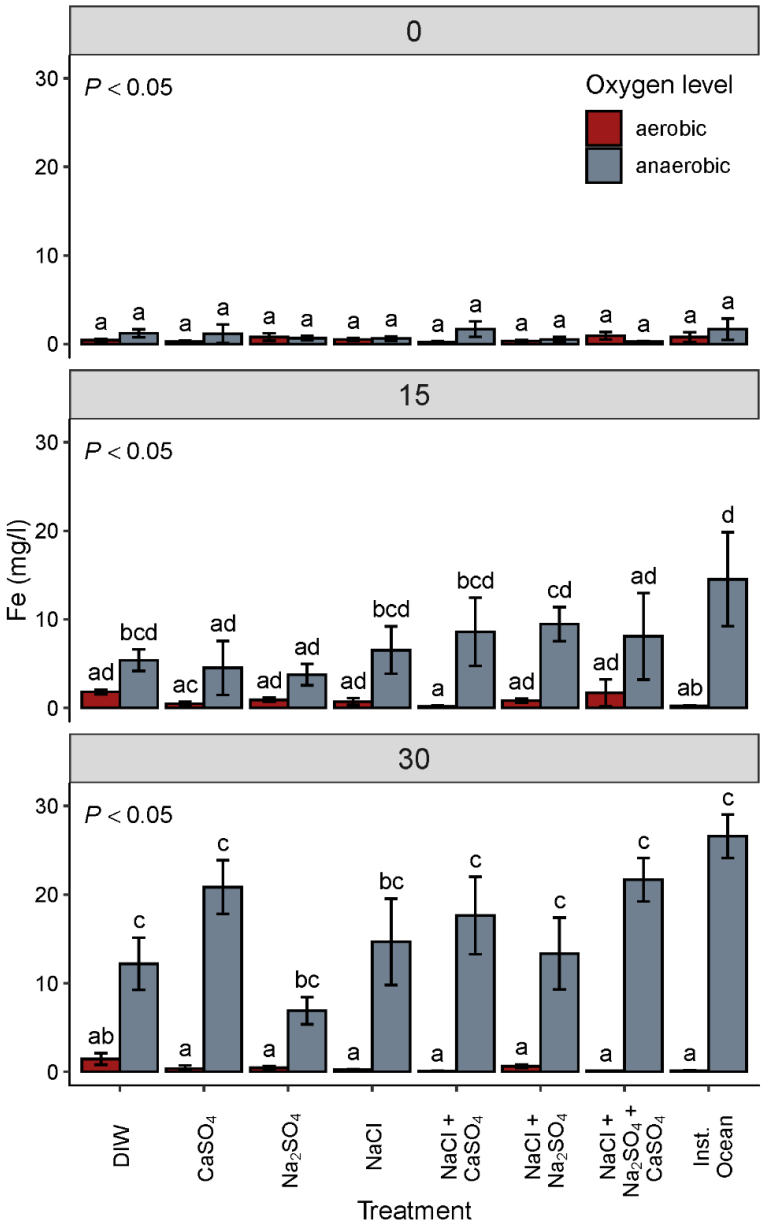

Figure 2-7

A: Poorly crystalline iron (Fe) concentrations in microcosm soil in mg Fe/g dry soil at days 0, 15, and 30 of the experiment under aerobic and anaerobic conditions (oxygen level). Error bars represent standard error of the mean. B: Total iron (Fe) concentrations in microcosm soil in mg Fe/g dry soil at days 0, 15, and 30 of the experiment under aerobic and anaerobic conditions. Error bars represent standard error of the mean.

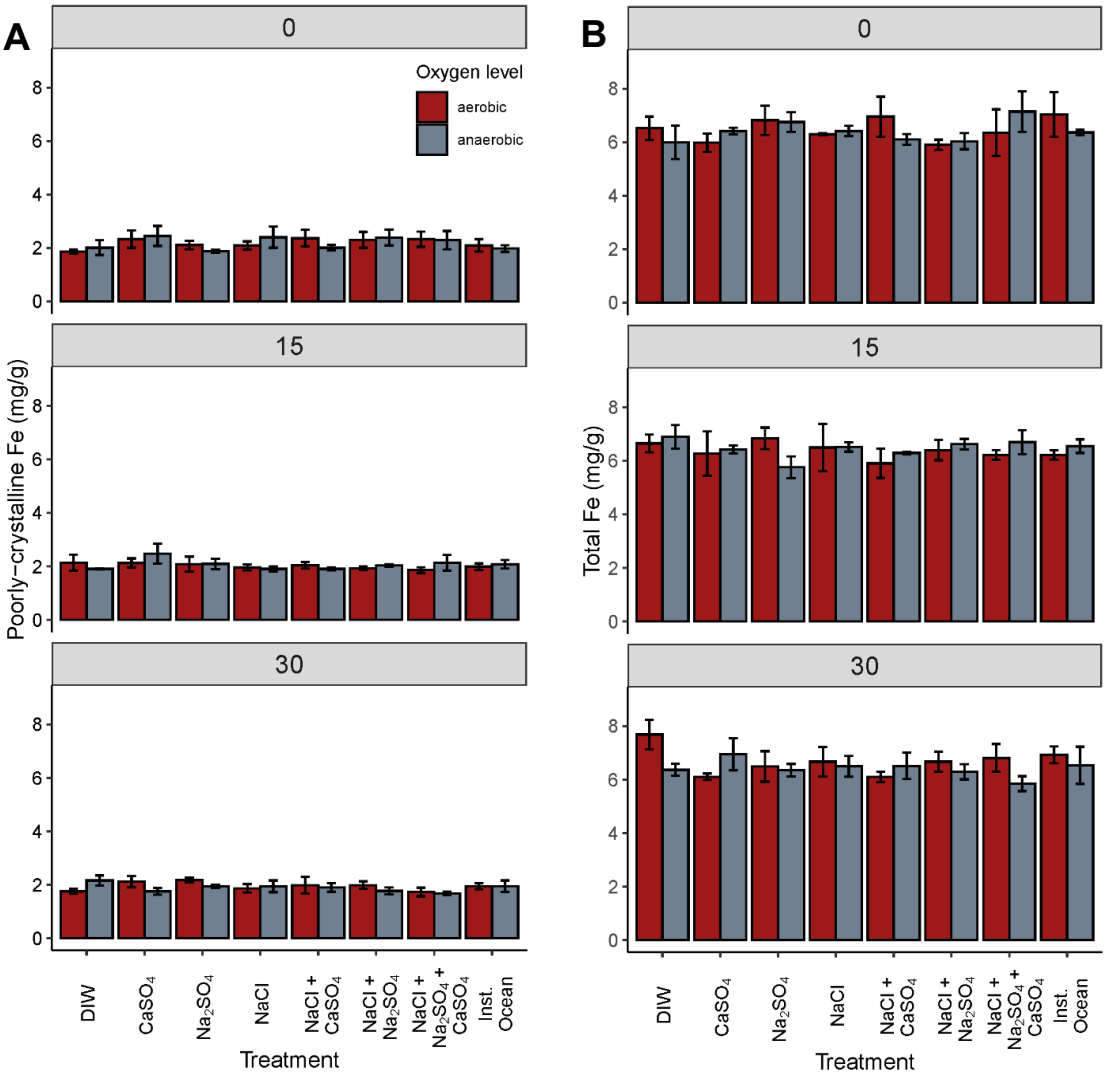

Works cited

Ardón M, Morse JL, Colman BP, Bernhardt ES (2013) Drought-induced saltwater incursion leads to increased wetland nitrogen export. Glob Chang Biol 19:2976–2985. https://doi.org/10.1111/gcb.12287

Bates D, Maechler M, Bolker B, et al (2018) lme4 Linear Mixed-Effects Models using "Eigen" and S4. https://cran.r-project.org/web/packages/lme4/lme4.pdf

Bhattachan A, Emanuel RE, Ardon M, et al (2018) Evaluating the effects of land-use change and future climate change on vulnerability of coastal landscapes to saltwater intrusion. Elem Sci Anth 6:62. https://doi.org/10.1525/elementa.316

Box GEP, Cox DR (1964) An analysis of transformations. J R Stat Soc Ser B 26:190–197

Brady NC, Weil RR (2016) The Nature and Properties of Soils, 15th edn. Pearson, Columbus

Burgin AJ, Hamilton SK (2007) Have we overemphasized the role of denitrification in aquatic ecosystems? A review of nitrate removal pathways. Front Ecol Environ 5:89–96. https://doi.org/10.1890/1540-9295(2007)5[89:HWOTRO]2.0.CO;2

Chambers RM, Odum WE (1990) Porewater oxidation, dissolved phosphate and the iron curtain - Iron-phosphorus relations in tidal freshwater marshes. Biogeochemistry 10:37–52. https://doi.org/10.1007/BF00000891

Darke AK, Walbridge MR (1994) Estimating non-crystalline and crystalline aluminum and iron by selective dissolution in a riparian forest soil. Commun Soil Sci Plant Anal 25:2089–2101

Fowler DN, King SL, Weindorf DC (2014) Evaluating Abiotic Influences on Soil Salinity of Inland Managed Wetlands and Agricultural Croplands in a Semi-Arid Environment. Wetlands 34:1229–1239. https://doi.org/10.1007/s13157-014-0585-3

Giblin AE, Tobias CR, Song B, et al (2013) The importance of dissimilatory nitrate reduction to ammonium (DNRA) in the nitrogen cycle of coastal ecosystems. Oceanography 26:124–131. https://doi.org/10.5670/oceanog.2013.54

Google Earth (2019) Google Earth imagery. http://www.earth.google.com. Accessed 4 Dec 2018

Goyne KW, Jun H-J, Anderson SH, Motavalli PP (2008) Phosphorus and nitrogen sorption to soils in the presence of poultry litter-derived dissolved organic matter. J Environ Qual 37:154–63. https://doi.org/10.2134/jeq2007.0141

Grubb KL, McGrath JM, Penn CJ, Bryant RB (2012) Effect of land application of phosphorus-saturated gypsum on soil phosphorus in a laboratory incubation. Appl Environ Soil Sci 2012:9–12. https://doi.org/10.1155/2012/506951

Grubb KL, McGrath JM, Penn CJ, Bryant RB (2011) Land application of spent gypsum from ditch filters: phosphorus source or sink? Agric Sci 02:364–374. https://doi.org/10.4236/as.2011.23048

Hartzell JL, Jordan TE (2012) Shifts in the relative availability of phosphorus and nitrogen along estuarine salinity gradients. Biogeochemistry 107:489–500. https://doi.org/10.1007/s10533-010-9548-9

Hartzell JL, Jordan TE, Cornwell JC (2017) Phosphorus Sequestration in Sediments Along the Salinity Gradients of Chesapeake Bay Subestuaries. Estuaries and

Coasts 40:1607–1625. https://doi.org/10.1007/s12237-017-0233-2

Helton AM, Bernhardt ES, Fedders A (2014) Biogeochemical regime shifts in coastal landscapes: The contrasting effects of saltwater incursion and agricultural pollution on greenhouse gas emissions from a freshwater wetland. Biogeochemistry 120:133–147. https://doi.org/10.1007/s10533-014-9986-x

Hothorn T, Bretz F, Westfall P, et al (2017) Simultaneous Inference in General Parametric Models. https://cran.r-project.org/web/packages/multcomp/

IPCC (2013) IPCC, 2013: Summary for Policymakers

Jessen S, Postma D, Thorling L, et al (2017) Decadal variations in groundwater quality: A legacy from nitrate leaching and denitrification by pyrite in a sandy aquifer. Water Resour Res 53:184–198. https://doi.org/10.1002/2016WR018995

Jordan TE, Cornwell JC, Boynton WR, et al (2008) Changes in phosphorus biogeochemistry along an estuarine salinity gradient: The iron conveyer belt. Limnol Oceanogr 53:172–184

Koop-jakobsen K, Giblin AE (2010) The effect of increased nitrate loading on nitrate reduction via denitrification and DNRA in salt marsh sediments. Limnol Oceanogr 55:789–802

Maryland Department of Natural Resources, NOAA [National Oceanic and Atmospheric Administration] (2008) Somerset County, Maryland: Rising Sea Level Guidance. https://dnr.maryland.gov/ccs/Publication/SeaLevel_Somerset.pdf. Accessed 1 May 2019

McDowell RW, Sharpley AN (2001) Soil phosphorus fractions in solution: Influence

of fertiliser and manure, filtration and method of determination. Chemosphere 45:737–748. https://doi.org/10.1016/S0045-6535(01)00117-5

Megonigal JP, Neubauer SC (2009) Biogeochemistry of Tidal Freshwater Wetlands. Coast Wetl An Integr Ecosyst Approach 535–562. https://doi.org/10.1016/B978-0-444-53103-2.00019-3

Moomaw WR, Chmura GL, Davies GT, et al (2018) Wetlands In a Changing Climate: Science, Policy and Management. Wetlands 38:183–205. https://doi.org/10.1007/s13157-018-1023-8

Moore PA, Miller DM (1994) Decreasing Phosphorus Solubility in Poultry Litter with Aluminum, Calcium, and Iron Amendments. J Environ Qual 23:325. https://doi.org/10.2134/jeq1994.00472425002300020016x

Nair VD, Clark MW, Reddy KR (2015) Evaluation of Legacy Phosphorus Storage and Release from Wetland Soils. J Environ Qual 44:1956. https://doi.org/10.2134/jeq2015.03.0154

Nair VD, Reddy KR, DeLaune RD, et al (2013) Phosphorus Sorption and Desorption in Wetland Soils. In: Methods in Biogeochemistry of Wetlands. Madison, WI, pp 667–681

National Oceanic and Atmospheric Administration - National Centers for Environmental Information [NOAA-NCEI] (2018) Climate Data Online. In: Natl. Ocean. Atmos. Adm. - Natl. Centers Environ. Inf. https://www.ncdc.noaa.gov/cdo-web/. Accessed 20 Nov 2018

Neubauer SC, Franklin RB, Berrier DJ (2013) Saltwater intrusion into tidal freshwater marshes alters the biogeochemical processing of organic carbon.

Biogeosciences 10:8171–8183. https://doi.org/10.5194/bg-10-8171-2013

R Studio Team (2019) RStudio: Integrated Development for R

Reddy KR, DeLaune RD (2008) Biogeochemistry of Wetlands, 1st edn. CRC Press, Boca Raton, Florida

Roman CT, Burdick DM (2012) Tidal Marsh Restoration. Island Press/Center for Resource Economics, Washington, DC

Schoepfer VA, Bernhardt ES, Burgin AJ (2014) Iron clad wetlands: Soil iron-sulfur buffering determines coastal wetland response to salt water incursion. J Geophys Res Biogeosciences Res 119:2209–2219. https://doi.org/10.1002/2014JG002739

Sharpley AN, Daniel T, Sims T, et al (2003) Agricultural Phosphorus and Eutrophication Second Edition. United States Dep Agric - Agric Res Serv ARS-149:1–43

Soil Survey Staff (2018) Web Soil Survey. In: USDA-NRCS Web Soil Surv. Website. https://websoilsurvey.sc.egov.usda.gov/. Accessed 4 Dec 2018

Steinmuller HE, Chambers LG (2018) Can Saltwater Intrusion Accelerate Nutrient Export from Freshwater Wetland Soils? An Experimental Approach. Soil Sci Soc Am J 82:283. https://doi.org/10.2136/sssaj2017.05.0162

Tobias CR, Macko SA, Anderson IC, et al (2001) Tracking the fate of a high concentration groundwater nitrate plume through a fringing marsh: A combined groundwater tracer and in situ isotope enrichment study. Limnol Oceanogr 46:1977–1989. https://doi.org/10.4319/lo.2001.46.8.1977

Tully KL, Gedan K, Epanchin-Niell R, et al (2019a) The Invisible Flood: The Chemistry, Ecology, and Social Implications of Coastal Saltwater Intrusion.

Bioscience 69:368–378. https://doi.org/10.1093/biosci/biz027

Tully KL, Weissman D, Wyner WJ, et al (2019b) Soils in transition: saltwater intrusion alters soil chemistry in agricultural fields. Biogeochemistry 142:339–356. https://doi.org/10.1007/s10533-019-00538-9

Viollier E, Inglett P., Hunter K, et al (2000) The ferrozine method revisited: Fe(II)/Fe(III) determination in natural waters. Appl Geochemistry 15:785–790. https://doi.org/10.1016/S0883-2927(99)00097-9

Waldrip HM, Pagliari PH, He Z, et al (2015) Legacy Phosphorus in Calcareous Soils: Effects of Long-Term Poultry Litter Application. Soil Sci Soc Am J 79:1601. https://doi.org/10.2136/sssaj2015.03.0090

Weissman DS, Tully KL (2020) Saltwater intrusion affects nutrient concentrations in soil porewater and surface waters of coastal habitats. Ecosphere 11:. https://doi.org/10.1002/ecs2.3041

Weston NB, Dixon RE, Joye SB (2006) Ramifications of increased salinity in tidal freshwater sediments: Geochemistry and microbial pathways of organic matter mineralization. J Geophys Res Biogeosciences 111:1–14. https://doi.org/10.1029/2005JG000071

White E, Kaplan D (2017) Restore or retreat? Saltwater intrusion and water management in coastal wetlands. Ecosyst Heal Sustain 3:e01258. https://doi.org/10.1002/ehs2.1258

Williams AA, Lauer NT, Hackney CT (2014) Soil phosphorus dynamics and saltwater intrusion in a florida estuary. Wetlands 34:535–544. https://doi.org/10.1007/s13157-014-0520-7

Zak D, Rossoll T, Exner H-J, et al (2009) Mitigation of sulfate pollution by rewetting of fens — A conflict with restoring their phosphorus sink function? Wetlands 29:1093–1103. https://doi.org/10.1672/09-102D.1

Chapter 3: Assessing the relationship between salinity and nutrient concentrations in tidal tributaries within the Chesapeake Bay watershed

Abstract

Nutrient pollution is a global problem and can lead to eutrophication and associated deleterious effects on water bodies. Trends in nutrient concentrations in waterways can be difficult to predict due to complex interactions between numerous environmental and anthropogenic drivers. Though streamflow is one of the dominant sources of nutrient inputs to water bodies, it is not always well-quantified in coastal waterways due to the mixing of freshwater and seawater. However, salinity may serve as a useful tracer of streamflow in predicting nutrient concentrations in tidal tributaries. Here we evaluate the strength of the relationship between salinity and nitrogen (N) and phosphorus (P) concentrations in the form of nitrite + nitrate-N ($NO_{2,3}$-N), ammonium-N (NH_4-N), soluble reactive P (SRP), and dissolved organic P (DOP), in ten tidal tributaries in the Delmarva Peninsula, Chesapeake Bay (CB), United States. To determine whether there was a clear pattern between salinity and nutrient concentrations, we compared detrended, long-term (1985-2018) salinity and nutrient data from the CB Program Water Quality Database at three tidal fresh (0-0.5 parts per thousand: ppt); three oligohaline (0.5-5 ppt), and four mesohaline (5-18 ppt) monitoring stations within tidal tributaries. We utilized a novel tool, the Coastal Salinity Index (CSI), to account for lag times between salinity changes and nutrient

concentrations at 1-, 2-, 3-, and 6-month intervals at each station. Contrary to what we expected, we did not observe long-term salinity increases at any of the stations, but instead we observed significant long-term decreases at two stations ($P < 0.0001$, in both cases), potentially due to increasing precipitation in the CB watershed. On monthly scales, we found that salinity was most strongly correlated with $NO_{2,3}$-N concentrations at all stations ($\rho = -0.524$, $P < 0.0001$) and that on annual scales, $NO_{2,3}$-N concentrations tended to be most strongly correlated with the 2-month CSI ($\rho = -0.728$, $P < 0.0001$). At some stations, SRP, NH_4-N, and DOP correlated strongly with salinity or the CSI, but not as consistently as $NO_{2,3}$-N. Our results suggest a potential for incorporating salinity into watershed models to improve predictions of nutrient concentrations in tidal tributaries, particularly when streamflow data are limited.

Introduction

Coastal watersheds support more than half of the global population and are some of the most economically and ecologically productive ecosystems in the world (Paerl et al. 2014). However, many of these areas have exhibited increasingly diminished water quality since the mid-twentieth century as a result of excess nutrient inputs from urban, agricultural, and industrial sources (Diaz and Rosenberg 2008). Human activities have spurred widespread eutrophication, leading to cascading deleterious effects on watersheds such as harmful algal blooms, fish kills, and loss of animal habitat (Deegan et al. 2012; Paerl et al. 2014). Therefore, it is important to understand and quantify the combined impacts that anthropogenically-driven activities are having on water quality in coastal areas.

Coastal estuaries are unique ecosystems because they encompass a gradient from freshwater to saltwater conditions (Bianchi 2007). We conducted our study in the Chesapeake Bay (CB), one of the largest estuaries in the world (Klemick et al. 2018). Streamflow is the dominant control on salinity in estuaries and the tidal tributaries that drain into them (Ross et al. 2015). Additionally, streamflow is an important variable in estimating loads of nutrients such as nitrogen (N) and phosphorus (P) in waterways as nutrient inputs increase during period of high flow and decrease during periods of low flow (Tango and Batiuk 2016). While there are continuous long-term (last 30+ years) streamflow data along some of the major tributaries that drain into in the CB, most streamflow monitoring stations are far upstream from the tributary mouth and fail to incorporate downstream flow additions. Further, many smaller tributaries, particularly those located along more saline gradients, do not have consistent publicly-available streamflow records. This is partially due to the difficulty in measuring streamflow in tidally-influenced areas, where flow is bi-directional and complicated by tidal regimes and the mixing of fresh and saline water (Austin 2002). Thus, towards the mouths of tidal tributaries, salinity levels may reflect the relationship between freshwater flow and nutrient inputs better than estimates of streamflow.

This study is the first to explore relationships between salinity changes and water quality (N and P concentrations) in tidal tributaries in the CB watershed. Recent studies that quantify trends in salinity focus on the CB mainstem, but there are few that explore the dynamics of salinity changes in smaller tributaries (Hilton et al. 2008). Though the Susquehanna River provides approximately half of the freshwater

inputs to the CB, inputs from smaller tributaries provide the remaining half, and are important sources of nutrients and sediments (Kemp et al. 2005; Jordan et al. 2018). These tributaries are ecologically and economically valuable. For example, they provide spawning and breeding habitat for fish and birds, buffer inland areas from storm surges with salt marsh vegetation, and serve as major recreational areas for boating and fishing (Boesch et al. 2001; Baldwin et al. 2009; Arkema et al. 2013). Thus, localized water quality issues are important to consider in smaller tidal tributaries as well as in the CB mainstem.

The dynamics of nutrient loading in waterways are complex with many drivers that can influence observed nutrient concentrations. Wastewater treatment plants are the main point source contribution of N and P to the CB watershed (Williams et al. 2010) but have been diminishing sources of nutrients due to plant upgrades in recent years (Eshleman and Sabo 2016). In 2018, these plants contributed 14% of N and 16% of P loading to the CB (Chesapeake Bay Program 2018). Nitrogen deposition is an important source of N to the CB watershed. However, the overall rate of N deposition is declining due to stricter emissions standards (Musolff et al. 2017b; Campbell et al. 2019) though NH_4-N deposition is increasing due to intensification of poultry and livestock operations (Loughner et al. 2016). In 1985, all sources of N deposition accounted for 86 million pounds of N loading to the CB but in 2018, they only accounted for 64 million pounds, which was about 24% of the total N loading to the CB for that year (Chesapeake Bay Program 2018). Urbanization and development have contributed to increased N and P delivery to watersheds (Van Meter et al. 2017). However, N and P inputs to the CB from agriculture have decreased since 1985. In

2018, agricultural activities contributed to 45% of N and 28% of P inputs to the CB, while developed land contributed another 18% of N and 18% of P inputs (Chesapeake Bay Program 2018). The overall strength of these different drivers varies spatially and can cause trends in N and P concentrations to vary by sub-watershed.

Because of their varying physical and chemical properties, organic and inorganic forms of N and P travel through landscapes to water bodies at different rates (Goyne et al. 2008). Soils in the study region have a net negative charge, hence they do not retain nitrate (NO_3^-) well. As a result, NO_3^- tends to leach quickly through the soil profile during precipitation or snowmelt events and into deeper soil layers, groundwater, streams, and rivers (Di and Cameron 2002). By contrast, soils tend to retain ammonium (NH_4^+) ions, because of their positive charge (Ardón et al. 2013). While dissolved inorganic P (DIP) in the form of phosphate (PO_4^{3-}) ions can be lost from soils quickly through surface runoff, it also tends to sorb to iron and build up in soils over time (Sharpley et al. 2014). Because it tends to bind to complexes, inorganic P is generally more recalcitrant in soils than organic P. Therefore, dissolved organic P (DOP) may reach surface waters faster than DIP (Turner and Haygarth 2000). In this study, we consider DIP in the form of SRP, which may include a small amount of organic P, and does not include an inorganic form of P known as hydrolyzable P. This discernment is based on sample collection and processing methods used in the datasets we analyzed (Chesapeake Bay Program 2019).

It is also important to understand the relationship between nutrient concentrations and salinity on different time scales. Nutrients may move more slowly through subsurface soil pathways rather than through overland flow (Turner and

Haygarth 2000; Ocampo et al. 2006) and saturated conditions in soils depend not only on current drought conditions, but conditions from previous months (Vicente-Serrano et al. 2010). To better understand these lag effects, we examined a newly developed tool, the Coastal Salinity Index (CSI), which incorporates lag effects in evaluating drought conditions in coastal areas, where salinity can be used as a drought indicator, in lieu of precipitation. The CSI is modeled after the Standardized Precipitation Evapotranspiration Index (SPEI), where index values are normalized to reflect a departure from the mean over the time period of observation. Using salinity measurements to compute coastal drought conditions in tidal tributaries is advantageous to other approaches because 1) salinity data are inexpensive to collect, 2) salinity is directly related to drought conditions along coastlines, and 3) salinity measurements integrate variables such as precipitation, tidal forcing, overland flow, and subsurface flow pathways (Conrads and Darby 2017).

Despite the many sources of N and P to the CB watershed, additive models that include a few major drivers can often capture a large amount of variability with good accuracy and provide considerable predictive capacity under different regulatory and climate change scenarios (Harding et al. 2016). The purpose of our study was to determine how well salinity could capture the cumulative effects of environmental drivers on nutrient concentrations in smaller tidal tributaries of agriculturally-dominated sub-watersheds that drain into the CB on both monthly and annual timescales. Though we were mainly interested in inorganic forms of N and P, we also included DOP in our analysis because of the legacy of P-rich fertilizer overapplication on farmland in the Delmarva Peninsula within the CB watershed

(Sharpley et al. 2014). The main objectives of this study were to 1) determine long-term trends in salinity and nutrient concentrations in the form of nitrate + nitrite-N ($NO_{2,3}$-N), ammonium-N (NH_4-N), soluble reactive P (SRP), and dissolved organic P (DOP) at monitoring stations along the Delmarva Peninsula in the CB and to 2) determine how well nutrient concentrations correlate with salinity and 1-, 2-, and 3-month interval CSI values on monthly and annual timescales (with an additional comparison with the 6-month CSI on annual timescales).

We expected to observe a significant increase in salinity at all monitoring stations based on prior studies that show that sea level rise is driving saltwater intrusion into many CB tributaries (Neubauer et al. 2013; Ross et al. 2015). Due to stricter regulations enacted since the 1980s, particularly for point sources, N and P loading has decreased in the CB overall (Boesch et al. 2001; Zhang et al. 2018; Fanelli et al. 2019). Nitrogen deposition has also been steadily decreasing since the 1990s due to reduced NO_x emissions (Eshleman and Sabo 2016). However, urban and rural land use has intensified in many watersheds (Van Meter et al. 2017). Therefore, we expected monitoring stations within tributary watersheds undergoing the greatest land use intensification to show increasing trends in N and P concentrations and others to show no change or decreasing trends. On monthly scales, we hypothesized that nutrient concentrations would correlate more highly with salinity than the 1-, 2-, or 3- month CSI, due to flow conditions being the dominant control on nutrient delivery to the tributary mouth. Specifically, we expected salinity to correlate more strongly with $NO_{2,3}$-N concentrations compared to other nutrient concentrations due to the tendency for $NO_{2,3}$-N to move quickly through hydrologic flow pathways. On

annual scales, we expected nutrient concentrations to correlate most closely with the 3-month CSI as it incorporates previous month's seasonal drought conditions which can account for lag effects due to nutrient movement through saturated soil subsurface pathways, particularly for $NO_{2,3}$-N and DOP.

Methods

This study represents first steps in understanding the strength of the association between salinity and nutrient concentrations in different tidal tributaries over decades using novel metrics of salinity. We analyzed data from 1) three tidal fresh (0-0.5 parts per thousand; ppt); 2) three oligohaline (0.5-5 ppt), and 3) four mesohaline (5-18 ppt) monitoring stations in order to compare the strengths of these relationships across different salinity regimes along the Delmarva Peninsula in the CB. We selected the CB as our study site for several reasons: 1) it is one of the largest and economically valuable estuaries in the world (Abler et al. 2002); 2) it has a wealth of long-term publicly-available data available on water quality parameters and salinity (Tango and Batiuk 2016), and; 3) it has been heavily targeted for water quality improvements (Klemick et al. 2018). More specifically, we focused on tidal tributaries along the Delmarva Peninsula that drain into the CB to capture potential differences in water quality patterns among tidal fresh, oligohaline, and mesohaline salinity regimes.

Data sources and monitoring station selection

Long-term water quality data were derived from the Chesapeake Bay Program (CBP) Water Quality Database (http://data.chesapeakebay.net/WaterQuality). The

CBP is a collaboration among the U.S. Environmental Protection Agency (EPA), the Chesapeake Bay Commission, the District of Columbia, and the states of Maryland, Pennsylvania, and Virginia, and provides monthly water quality measurements from July 1984-present (Chesapeake Bay Program 2019). The data follow rigorous sampling and analytical quality assurance protocols approved by the EPA (CBP DIWG and Nontidal WG 2017). The locations of monitoring stations are shown on the map in Figure 3-1 and station metadata is detailed in Table 3-1. We used salinity, $NO_{2,3}$-N, NH_4-N, SRP, and DOP data from surface water (50 cm depth) measurements. A small percentage of months (~ 2%) contained missing data, and we linearly interpolated the missing values. Less than 5% of values for $NO_{2,3}$-N, NH_4-N, and SRP were under the detection limit for their corresponding method. In these cases, we replaced the values with values that were half of the detection limit (0.02 mg N/l, 0.003 mg N/l, and 0.004 mg SRP/l; respectively). Ten tidal monitoring stations with a continuous period of record from 1987 or earlier to present were selected for analysis and labeled s1-s10 from highest to lowest latitude (Figure 3-2). All stations are part of the tributary monitoring project except for s2, which is located in the mainstem of the CB and was the only station with a pycnocline.

Throughout the CB, streamflow data are available at U.S. Geological Survey (USGS) gauges. In order to compare correlation coefficients between salinity and nutrient concentrations versus streamflow and nutrient concentrations, we analyzed streamflow data from the USGS National Water Information System database (https://nwis.waterdata.usgs.gov/nwis; USGS 2019). Of the ten CBP stations we analyzed, only two (s3 and s9) had consistent, long-term streamflow data at nearby

USGS gauges. In both cases, the gauges did not geographically coincide with CBP monitoring stations, rather they were upstream of the CBP stations, along the same major tributary. For s3, the period of record was August 1996 to August 2018 with a gap in the dataset from October 2002 to June 2011. For s9, the period of record was January 1986 to August 2018 with no gaps in the dataset.

To determine change in land cover in the sub-watershed surrounding each tributary where a monitoring station is located, we used the USGS Chesapeake Bay Watershed Land Cover Data Series (Irani 2015), which consists of raster datasets for the years 1984, 1992, 2001, 2006 and 2011. We quantified the percentage of land in each land use category and the change in land cover from 1984 to 2011 in each sub-watershed by overlaying hydrologic unit code (HUC)-8 boundaries from the Maryland Department of Natural Resources (MD-DNR 1998) and extracting land use data from within each boundary. Sub-watersheds correspond to the unique HUC-8 codes for each tributary, which represent medium-sized river basins, along which the CBP monitoring stations selected for this study are located.

To determine whether there was a close relationship between salinity and precipitation at each station, we compared CSI values to corresponding monthly SPEI values. We drew SPEI data from the SPEI Global database (Beguería et al. 2020), which has 0.5 degree spatial resolution. Correlations between the CSI and SPEI, though significant, were weak. Thus, we did not further include the SPEI in our analyses.

Generation of CSI values

We computed monthly CSI values for each station using the R-package *CSI* (McCloskey 2019). The CSI uses salinity as an indicator of coastal drought, where times of higher salinity represent drought and times of lower salinity represent greater freshwater conditions at a station. Index values are computed by first fitting monthly salinity values to a gamma distribution function and then normalizing them through a probability density function. Index values represent standard deviations from median values. More detail on how CSI values are calculated is provided in Conrads and Darby (2017). Plots of 1- and 2-month CSI at each station are included in the Supplemental Figures for this chapter (Figures S 3-1 - S 3-20).

Statistical analyses

We completed all statistical analyses and maps in R Studio (R Studio Team 2019). To determine the slope and significance of monthly trends, we computed the Sen slope and ran modified Mann-Kendall tests for each variable (salinity, $NO_{2,3}$-N, NH_4-N, SRP, and DOP) at each station using the "mmkh" function in the R-package *modifiedmk* (Patakamuri and O'Brien 2019). The modified test accounts for serial correlation in trend analyses, since time series data are frequently influenced by previous observations (Hamed and Rao 1998). To determine patterns on annual timescales, we used the average value for each variable weighted by the numbers of days in each month for each year. For both monthly and annually-averaged data, we first detrended the time series if a significant trend was present to avoid spurious correlations. We then conducted Spearman correlation tests for each variable against salinity and the 1-, 2-, and 3-month (and 6-month for annually-averaged data) CSI

values with the function "cor.test" in the package *Hmisc* (Harrel Jr. 2018). We chose the Spearman test for its strength in incorporating monotonic relationships rather than simple linear relationships as in the case of the Pearson test (Hauke and Kossowski 2011).

To determine how the strength of correlations changed during periods of high salinity, we also conducted Spearman correlation tests for the top 15% highest salinity values recorded at each station for monthly data only. We refer to these periods of high salinity as "saltwater intrusion" herein. Since the strongest correlations were between annually averaged 1 and 2-month CSI values and annually-averaged $NO_{2,3}$-N concentrations, we plotted spline graphs to visualize these relationships. We fitted smoothed splines through the data points using the "geom_spline" function in the package *ggformula* (Kaplan and Pruim 2020) to represent the monotonic relationships reflected by the Spearman correlation tests.

Results

Change in land cover within each sub-watershed from 1984 to 2011 was relatively small as most land cover only increased or decreased by 0.5% or less of total sub-watershed area. The largest change in agricultural land was in the Lower Wicomico River where it decreased by 1.1% of the total sub-watershed area (from 29.3% to 28.2%). The largest change in developed land was also in this watershed where it increased by 0.9% of the total sub-watershed area (from 7.9% to 8.8%). The largest change in a category of land cover in a sub-watershed was in forests of the Upper Pocomoke River, which decreased by 2.1% of the total sub-watershed area (48.3% to 46.1%; Table 3-2).

Most stations showed no significant changes or decreasing trends in nutrient concentrations while a few showed increasing trends over the period of record analyzed (Table 3-3). There was no significant trend in salinity at most stations, except for s7 and s8, which showed decreasing trends ($P < 0.01$; Table 3-3). Salinity at s7 decreased by 2.1 ppt while salinity at s8 decreased by 1.6 ppt. There were no changes in SRP at s2, s3, and s7, and downward trends at s1, s5, s6, s9, and s10 (0.01 mg P/l, on average; $P < 0.01$). Station 4 was the only station that showed an increase in SRP (0.01 mg P/l; $P < 0.01$; Table 3-3). At s2, s5, s7, s8, and s10 there was a decrease in NH_4-N (-0.03 mg NH_4-N/l, $P < 0.01$), while the rest of the stations had no significant change. At s4 and s6 there was an increase in $NO_{2,3}$-N (0.76 mg N/l; $P < 0.01$), while there was a decrease at s9 and s10 (-0.22 mg N/l; $P < 0.01$), and the other stations showed no changes. Dissolved organic P increased at s3 (0.02 mg DOP/l; $P < 0.01$), decreased at s5 (0.01 mg DOP/l; $P < 0.01$), and did not change at other stations (Table 3-3).

In most cases, monthly measurements of nutrient concentrations were most strongly correlated with salinity, as opposed to the 1-, 2-, or 3-month CSI (Table 3-4). A negative correlation indicates that the nutrient concentration decreased with increasing salinity, while a positive correlation indicates that the nutrient concentration increased with increasing salinity. Station 2 was the only station where SRP concentrations increased with salinity ($\rho = 0.24$; $P < 0.01$). At stations, s1, s2, s3, s4, s6, s7, s8, and s10, SRP concentrations declined as salinity increased ($\rho = -0.34$, on average; $P < 0.01$). At stations s3, s4, s5, s6, s7, s8, and s10, NH_4-N concentrations declined as salinity increased ($\rho = -0.28$, on average; $P < 0.01$). Except

for at s1, $NO_{2,3}$-N concentrations declined as salinity increased at all stations (ρ = -0.58, on average; $P < 0.01$). As compared to other nutrients, $NO_{2,3}$-N concentrations were most strongly correlated with salinity at all stations except s1. Stations s2 and s9 were the only stations where DOP concentrations increased as salinity increased (ρ = 0.18, 0.20, respectively; $P < 0.01$). At stations s1, s3, s4, and s10, DOP concentrations decreased as salinity increased (ρ = -0.27, on average; $P < 0.01$; Table 3-4).

There was streamflow data from USGS gauges near only two of the ten total water quality monitoring stations analyzed in this study. There were no significant correlations between monthly salinity or nutrient concentrations at s3 and streamflow at the closest USGS station. The period of record for this station was 12 years total, with gaps in the record. There was a decrease in salinity with increased streamflow and an increase in $NO_{2,3}$-N concentrations with increased streamflow at s9 and the closest USGS station (ρ = -0.60 and ρ = 0.40, respectively; $P < 0.01$). The period of record for this station was 32.5 years total, with no gaps in the record (Table 3-5).

For most of the nutrients analyzed, relationships between concentrations and salinity weakened during periods of extreme saltwater intrusion. We classified these periods as the top 15% of months with the highest salinity measurements. To account for the reduced sample size of these datasets, we shifted our significance threshold from $P < 0.01$ to $P < 0.05$ to better detect significant correlations. Only s10 showed a decline in SRP concentrations with increased salinity (ρ = -0.54), while at s4, SRP concentrations switched from decreasing with increased salinity to increasing with increased salinity (ρ = 0.57; $P < 0.05$). At s2, SRP concentrations remained increasing

with increasing salinity ($\rho = 0.29$; $P < 0.05$). Station 2 was the only station to show a significant correlation between NH_4-N and salinity for the threshold values ($\rho = -0.28$; $P < 0.05$). Only half of stations retained increasing $NO_{2,3}$-N concentrations with increasing salinity but these correlations were weaker compared to the full dataset ($\rho = -0.35$, on average; $P < 0.05$). In contrast to the other nutrients, DOP behaved differently at threshold values. At s10, DOP switched from increasing with increasing salinity to decreasing with increasing salinity ($\rho = -0.36$), while at s8 switched from decreasing with increasing salinity to increasing with increasing salinity ($\rho = 0.34$), and s6 remained increasing with increasing salinity ($\rho = 0.28$; in all cases $P < 0.05$; Tables 3-4 and 3-6).

On annual versus monthly timescales, our comparison between nutrients and salinity or the 1-, 2-, 3-, and 6-month CSI generally yielded stronger correlations for $NO_{2,3}$ but weaker correlations for the other nutrients analyzed. For annually-averaged data, the strongest correlations were between $NO_{2,3}$-N and the 2-month CSI ($\rho = 0.73$, on average; $P < 0.01$). The strongest correlation was between $NO_{2,3}$-N and the 2-month CSI at s6 (Table 3-7). For each station, visual representations of relationships between the 1-month CSI and $NO_{2,3}$-N concentrations are plotted in Figure 3-2A and relationships between the 2-month CSI and $NO_{2,3}$-N are plotted in Figure 3-2B. at all stations, $NO_{2,3}$-N concentrations increased monotonically with the 1- or 2-month CSI (Figure 3-2A and 3-2B).

Discussion

Overall, several clear patterns emerged, particularly regarding $NO_{2,3}$-N. On monthly scales, salinity was strongly correlated with $NO_{2,3}$-N concentrations (Table

3-4), and on annual scales, the 1- and 2-month CSI was strongly correlated with $NO_{2,3}$-N concentrations (Table 3-7), which suggests that salinity may be used as an tracer of streamflow to explain a large amount of the variability in these concentrations. Even though correlations between salinity and concentrations of SRP, NH_4-N, and DOP were generally not as strong, they were still significant in many cases (Tables 3-4 and 3-6) and should be further explored for their ability to explain variability in nutrient concentrations in corresponding tributaries.

Though we expected to see measurable increases in salinity at most stations due to sea level rise, we observed downward trends at two stations and no significant changes at the others (Table 3-3), possibly due to changing precipitation patterns. There has been an observed 8% increase in precipitation in the CB watershed over the past 100 years. This increase has been largely attributed to climate change, and has resulted in greater freshwater flow in many tributaries (Najjar et al. 2009). Therefore, increases in precipitation may mute the effects of increasing salinity delivered to tributaries as a result of sea level rise. Surprisingly, few studies have assessed long-term changes in salinity in the CB watershed, and of those that do, almost all of them focus on the mainstem, not tidal tributaries. For example, one study found that on average, salinity in the CB mainstem increased by 0.5 ppt from 1949 to 2006. However, changes ranged from -2.0 to 2.2 ppt in different portions of the mainstem (Hilton et al. 2008). We are only aware of one study that assesses salinity trends in CB tributaries. This study predicted that with 50 cm of sea-level rise, salinity in the James River would increase by 2 ppt and salinity at the mouth of the Chickahominy River would increase by over 4 ppt (Rice et al. 2012). Similar modelling approaches

should be conducted to predict how the competing drivers of sea-level rise and increased precipitation will affect future salinity trends in other tidal tributaries of the CB watershed.

Despite a long-term decrease in N deposition in the CB watershed (Van Meter et al. 2017), most stations exhibited no change in $NO_{2,3}$-N concentrations, and s4 and s6 exhibited increasing trends (Table 3-3) potentially due to other drivers such as increased precipitation, intensified land use, and groundwater sources. The fact that we observed little change in land cover categories in each sub-watershed (Table 3-2) suggests that the intensity of practices is a larger driver of nutrient trends than land use change itself. Additionally, studies have shown that water quality in the CB may take years to decades to improve due to lag times between on-the-ground nutrient application and residence time of nutrients in groundwater, particularly for NO_3-N (Sanford and Pope 2013; Jessen et al. 2017). Groundwater aquifers in the Delmarva Peninsula are deep and porous, thus water may take on the order of years to decades to leave the groundwater to travel to surface water bodies such as streams and rivers (Sanford and Pope 2013).

Monthly nutrient concentrations were most highly correlated with salinity rather than the CSI in most cases (Table 3-4), likely because changes in freshwater flow result in almost immediate changes in CB salinity (Austin 2002). Of all the nutrients, $NO_{2,3}$-N was most highly correlated with salinity (ρ = -0.524; Table 3-4), which supports the idea that it is readily mobilized during wetter conditions associated with periods of greater streamflow. At s9, the only station for which we had consistent nearby streamflow data, the correlation between streamflow and

$NO_{2,3}$-N concentrations was similar in magnitude to that of salinity and $NO_{2,3}$-N (ρ = 0.040 and ρ = -0.385, respectively; Tables 3-4 and 3-5), which suggests that salinity may be a reliable tracer of streamflow. However, we were are unable to determine if this is the case at other monitoring stations due to the lack of long-term streamflow data at nearby gauges. Though DOP is also highly mobile in soil, differences in properties of sources of organic P have been shown to affect DOP solubility (White et al. 2010). In a few cases, such as for SRP and DOP concentrations at s10, incorporating the previous month's salinity in the form of the 1-month CSI yielded a stronger correlation (Table 3-4). It is possible that subsurface flow pathways are more important to overall nutrient concentrations at these stations, resulting in a lag between salinity and nutrient concentrations. Phosphorus concentrations at s2 may have been governed less by freshwater flow and more by chemical interactions between saltwater and sediments as s2 was the only station located in the mainstem of the CB rather than in a tidal tributary. It was also the only station that showed a significant positive correlation between salinity and SRP and salinity and DOP (ρ = 0.235 and ρ = 0.180, respectively; Table 3-4), potentially due to the tendency for P release from bottom water attributed to anoxic conditions in the sediment (Caraco et al. 1990). Overall, there were no clear patterns between salinity regime and strength of correlation between salinity and nutrients. For example, in s3, a tidal fresh station, salinity and SRP were strongly correlated (ρ = -0.604) but in another tidal fresh station, s10, the strength of this relationship was much weaker (ρ = -0.195; Table 3-4), which suggests that freshwater flow may be a more dominant driver of SRP concentrations at s3 than at s10. The varying strength of correlations between salinity

and nutrient concentrations from station to station suggest that models of nutrient concentrations need to be individualized on the tributary or tributary segment level in order to understand the relative importance of different drivers.

Many of the strong and significant correlations between salinity and nutrient concentrations weakened and became non-significant or reversed in directionality when we considered only periods of extreme saltwater intrusion at each station (Table 3-6). During these periods, it is possible that not only streamflow, but other drivers played a dominant role in nutrient delivery to the tributaries. One explanation for part of the observed shifts in relationships may be attributed to biogeochemical interactions between saltwater and soils of lands bordering tributaries, that can lead to nutrient export from these soils, particularly in Coastal Plain areas with low elevation such as the Delmarva Peninsula (Steinmuller and Chambers 2018; Tully et al. 2019b; Weissman and Tully 2020). For example, studies have shown that saltwater intrusion can cause coastal agricultural soils to export large quantities of NH_4-N into adjacent water bodies due to mechanisms of cation exchange (Weston et al. 2006; Ardón et al. 2013). One study found that as salinity increased in a sub-watershed, NO_3-N concentrations decreased, but NH_4-N concentrations increased (Jordan et al. 2018). Other studies have shown that interactions between iron, sulfur, and P as a result of saltwater intrusion can cause release of P from soils and sediments (Williams et al. 2014; Hartzell et al. 2017). Therefore, the role of saltwater intrusion should be considered for inclusion in models of nutrient export from sub-watersheds in coastal areas.

It is important to consider the degree to which nutrient concentrations measured at each monitoring station are a result of contributions from their surrounding sub-watershed rather than contributions from the CB mainstem that have travelled into the tributary from other sub-watersheds. These relative contributions depend on factors such as the ratio of tributary area to sub-watershed area as well as the distance from the station to the head of the CB, where nutrient inputs from the Susquehanna River may affect concentrations in other tributaries (Jordan et al. 2018). For example, one study in the Rhode River, a CB tributary, found that DIP concentrations were mainly a result of upland nutrient inputs in the sub-watershed, but the tributary was a net importer of NO_3-N from the estuary mainstem (Jordan et al. 1991). Therefore, during periods of higher salinity and lower freshwater flow, tidal tributaries may import a significant proportion of nutrients from outside of the sub-watershed and weaken the unidirectional relationship between salinity and nutrient concentrations.

On annual timescales, incorporating lag effects strengthened relationships between salinity and nutrients (Table 3-7), likely due to pathways that delivered nutrients to water bodies less immediately than overland flow, particularly for $NO_{2,3}$-N. The soils of the Delmarva Peninsula are generally sandy, and the topsoil is usually underlain by a less permeable clay layer (B horizon; Kleinman et al. 2015). These soil characteristics are conducive to facilitating subsurface flow of $NO_{2,3}$-N vertically to groundwater and laterally through soil layers (Ocampo et al. 2006). While $NO_{2,3}$-N can take years or decades to leave groundwater sources, it can move more quickly through saturated soils and shallow aquifers into downstream surface waters on the

scale of weeks to months (Sanford and Pope 2013). In contrast to $NO_{2,3}$-N, our analysis of NH_4-N, SRP, and DOP concentrations on annual timescales generally resulted in weaker relationships between nutrients and salinity than on monthly timescales, potentially due to a more dominant role of monthly to seasonal drivers such as timing of fertilizer application and spring precipitation (Ryberg et al. 2018).

Because estuaries and their surrounding watersheds differ vastly in their physical, chemical, and biological characteristics, it is important not to over-generalize models and processes when predicting how they will behave under different climate change and land use scenarios. Furthermore, processes within estuaries are spatially heterogenous, and predictor variables that explain an outcome well in one area may fail to do so in another (Hartzell and Jordan 2012; Jordan et al. 2018). As we have illustrated in this study, the strength of the relationships between salinity and nutrient concentrations vary greatly both spatially and temporally in the CB watershed, suggesting that more focus should be given to exploring dominant drivers of water quality at the sub-watershed level.

Conclusion

Our analysis represents initial steps in characterizing the link between salinity and nutrient concentrations in tidal tributaries of the CB. After accounting for long-term trends in our data, we found many strong correlations between salinity and nutrient concentrations on monthly timescales and between the 2-month CSI and nutrient concentrations on annual timescales, particularly for $NO_{2,3}$-N. These strong relationships suggest that salinity and indices of salinity may be incorporated into models to enhance accuracy of causal mechanisms for changes in water quality in

different sub-watersheds of the CB. For example, our findings can be used to develop structural equation models where salinity or CSI values reflect the effects of the latent variable streamflow, for which direct measurements are limited or non-existent for the stations we analyzed. Building water quality models for individual tributaries rather than deriving inferences about these tributaries based on results from general models about the CB mainstem may allow for more targeted approaches to nutrient load reductions in sub-watersheds of the CB.

Tables and figures

Table 3-1

Descriptions of Chesapeake Bay Program (CBP) monitoring stations selected for analysis. Station ID is CBP assigned station name. Duration is time span of data record. HUC-8 is hydrologic unit code 8 for each sub-watershed.

Station	Station ID	Sub-watershed	Salinity regime	Duration	Latitude	Longitude	HUC-8
s1	ET3.1	Sassafrass River	Oligohaline	1985-2018	39.364	-75.882	2130610
s2	CB2.2	Chesapeake Bay: Mid-Channel	Oligohaline	1984-2018	39.349	-76.176	2139997
s3	ET4.1	Chester River	Tidal fresh	1984-2018	39.244	-75.925	2130510
s4	ET5.1	Upper Choptank River	Oligohaline	1984-2018	38.806	-75.910	2130404
s5	ET5.2	Lower Choptank River	Mesohaline	1984-2018	38.581	-76.059	2130403
s6	ET6.1	Upper Nanticoke River	Tidal fresh	1984-2018	38.548	-75.703	2130305
s7	ET6.2	Lower Nanticoke River	Mesohaline	1986-2018	38.341	-75.888	2130305
s8	ET7.1	Lower Wicomico River	Mesohaline	1986-2018	38.268	-75.788	2130301
s9	ET8.1	Manokin River	Mesohaline	1986-2018	38.138	-75.814	2130208
s10	ET10.1	Upper Pocomoke River	Tidal fresh	1986-2018	38.076	-75.571	2130203

Table 3-2

Percentage of land and percent change (Δ) in land cover in each land cover category from 1984 to 2011 in the sub-watershed surrounding each tributary where a monitoring station is located. Land cover data were derived from the USGS Chesapeake Bay Watershed Land Cover Data Series (Irani 2015). Land cover categories are described in greater detail in Irani et al (2015). Watershed boundaries were derived from the Maryland Department of Natural Resources (MD-DNR 1998). Note: stations s6 and s7 are located within the same sub-watershed.

Station	Sub-watershed	Agriculture			Developed			Developed open space			Emergent wetlands		
		1984	2011	% Δ	1984	2011	% Δ	1984	2011	% Δ	1984	2011	% Δ
s1	Sassafrass River	59.8	59.7	**-0.1**	0.7	0.7	**0.0**	0.8	0.8	**0.0**	1.5	1.4	**-0.1**
s2	Chesapeake Bay: Mid-Channel	0.0	0.0	**0.0**	0.0	0.0	**0.0**	0.0	0.0	**0.0**	0.4	0.3	**-0.2**
s3	Chester River	63.9	63.8	**-0.1**	0.9	1.0	**0.1**	1.0	1.1	**0.1**	0.7	0.7	**0.0**
s4	Upper Choptank River	61.2	61.1	**-0.2**	1.4	1.6	**0.3**	1.3	1.5	**0.2**	2.2	2.2	**0.0**
s5	Lower Choptank River	33.8	33.1	**-0.7**	3.2	3.7	**0.5**	2.5	2.9	**0.4**	1.5	1.5	**0.0**
s6 & s7	Nanticoke River	32.3	32.7	**0.4**	0.9	1.0	**0.1**	0.8	0.9	**0.0**	11.5	11.7	**0.2**
s8	Lower Wicomico River	29.3	28.2	**-1.1**	7.9	8.8	**0.9**	4.7	5.6	**0.9**	8.0	8.1	**0.1**
s9	Manokin River	22.6	22.2	**-0.4**	1.4	1.7	**0.3**	0.8	0.9	**0.1**	14.5	14.9	**0.4**
s10	Upper Pocomoke River	44.9	44.6	**-0.3**	1.1	1.2	**0.1**	0.9	1.1	**0.2**	0.2	0.7	**0.6**
Station	Sub-watershed	Forest			Grassland/shrub			Unconsolidated shoreline			Water		
		1984	2011	% Δ	1984	2011	% Δ	1984	2011	% Δ	1984	2011	% Δ
s1	Sassafrass River	21.3	21.2	**-0.1**	1.6	1.6	**0.1**	0.2	0.2	**0.0**	14.2	14.3	**0.1**
s2	Chesapeake Bay: Mid-Channel	0.2	0.2	**0.0**	0.0	0.0	**0.0**	0.2	0.9	**0.7**	99.2	98.6	**-0.6**
s3	Chester River	30.4	30.4	**0.0**	1.6	1.7	**0.0**	0.1	0.0	**0.0**	1.3	1.4	**0.0**
s4	Upper Choptank River	28.8	28.1	**-0.7**	2.4	2.7	**0.3**	0.1	0.1	**0.1**	2.7	2.8	**0.0**
s5	Lower Choptank River	15.1	14.7	**-0.4**	2.6	2.8	**0.1**	0.3	0.2	**-0.1**	41.0	41.1	**0.1**
s6 & s7	Nanticoke River	35.3	33.7	**-1.6**	5.3	6.3	**1.0**	0.2	0.0	**-0.2**	13.8	13.8	**0.0**
s8	Lower Wicomico River	34.6	32.9	**-1.7**	6.4	7.2	**0.8**	0.2	0.2	**0.0**	9.0	9.0	**0.0**
s9	Manokin River	34.1	33.1	**-1.0**	5.9	6.4	**0.5**	0.1	0.1	**0.0**	20.7	20.7	**0.0**
s10	Upper Pocomoke River	48.3	46.1	**-2.1**	4.6	6.0	**1.3**	0.0	0.1	**0.1**	0.1	0.2	**0.1**

Table 3-3

Trends in salinity, soluble reactive phosphorus (SRP), ammonium-N (NH_4-N), nitrite + nitrate-nitrogen ($NO_{2,3}$-N), and dissolved organic P concentrations at each monitoring station over the duration of data record for that station (1986 or earlier to 2018). Yellow shaded boxes show no significant trend. Numbers in boxes represent magnitude of trend in parts per thousand for salinity, mg P/l for SRP and DOP and mg N/l for $NO_{2,3}$-N and NH_4-N.

Salinity regime	Station	Change in concentration over period of record				
		Salinity ppt	$NO_{2,3}$-N mg/l	NH_4-N mg/l	SRP mg/l	DOP mg/l
Tidal fresh	s3					0.015
Tidal fresh	s6		0.906		-0.007	
Tidal fresh	s10		-0.423	-0.020	-0.016	0.000
Oligohaline	s1				-0.002	
Oligohaline	s2			-0.037		
Oligohaline	s4		0.620		0.010	
Mesohaline	s5			-0.027	-0.009	-0.012
Mesohaline	s7	-2.101		-0.015		
Mesohaline	s8	-1.633		-0.032	-0.003	
Mesohaline	s9		-0.019		-0.002	
	Increasing trend		Decreasing trend		No change	

Table 3-4

Spearman correlations between monthly detrended salinity or the 1-, 2-, or 3-month coastal salinity index (CSI) values and soluble reactive phosphorus (SRP), ammonium-N (NH_4-N), nitrite + nitrate-nitrogen ($NO_{2,3}$-N), and dissolved organic P concentrations at each monitoring station over the duration of data record for that station (1986 or earlier to 2018). Correlations significant at $P < 0.01$ are in green shaded boxes.

Salinity regime	Station	Spearman correlations between metrics of salinity and nutrient concentrations											
		Salinity				$NO_{2,3}$-N				NH_4-N			
		Monthly salinity	CSI value			Monthly salinity	CSI value			Monthly salinity	CSI value		
			1-month	2-month	3-month		1-month	2-month	3-month		1-month	2-month	3-month
Tidal fresh	s3	1.000	-0.803	-0.724	-0.633	-0.642	0.350	0.369	0.335	-0.371	0.163	0.142	0.104
Tidal fresh	s6	1.000	-0.757	-0.668	-0.582	-0.608	0.114	0.200	0.224	-0.257	-0.001	0.083	0.087
Tidal fresh	s10	1.000	-0.679	-0.578	-0.521	-0.465	0.093	0.121	0.098	-0.136	-0.238	-0.277	-0.234
Oligohaline	s1	1.000	-0.841	-0.796	-0.738	-0.066	0.140	0.119	0.109	0.059	-0.026	-0.054	-0.053
Oligohaline	s2	1.000	-0.838	-0.682	-0.583	-0.580	0.388	0.325	0.279	0.035	-0.099	-0.087	-0.085
Oligohaline	s4	1.000	-0.835	-0.718	-0.624	-0.757	0.439	0.418	0.363	-0.368	0.118	0.010	-0.056
Mesohaline	s5	1.000	-0.856	-0.824	-0.785	-0.517	0.375	0.334	0.299	-0.131	0.046	0.021	-0.004
Mesohaline	s7	1.000	-0.861	-0.777	-0.706	-0.612	0.386	0.354	0.323	-0.271	0.186	0.126	0.085
Mesohaline	s8	1.000	-0.865	-0.775	-0.711	-0.607	0.328	0.285	0.255	-0.422	0.222	0.181	0.144
Mesohaline	s9	1.000	-0.861	-0.803	-0.748	-0.385	0.257	0.214	0.195	-0.067	0.049	0.027	0.019

Salinity regime	Station	Spearman correlations between metrics of salinity and nutrient concentrations							
		SRP				DOP			
		Monthly salinity	CSI value			Monthly salinity	CSI value		
			1-month	2-month	3-month		1-month	2-month	3-month
Tidal fresh	s3	-0.604	0.562	0.487	0.428	-0.342	0.371	0.326	0.280
Tidal fresh	s6	-0.418	0.373	0.347	0.296	-0.108	0.283	0.178	0.133
Tidal fresh	s10	-0.195	0.401	0.361	0.333	-0.159	0.326	0.295	0.247
Oligohaline	s1	-0.225	0.227	0.176	0.150	-0.274	0.194	0.151	0.114
Oligohaline	s2	0.235	0.070	0.061	0.057	0.180	-0.063	-0.146	-0.189
Oligohaline	s4	-0.258	0.353	0.234	0.167	-0.306	0.339	0.254	0.220
Mesohaline	s5	0.001	0.141	0.108	0.079	0.126	0.070	-0.076	-0.075
Mesohaline	s7	-0.183	0.322	0.252	0.199	0.087	-0.010	-0.015	-0.022
Mesohaline	s8	-0.463	0.483	0.415	0.361	-0.059	0.078	0.056	0.048
Mesohaline	s9	-0.059	0.123	0.089	0.049	0.196	-0.106	-0.097	-0.088

$P < 0.01$

Table 3-5

Spearman correlations between monthly-averaged detrended streamflow at USGS stream gauges and soluble reactive phosphorus (SRP), ammonium-N (NH_4-N), nitrite + nitrate-nitrogen ($NO_{2,3}$-N), and dissolved organic P concentrations at each Chesapeake Bay Program (CBP) monitoring station over the duration of data record for that station (1986 or earlier to 2018). Correlations significant at $P < 0.01$ are in green shaded boxes. Note: streamflow stations are geographically distinct from CBP water quality monitoring stations and distance between stations is indicated.

USGS stream gauge	Downstream station	Distance to station (km)	Tributary	Spearman correlations between streamflow and nutrient concentrations				
				Salinity	$NO_{2,3}$-N	NH_4-N	SRP	DOP
1493112	s3	2	Chester River	-0.297	0.552	0.406	0.479	0.273
1486000	s9	15	Manokin River	-0.598	0.402	0.073	0.298	-0.212

$P < 0.05$

Table 3-6

Spearman correlations between the top 15% of monthly detrended salinity values and corresponding soluble reactive phosphorus (SRP), ammonium-N (NH_4-N), nitrite + nitrate-nitrogen ($NO_{2,3}$-N), and dissolved organic P concentrations at each monitoring station over the duration of data record for that station (1986 or earlier to 2018). Tidal fresh (0-0.5 parts per thousand: ppt) stations are shaded in blue, oligohaline stations (0.5-5 ppt) are shaded in light green, and mesohaline (5-18 ppt) stations are shaded in dark green. Correlations significant at $P < 0.05$ are in green shaded boxes.

Salinity regime	Station	Spearman correlations between top 15% salinity values and nutrient concentrations				
		Salinity	$NO_{2,3}$-N	NH_4-N	SRP	DOP
Tidal fresh	s3	1.000	-0.444	0.118	0.243	0.148
Tidal fresh	s6	1.000	-0.272	-0.195	-0.180	0.277
Tidal fresh	s10	1.000	-0.461	-0.124	-0.539	-0.359
Oligohaline	s1	1.000	0.033	0.082	0.121	0.240
Oligohaline	s2	1.000	-0.181	-0.281	0.291	0.282
Oligohaline	s4	1.000	-0.152	-0.013	0.574	-0.036
Mesohaline	s5	1.000	-0.288	-0.214	-0.196	-0.008
Mesohaline	s7	1.000	-0.132	-0.069	-0.089	-0.051
Mesohaline	s8	1.000	-0.272	-0.123	-0.032	0.343
Mesohaline	s9	1.000	0.007	-0.047	0.042	0.076
		$P < 0.05$				

Table 3-7

Spearman correlations between annually-averaged detrended salinity or the 1-, 2-, 3-, or 6-month coastal salinity index (CSI) values and soluble reactive phosphorus (SRP), ammonium-N (NH_4-N), nitrite + nitrate-nitrogen ($NO_{2,3}$-N), and dissolved organic P concentrations at each monitoring station over the duration of data record for that station (1986 or earlier to 2018). Correlations significant at $P < 0.01$ are in green shaded boxes and correlations significant at $P < 0.05$ are in pink shaded boxes.

Salinity regime	Station	Spearman correlations between metrics of salinity and nutrient concentrations														
		Salinity					$NO_{2,3}$-N					NH4-N				
		Annually-averaged salinity	Annually-averaged CSI value				Annually-averaged salinity	Annually-averaged CSI value				Annually-averaged salinity	Annually-averaged CSI value			
			1-month	2-month	3-month	6-month		1-month	2-month	3-month	6-month		1-month	2-month	3-month	6-month
Tidal fresh	s3	1.000	-0.971	-0.966	-0.935	-0.819	-0.695	0.741	0.748	0.746	0.830	-0.250	0.267	0.219	0.167	0.057
Tidal fresh	s6	1.000	-0.972	-0.968	-0.945	-0.736	-0.844	0.840	0.863	0.859	0.696	-0.378	0.412	0.392	0.370	0.217
Tidal fresh	s10	1.000	-0.977	-0.976	-0.914	-0.765	-0.738	0.740	0.749	0.683	0.547	0.036	-0.035	0.021	0.133	0.291
Oligohaline	s1	1.000	-0.857	-0.831	-0.807	-0.726	-0.696	0.779	0.801	0.795	0.833	-0.087	0.014	-0.008	-0.018	-0.083
Oligohaline	s2	1.000	-0.939	-0.916	-0.892	-0.823	-0.717	0.582	0.598	0.538	0.469	0.101	-0.189	-0.169	-0.134	-0.097
Oligohaline	s4	1.000	-0.931	-0.893	-0.859	-0.760	-0.714	0.767	0.784	0.778	0.693	-0.135	0.047	-0.022	-0.098	-0.245
Mesohaline	s5	1.000	-0.991	-0.991	-0.989	-0.939	-0.800	0.785	0.801	0.810	0.794	-0.076	0.064	0.058	0.035	0.003
Mesohaline	s7	1.000	-0.950	-0.946	-0.923	-0.829	-0.670	0.739	0.756	0.758	0.794	-0.366	0.379	0.412	0.409	0.343
Mesohaline	s8	1.000	-0.915	-0.912	-0.901	-0.822	-0.579	0.626	0.658	0.695	0.707	-0.237	0.142	0.133	0.116	0.058
Mesohaline	s9	1.000	-0.993	-0.987	-0.984	-0.929	-0.496	0.482	0.527	0.554	0.546	0.053	-0.052	-0.033	-0.022	-0.031

Salinity regime	Station	Spearman correlations between metrics of salinity and nutrient concentrations									
		SRP					DOP				
		Annually-averaged salinity	Annually-averaged CSI value				Annually-averaged salinity	Annually-averaged CSI value			
			1-month	2-month	3-month	6-month		1-month	2-month	3-month	6-month
Tidal fresh	s3	-0.657	0.680	0.649	0.587	0.459	-0.604	0.572	0.556	0.511	0.372
Tidal fresh	s6	-0.487	0.462	0.485	0.473	0.342	-0.260	0.224	0.241	0.270	0.224
Tidal fresh	s10	-0.597	0.656	0.675	0.645	0.605	-0.464	0.491	0.503	0.583	0.581
Oligohaline	s1	-0.337	0.393	0.371	0.333	0.315	-0.217	0.305	0.266	0.212	0.183
Oligohaline	s2	0.125	-0.145	-0.145	-0.110	-0.125	0.147	-0.118	-0.100	-0.106	-0.080
Oligohaline	s4	-0.477	0.405	0.335	0.243	0.051	-0.439	0.407	0.359	0.345	0.282
Mesohaline	s5	-0.033	-0.024	0.027	0.028	0.046	0.337	-0.339	-0.354	-0.385	-0.417
Mesohaline	s7	-0.304	0.283	0.391	0.405	0.337	0.090	-0.259	-0.187	-0.171	-0.126
Mesohaline	s8	-0.574	0.644	0.632	0.616	0.572	-0.071	0.037	0.060	0.087	0.098
Mesohaline	s9	-0.180	0.184	0.150	0.149	0.066	0.593	-0.573	-0.561	-0.578	-0.585

$P < 0.05$

$P < 0.01$

Figure 3-1

Map of the location of monitoring stations within the Chesapeake Bay, along the Delmarva Peninsula. Maryland counties are shaded in gray. The salinity regime of each station is indicated by different colored dots as tidal fresh (0-0.5 parts per thousand: ppt); oligohaline (0.5-5 ppt), or mesohaline (5-18 ppt).

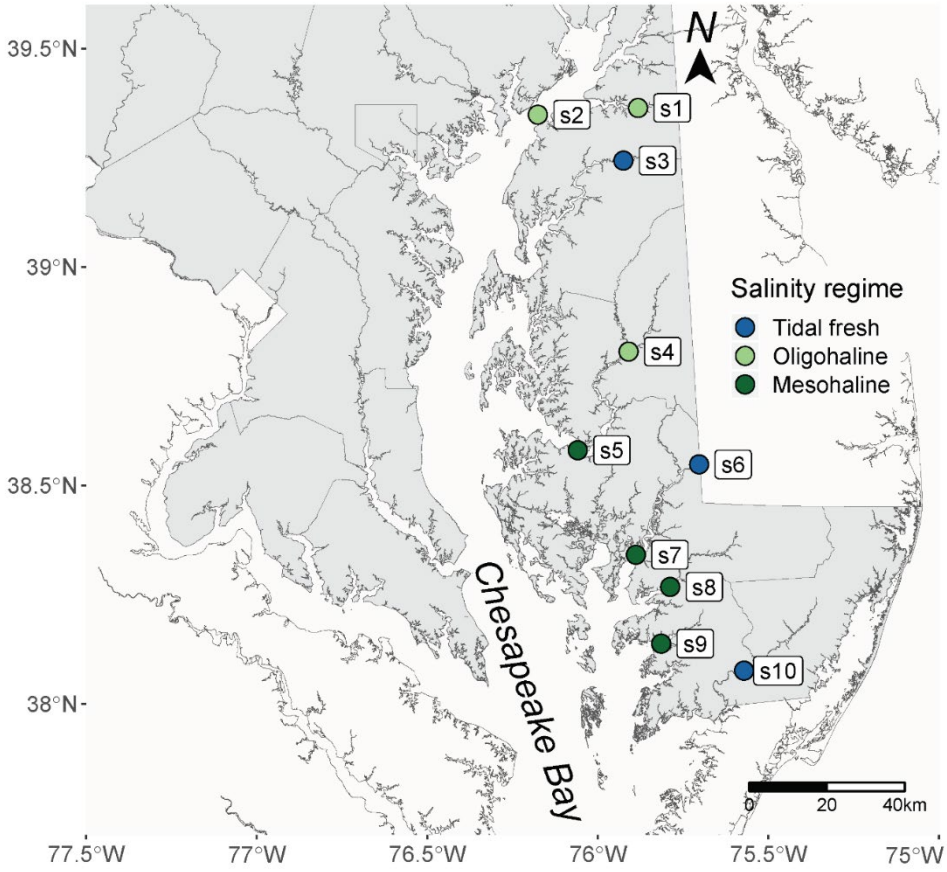

Figure 3-2

Spline graphs illustrating monotonic relationships between detrended, annually-averaged nitrite + nitrate nitrogen ($NO_{2,3}$-N) concentrations (mg N/l) and A) annually-averaged 1-month coastal salinity index (CSI) values and B) annually-averaged 2-month CSI values at each monitoring station

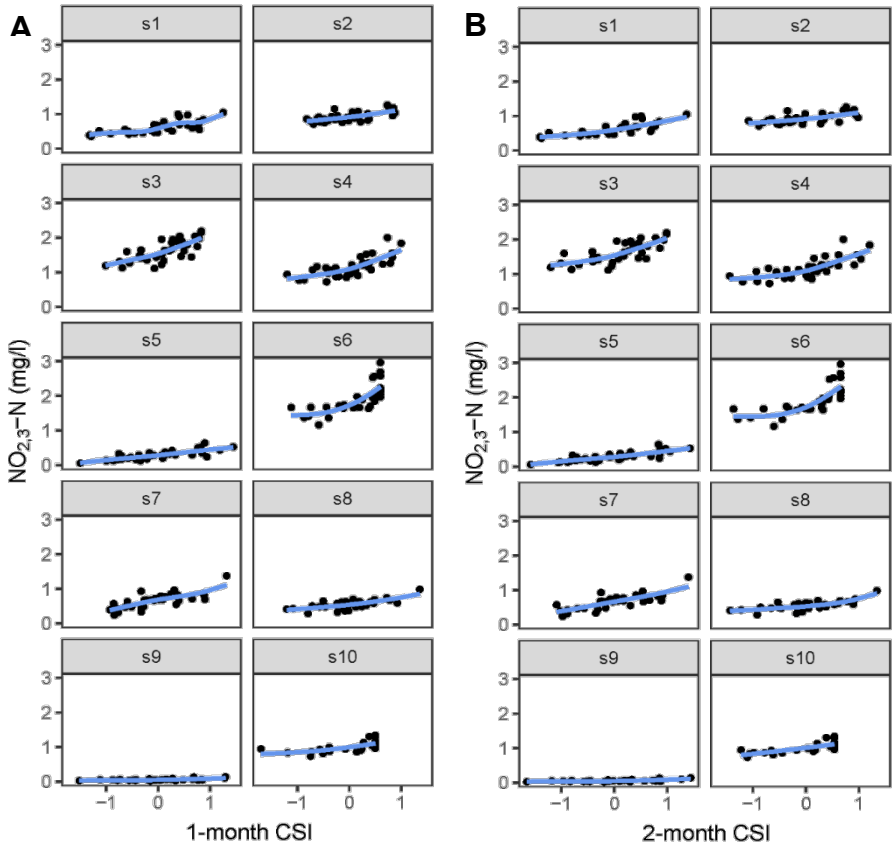

Works cited

Abler, D., J. Shortle, J. Carmichael, and R. Horan. 2002. Climate change, agriculture, and water quality in the Chesapeake Bay region. Climatic Change 55:339–359.

Ardón, M., J. L. Morse, B. P. Colman, and E. S. Bernhardt. 2013. Drought-induced saltwater incursion leads to increased wetland nitrogen export. Global Change Biology 19:2976–2985.

Arkema, K. K., G. Guannel, G. Verutes, S. A. Wood, A. Guerry, M. Ruckelshaus, P. Kareiva, M. Lacayo, and J. M. Silver. 2013. Coastal habitats shield people and property from sea-level rise and storms. Nature Climate Change 3:913–918.

Austin, J. A. 2002. Estimating the mean ocean-bay exchange rate of the Chesapeake Bay. Journal of Geophysical Research C: Oceans 107:13–1.

Baldwin, A. H., P. J. Kangas, J. P. Megonigal, M. C. Perry, and D. F. Whigham. 2009. Coastal Wetlands of the Chesapeake Bay. Pages 29–43 *in* A. H. Baldwin, editor. Wetland Habitats of North America - Ecology and Conservation Concerns. First edition. University of California Press, Berkeley, CA.

Beguería, S., B. Latorre, F. Reig, and S. M. Vicente-Serrano. 2020. Standardized Precipitation Evapotranspiration Index Global Database. https://spei.csic.es/database.html.

Bianchi, T. S. 2007. Estuarine Science and Biogeochemical Cycles. Pages 3–10 Biogeochemistry of Estuaries. Oxford University Press, Oxford.

Boesch, D. F., R. B. Brinsfield, and R. E. Magnien. 2001. Chesapeake Bay Eutrophication. Journal of Environmental Quality 30:303–320.

Campbell, P. C., J. O. Bash, C. G. Nolte, T. L. Spero, E. J. Cooter, K. Hinson, and L.

C. Linker. 2019. Projections of Atmospheric Nitrogen Deposition to the Chesapeake Bay Watershed. Journal of Geophysical Research: Biogeosciences:3307–3326.

Caraco, N., J. Cole, and G. E. Likens. 1990. A comparison of phosphorus immobilization in sediments of freshwater and coastal marine systems. Biogeochemistry 9:277–290.

CBP Data Integrity Workgroup (DIWG), and Nontidal Workgroup. 2017. Methods and Quality Assurance for Chesapeake Bay Water Quality Monitoring Programs - CBP/TRS-319. https://www.chesapeakebay.net/documents/Methods_Manual.pdf.

Chesapeake Bay Program. 2018. 2017 and 2025 Watershed Implementation Plans (WIPs). https://www.chesapeakeprogress.com/clean-water/watershed-implementation-plans.

Chesapeake Bay Program. 2019. Chesapeake Bay Program: Water Quality Database. https://www.chesapeakebay.net/what/downloads/cbp_water_quality_database_1984_present.

Conrads, P. A., and L. S. Darby. 2017. Development of a coastal drought index using salinity data. Bulletin of the American Meteorological Society 98:753–766.

Deegan, L. A., D. S. Johnson, R. S. Warren, B. J. Peterson, J. W. Fleeger, S. Fagherazzi, and W. M. Wollheim. 2012. Coastal eutrophication as a driver of salt marsh loss. Nature 490:388–392.

Di, H. J., and K. C. Cameron. 2002. Nitrate leaching in temperate agroecosystems: Sources, factors and mitigating strategies. Nutrient Cycling in Agroecosystems

64:237–256.

Diaz, R. J., and R. Rosenberg. 2008. Spreading dead zones and consequences for marine ecosystems. Science 321:926–929.

Eshleman, K. N., and R. D. Sabo. 2016. Declining nitrate-N yields in the Upper Potomac River Basin: What is really driving progress under the Chesapeake Bay restoration? Atmospheric Environment 146:280–289.

Fanelli, R. M., J. D. Blomquist, and R. M. Hirsch. 2019. Point sources and agricultural practices control spatial-temporal patterns of orthophosphate in tributaries to Chesapeake Bay. Science of the Total Environment 652:422–433.

Goyne, K. W., H.-J. Jun, S. H. Anderson, and P. P. Motavalli. 2008. Phosphorus and nitrogen sorption to soils in the presence of poultry litter-derived dissolved organic matter. Journal of environmental quality 37:154–63.

Hamed, K. H., and A. R. Rao. 1998. A modified Mann-Kendall trend test for autocorrelated data. Journal of Hydrology 204:182–196.

Harding, L. W., C. L. Gallegos, E. S. Perry, W. D. Miller, J. E. Adolf, M. E. Mallonee, and H. W. Paerl. 2016. Long-Term Trends of Nutrients and Phytoplankton in Chesapeake Bay. Estuaries and Coasts 39:664–681.

Harrel Jr., F. E. 2018. Package ‘HMisc’ for R.

Hartzell, J. L., and T. E. Jordan. 2012. Shifts in the relative availability of phosphorus and nitrogen along estuarine salinity gradients. Biogeochemistry 107:489–500.

Hartzell, J. L., T. E. Jordan, and J. C. Cornwell. 2017. Phosphorus Sequestration in Sediments Along the Salinity Gradients of Chesapeake Bay Subestuaries. Estuaries and Coasts 40:1607–1625.

Hauke, J., and T. Kossowski. 2011. Comparison of values of pearson's and spearman's correlation coefficients on the same sets of data. Quaestiones Geographicae 30:87–93.

Hilton, T. W., R. G. Najjar, L. Zhong, and M. Li. 2008. Is there a signal of sea-level rise in Chesapeake Bay salinity? Journal of Geophysical Research: Oceans 113:1–12.

Irani, F. . 2015. Chesapeake Bay Watershed 2011 Edition Land Cover Data Release. https://www.sciencebase.gov/catalog/item/557b238fe4b0c350d7b9abb8.

Jessen, S., D. Postma, L. Thorling, S. Müller, J. Leskelä, and P. Engesgaard. 2017. Decadal variations in groundwater quality: A legacy from nitrate leaching and denitrification by pyrite in a sandy aquifer. Water Resources Research 53:184–198.

Jordan, T. E., D. L. Correll, J. Miklas, and D. E. Weller. 1991. Nutrients and chlorophyll at the interface of a watershed and an estuary. Limnology and Oceanography 36:251–267.

Jordan, T. E., D. E. Weller, and C. E. Pelc. 2018. Effects of Local Watershed Land Use on Water Quality in Mid-Atlantic Coastal Bays and Subestuaries of the Chesapeake Bay. Estuaries and Coasts 41:38–53.

Kaplan, D., and R. Pruim. 2020. ggformula: Formula Interface to the Grammar of Graphics. CRAN.

Kemp, W. M., W. R. Boynton, J. E. Adolf, D. F. Boesch, W. C. Boicourt, G. Brush, J. C. Cornwell, T. R. Fisher, P. M. Glibert, J. D. Hagy, L. W. Harding, E. D. Houde, D. G. Kimmel, W. D. Miller, R. I. E. Newell, M. R. Roman, E. M.

Smith, and J. C. Stevenson. 2005. Eutrophication of Chesapeake Bay: historical trends and ecological interactions. Marine Ecology Progress Series 303:1–29.

Kleinman, P. J. A., C. Church, L. S. Saporito, J. M. McGrath, M. S. Reiter, A. L. Allen, S. Tingle, G. D. Binford, K. Han, and B. C. Joern. 2015. Phosphorus leaching from agricultural soils of the Delmarva Peninsula, USA. Journal of Environmental Quality 44:524–534.

Klemick, H., C. Griffiths, D. Guignet, and P. Walsh. 2018. Improving Water Quality in an Iconic Estuary: An Internal Meta-analysis of Property Value Impacts Around the Chesapeake Bay. Environmental and Resource Economics 69:265–292.

Loughner, C. P., M. Tzortziou, S. Shroder, and K. E. Pickering. 2016. Enhanced dry deposition of nitrogen pollution near coastlines: A case study covering the chesapeake bay estuary and atlantic ocean coastline. Journal of Geophysical Research 121:14,221-14,238.

Maryland Department of Natural Resources. 1998. Maryland Watersheds - 8 Digit Watersheds. https://geodata.md.gov/imap/rest/services/Hydrology/MD_Watersheds/FeatureServer/1.

McCloskey, B. 2019. R - Coastal salinity index package. R.

Van Meter, K. J., N. B. Basu, and P. Van Cappellen. 2017. Two centuries of nitrogen dynamics: Legacy sources and sinks in the Mississippi and Susquehanna River Basins. Global Biogeochemical Cycles 31:2–23.

Musolff, A., B. Selle, O. Büttner, M. Opitz, and J. Tittel. 2017. Unexpected release of

phosphate and organic carbon to streams linked to declining nitrogen depositions. Global Change Biology 23:1891–1901.

Najjar, R., L. Patterson, and S. Graham. 2009. Climate simulations of major estuarine watersheds in the Mid-Atlantic region of the US. Climatic Change 95:139–168.

Neubauer, S. C., R. B. Franklin, and D. J. Berrier. 2013. Saltwater intrusion into tidal freshwater marshes alters the biogeochemical processing of organic carbon. Biogeosciences 10:8171–8183.

Ocampo, C. J., C. E. Oldham, and M. Sivapalan. 2006. Nitrate attenuation in agricultural catchments: Shifting balances between transport and reaction. Water Resources Research 42:1–16.

Paerl, H. W., N. S. Hall, B. L. Peierls, and K. L. Rossignol. 2014. Evolving Paradigms and Challenges in Estuarine and Coastal Eutrophication Dynamics in a Culturally and Climatically Stressed World. Estuaries and Coasts 37:243–258.

Patakamuri, S. K., and N. O'Brien. 2019. modifiedmk: Modified Versions of Mann Kendall and Spearman's Rho Trend Tests. CRANR.

R Studio Team. 2019. RStudio: Integrated Development for R. R Studio Incorporated, Boston, MA.

Rice, K. C., B. Hong, and J. Shen. 2012. Assessment of salinity intrusion in the James and Chickahominy Rivers as a result of simulated sea-level rise in Chesapeake Bay, East Coast, USA. Journal of Environmental Management 111:61–69.

Ross, A. C., R. G. Najjar, M. Li, M. E. Mann, S. E. Ford, and B. Katz. 2015. Sea-level rise and other influences on decadal-scale salinity variability in a coastal plain estuary. Estuarine, Coastal and Shelf Science 157:79–92.

Ryberg, K. R., J. D. Blomquist, L. A. Sprague, A. J. Sekellick, and J. Keisman. 2018. Modeling drivers of phosphorus loads in Chesapeake Bay tributaries and inferences about long-term change. Science of the Total Environment 616–617:1423–1430.

Sanford, W. E., and J. P. Pope. 2013. Quantifying groundwater's role in delaying improvements to Chesapeake Bay water quality. Environmental Science and Technology 47:13330–13338.

Sharpley, A. N., H. P. Jarvie, A. R. Buda, L. May, B. Spears, and P. J. A. Kleinman. 2014. Phosphorus Legacy: Overcoming the Effects of Past Management Practices to Mitigate Future Water Quality Impairment. Journal of Environmental Quality 42:1308–1326.

Steinmuller, H. E., and L. G. Chambers. 2018. Can Saltwater Intrusion Accelerate Nutrient Export from Freshwater Wetland Soils? An Experimental Approach. Soil Science Society of America Journal 82:283.

Tango, P. J., and R. A. Batiuk. 2016. Chesapeake Bay recovery and factors affecting trends: Long-term monitoring, indicators, and insights. Regional Studies in Marine Science 4:12–20.

Tully, K. L., D. Weissman, W. J. Wyner, J. Miller, and T. Jordan. 2019. Soils in transition: saltwater intrusion alters soil chemistry in agricultural fields. Biogeochemistry 142:339–356.

Turner, B. L., and P. M. Haygarth. 2000. Phosphorus Forms and Concentrations in Leachate under Four Grassland Soil Types. Soil Science Society of America Journal 64:1090–1099.

USGS. 2019. National Water Information System. https://nwis.waterdata.usgs.gov/nwis.

Vicente-Serrano, S. M., S. Beguería, J. I. López-Moreno, M. Angulo, and A. El Kenawy. 2010. A new global 0.5° gridded dataset (1901-2006) of a multiscalar drought index: Comparison with current drought index datasets based on the palmer drought severity index. Journal of Hydrometeorology 11:1033–1043.

Weissman, D. S., and K. L. Tully. 2020. Saltwater intrusion affects nutrient concentrations in soil porewater and surface waters of coastal habitats. Ecosphere 11.

Weston, N. B., R. E. Dixon, and S. B. Joye. 2006. Ramifications of increased salinity in tidal freshwater sediments: Geochemistry and microbial pathways of organic matter mineralization. Journal of Geophysical Research: Biogeosciences 111:1–14.

White, J. W., F. J. Coale, J. T. Sims, and A. L. Shober. 2010. Phosphorus Runoff from Waste Water Treatment Biosolids and Poultry Litter Applied to Agricultural Soils. Journal of Environmental Quality 39:314–323.

Williams, A. A., N. T. Lauer, and C. T. Hackney. 2014. Soil phosphorus dynamics and saltwater intrusion in a florida estuary. Wetlands 34:535–544.

Williams, M. R., S. Filoso, B. J. Longstaff, and W. C. Dennison. 2010. Long-Term Trends of Water Quality and Biotic Metrics in Chesapeake Bay: 1986 to 2008. Estuaries and Coasts 33:1279–1299.

Zhang, Q., R. R. Murphy, R. Tian, M. K. Forsyth, E. M. Trentacoste, J. Keisman, and P. J. Tango. 2018. Chesapeake Bay's water quality condition has been

recovering: Insights from a multimetric indicator assessment of thirty years of tidal monitoring data. Science of the Total Environment 637–638:1617–1625.

Supplemental Figures

Figure S 3-1

1-month coastal salinity index (CSI) at station s1. Black line indicates 1-month rolling average salinity. Colors in background represent periods of drought (yellow to red colors) or periods of wetter conditions (light blue to dark blue). Green background indicates linearly interpolated data. A more comprehensive explanation of colored categories is detailed in Conrads and Darby 2017.

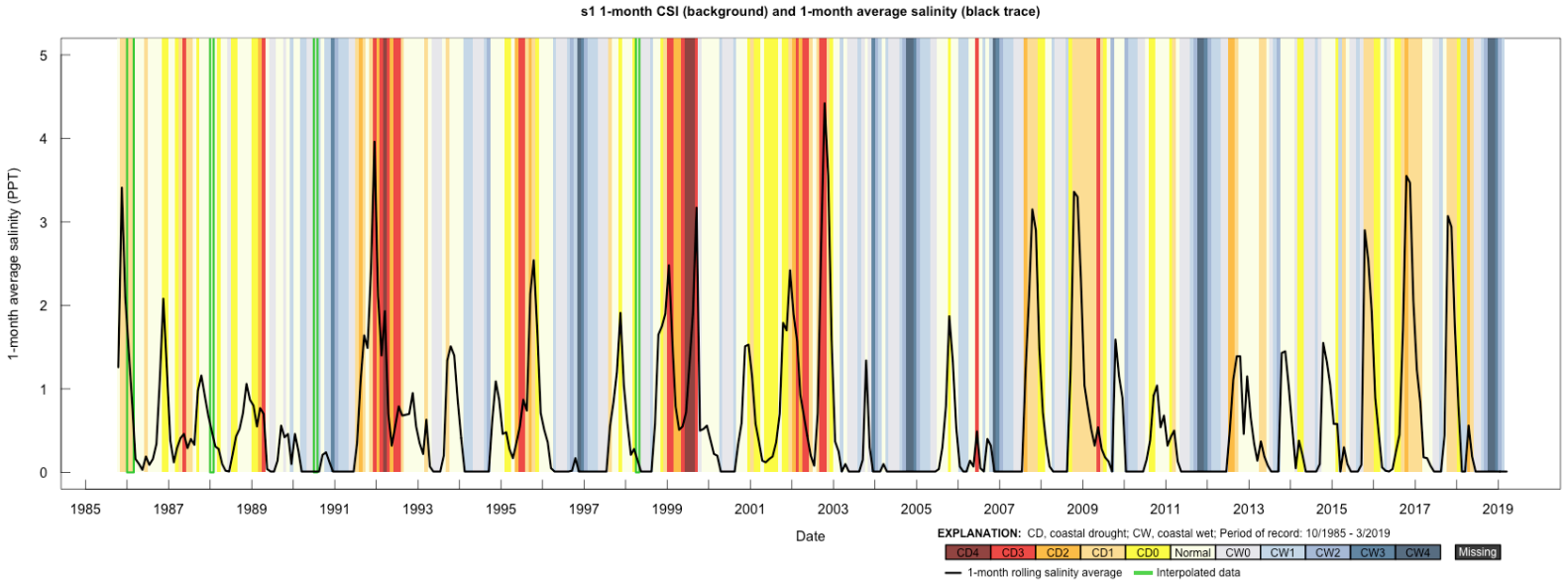

Figure S 3-2

2-month coastal salinity index (CSI) at station s1. Black line indicates 2-month rolling average salinity. Colors in background represent periods of drought (yellow to red colors) or periods of wetter conditions (light blue to dark blue).

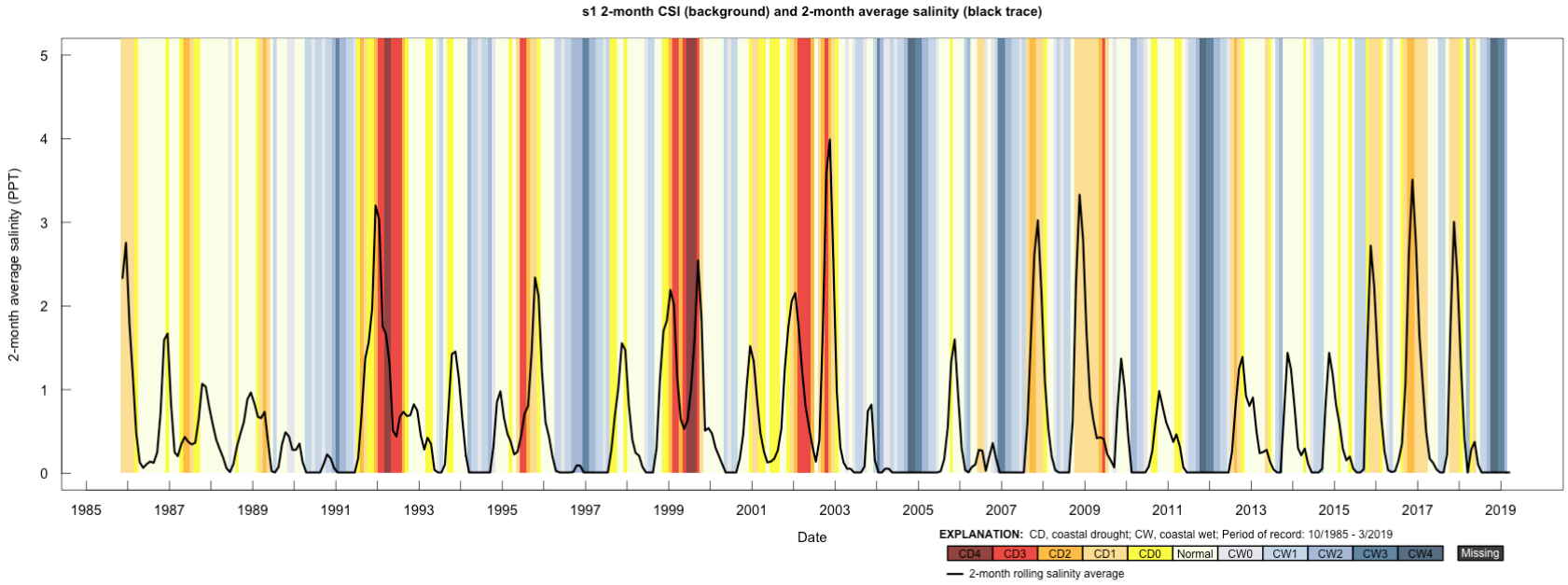

Figure S 3-3

1-month coastal salinity index (CSI) at station s2. Black line indicates 1-month rolling average salinity. Colors in background represent periods of drought (yellow to red colors) or periods of wetter conditions (light blue to dark blue). Green background indicates linearly interpolated data.

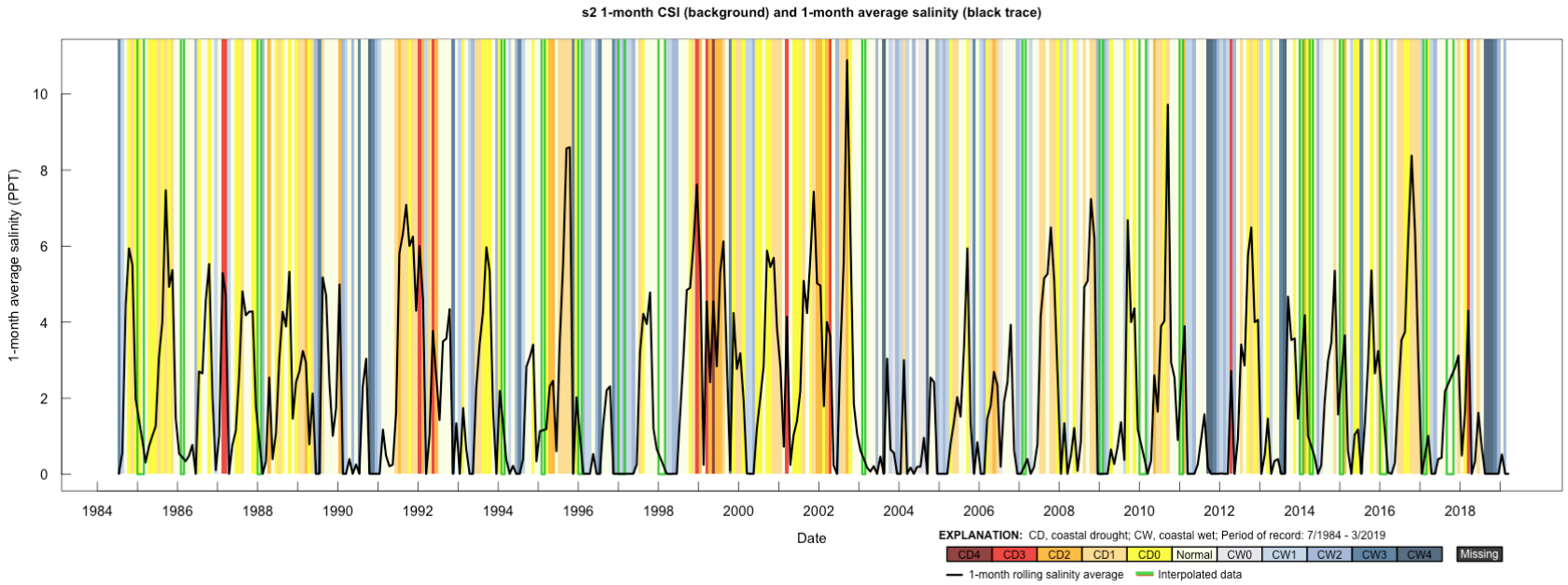

Figure S 3-4

2-month coastal salinity index (CSI) at station s2. Black line indicates 2-month rolling average salinity. Colors in background represent periods of drought (yellow to red colors) or periods of wetter conditions (light blue to dark blue).

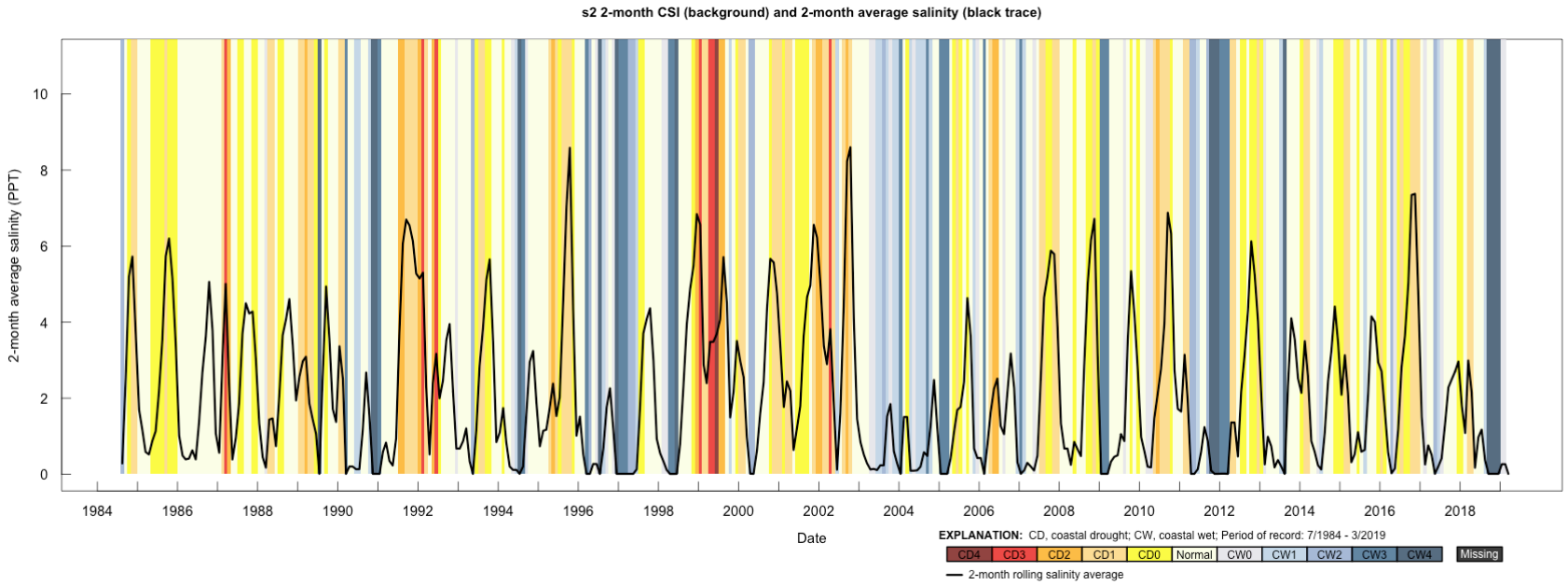

Figure S 3-5

1-month coastal salinity index (CSI) at station s3. Black line indicates 1-month rolling average salinity. Colors in background represent periods of drought (yellow to red colors) or periods of wetter conditions (light blue to dark blue). Green background indicates linearly interpolated data.

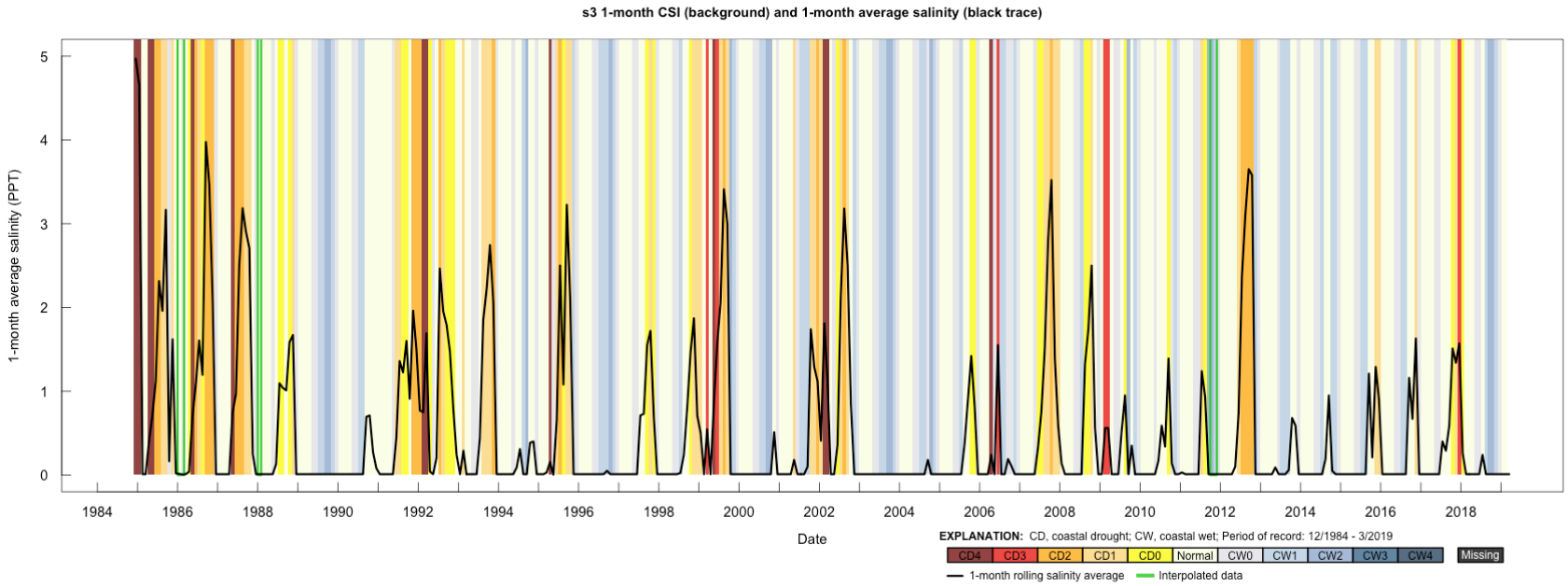

Figure S 3-6

2-month coastal salinity index (CSI) at station s3. Black line indicates 2-month rolling average salinity. Colors in background represent periods of drought (yellow to red colors) or periods of wetter conditions (light blue to dark blue).

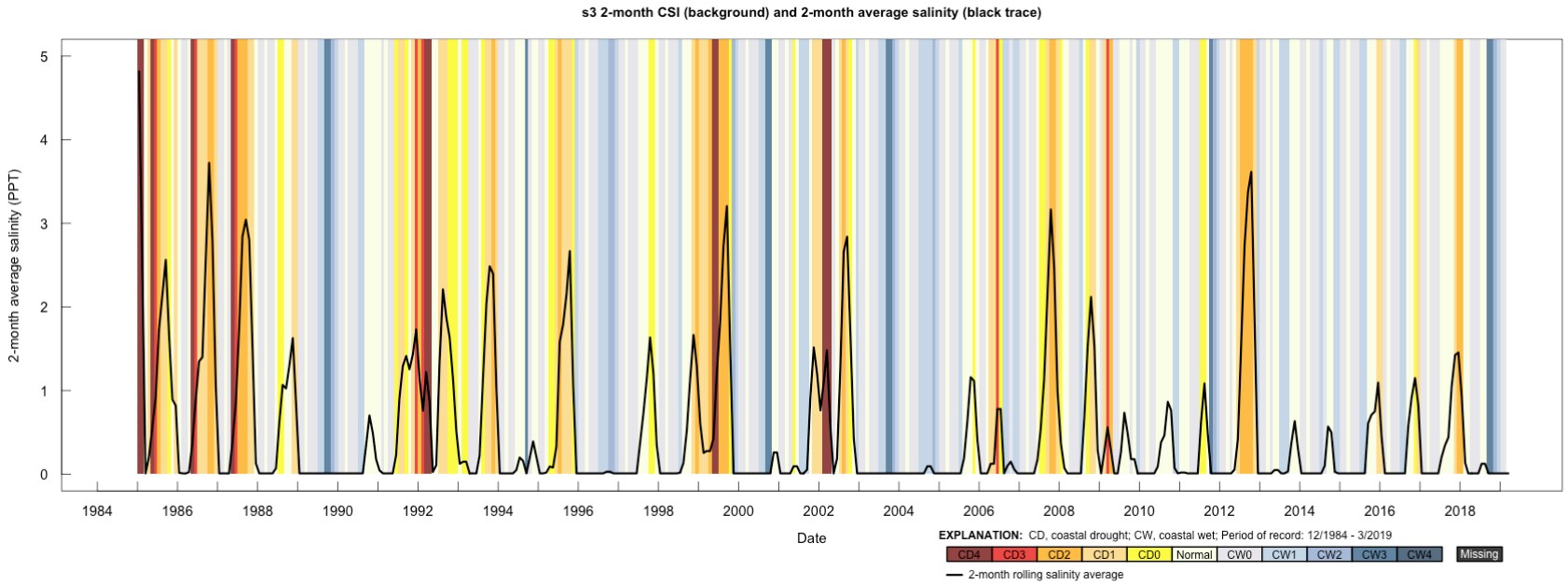

Figure S 3-7

1-month coastal salinity index (CSI) at station s4. Black line indicates 1-month rolling average salinity. Colors in background represent periods of drought (yellow to red colors) or periods of wetter conditions (light blue to dark blue). Green background indicates linearly interpolated data.

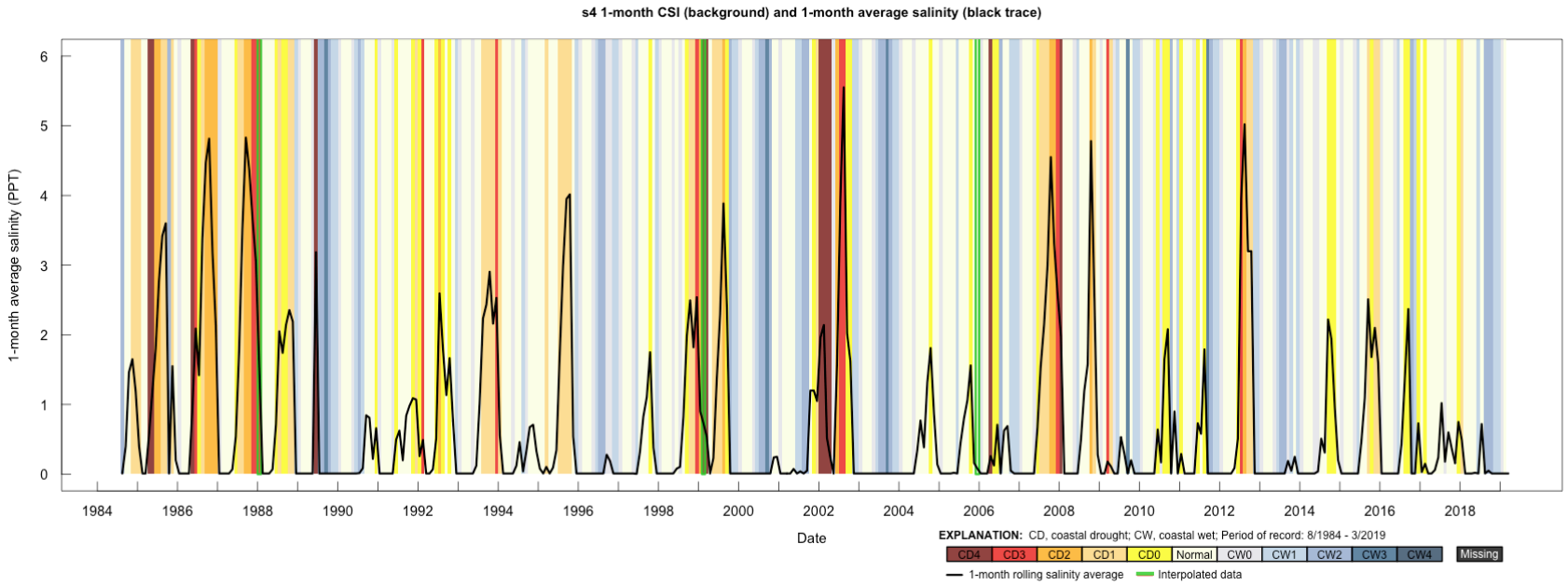

Figure S 3-8

2-month coastal salinity index (CSI) at station s4. Black line indicates 2-month rolling average salinity. Colors in background represent periods of drought (yellow to red colors) or periods of wetter conditions (light blue to dark blue).

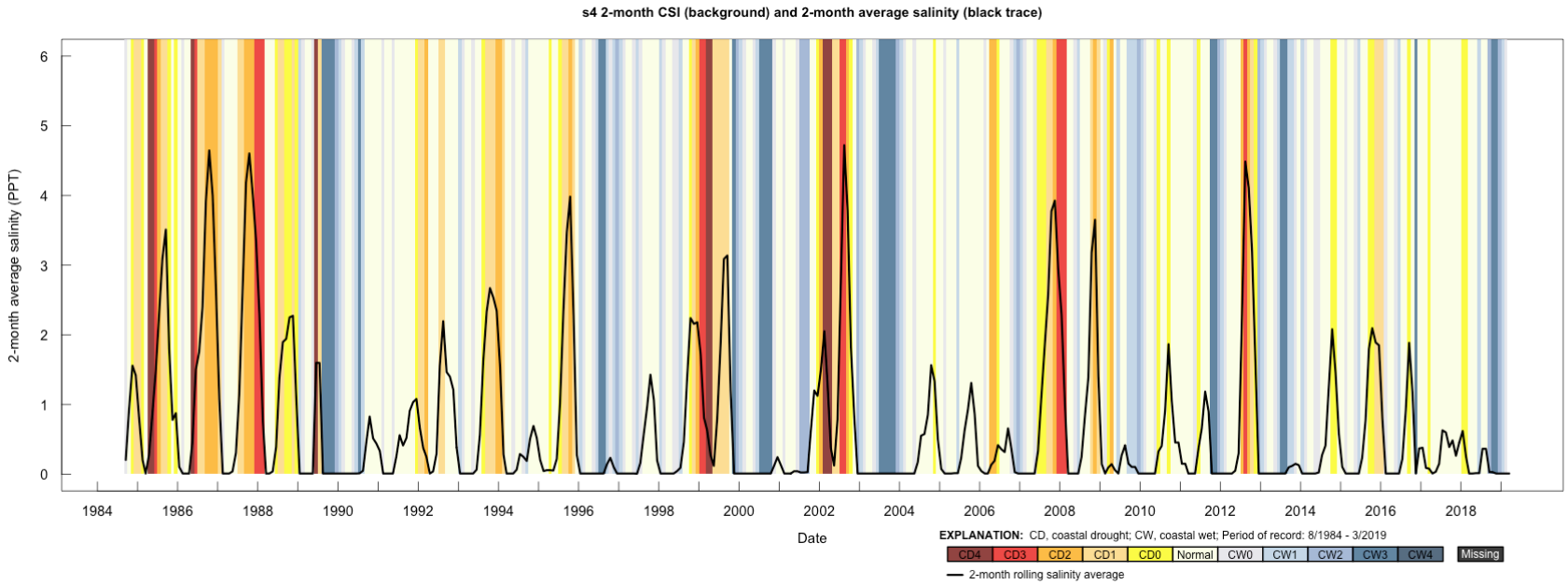

Figure S 3-9

1-month coastal salinity index (CSI) at station s5. Black line indicates 1-month rolling average salinity. Colors in background represent periods of drought (yellow to red colors) or periods of wetter conditions (light blue to dark blue). Green background indicates linearly interpolated data.

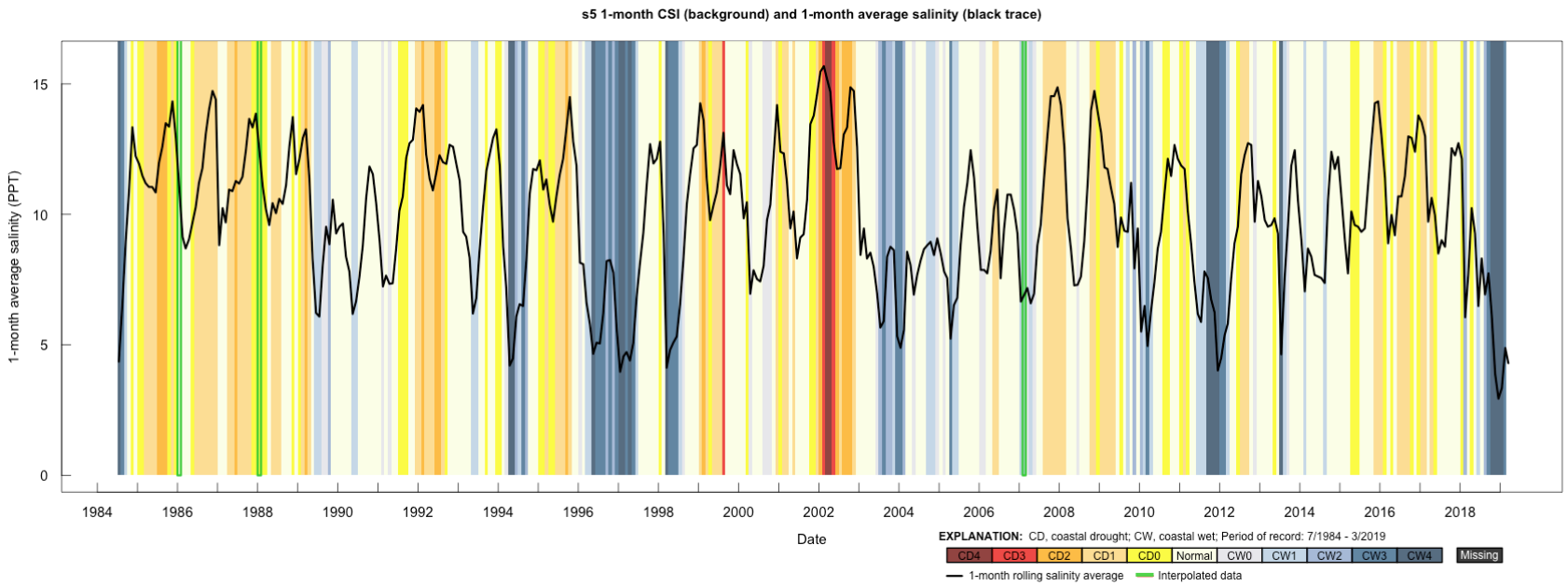

Figure S 3-10

2-month coastal salinity index (CSI) at station s5. Black line indicates 2-month rolling average salinity. Colors in background represent periods of drought (yellow to red colors) or periods of wetter conditions (light blue to dark blue).

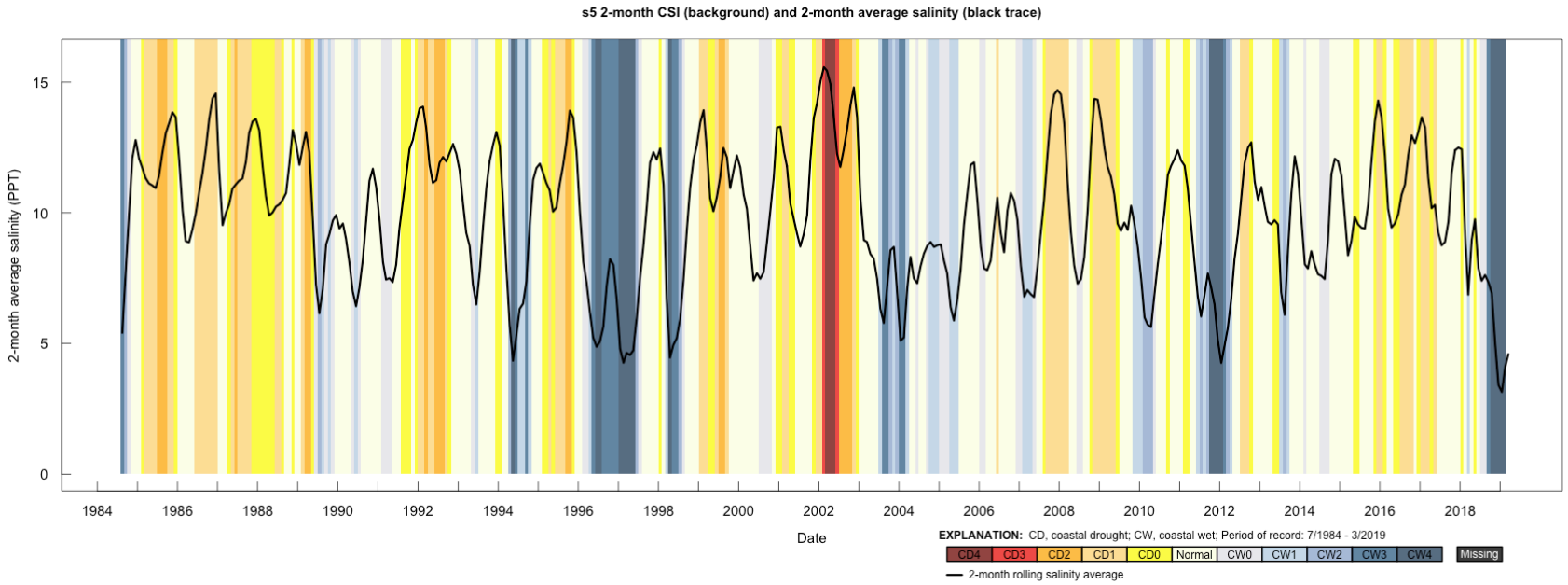

Figure S 3-11

1-month coastal salinity index (CSI) at station s6. Black line indicates 1-month rolling average salinity. Colors in background represent periods of drought (yellow to red colors) or periods of wetter conditions (light blue to dark blue). Green background indicates linearly interpolated data.

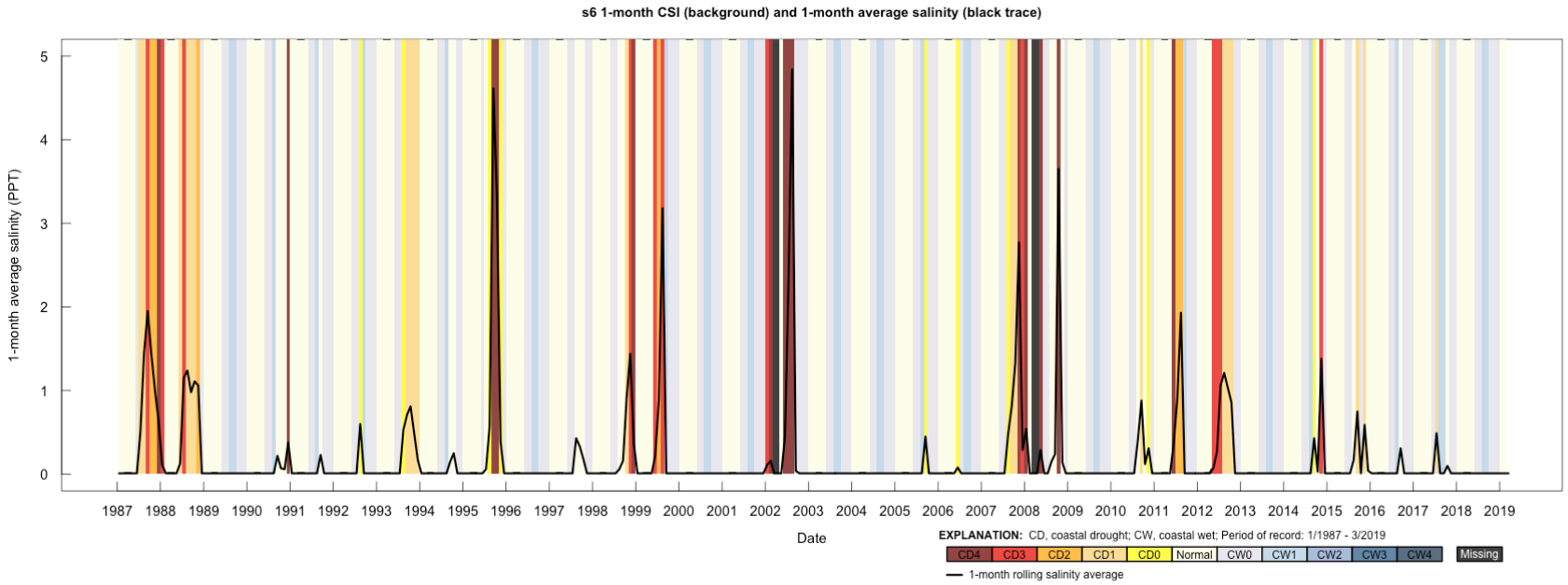

Figure S 3-12

2-month coastal salinity index (CSI) at station s6. Black line indicates 2-month rolling average salinity. Colors in background represent periods of drought (yellow to red colors) or periods of wetter conditions (light blue to dark blue).

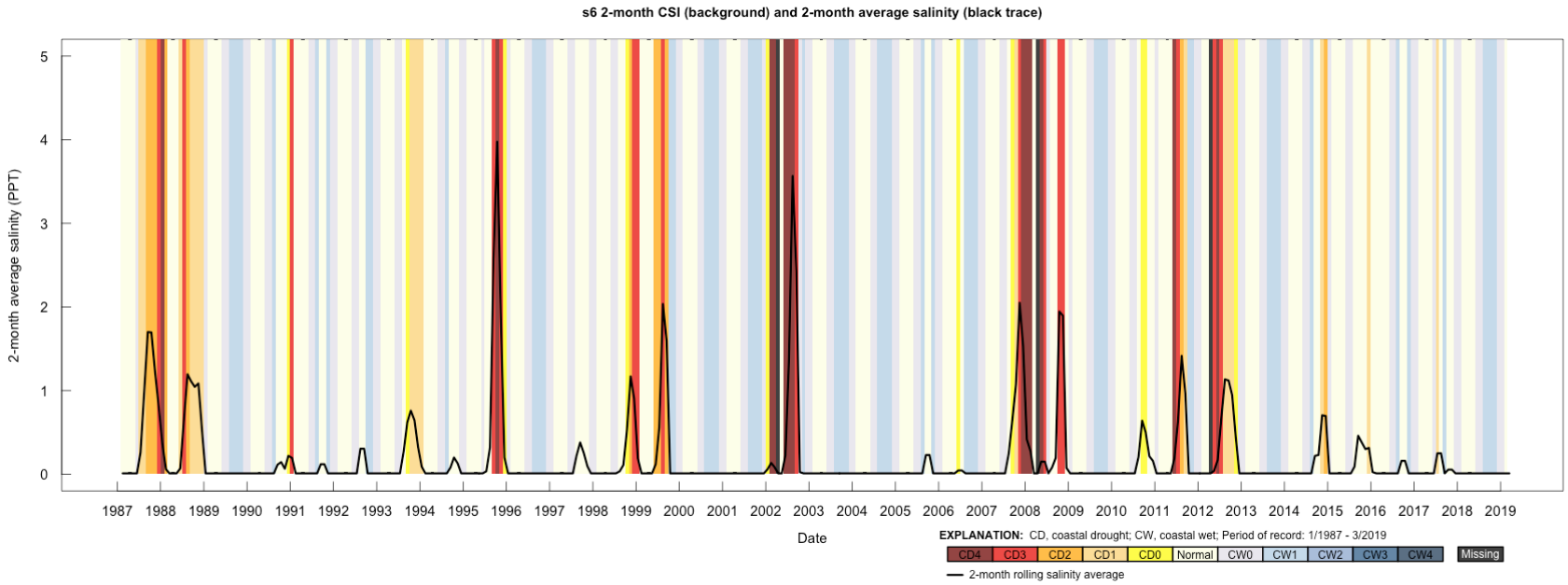

Figure S 3-13

1-month coastal salinity index (CSI) at station s7. Black line indicates 1-month rolling average salinity. Colors in background represent periods of drought (yellow to red colors) or periods of wetter conditions (light blue to dark blue). Green background indicates linearly interpolated data.

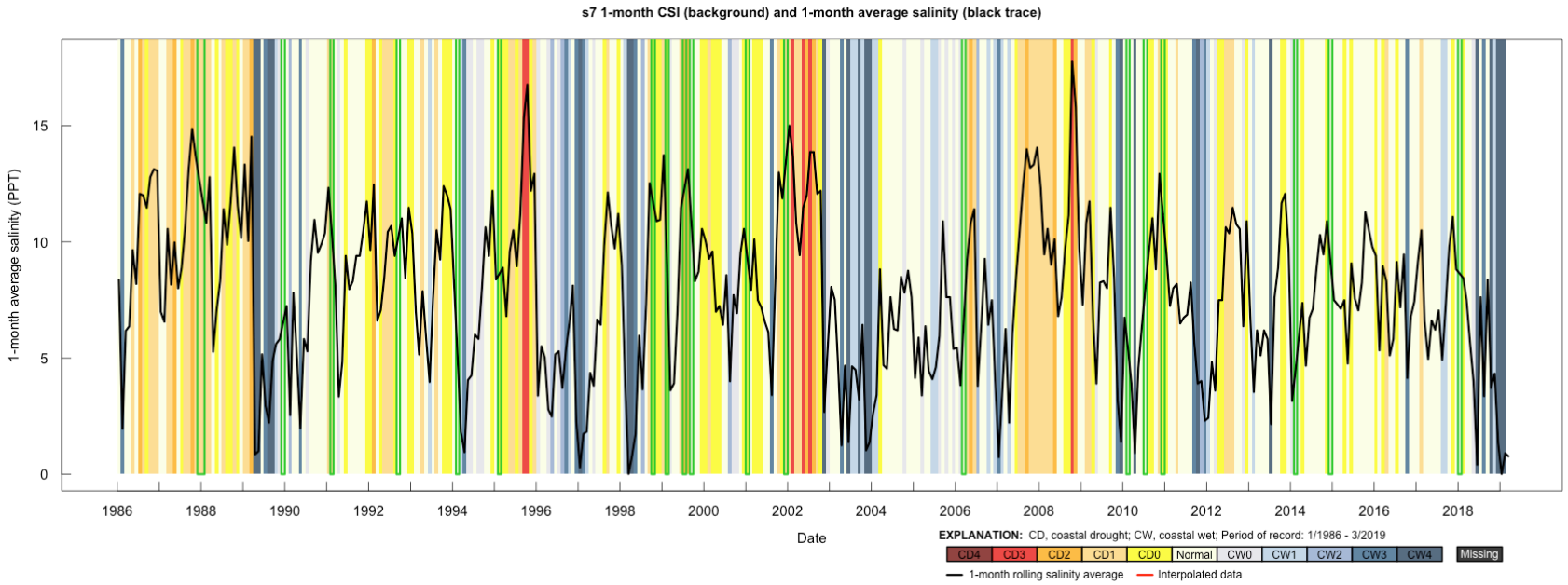

Figure S 3-14

2-month coastal salinity index (CSI) at station s7. Black line indicates 2-month rolling average salinity. Colors in background represent periods of drought (yellow to red colors) or periods of wetter conditions (light blue to dark blue).

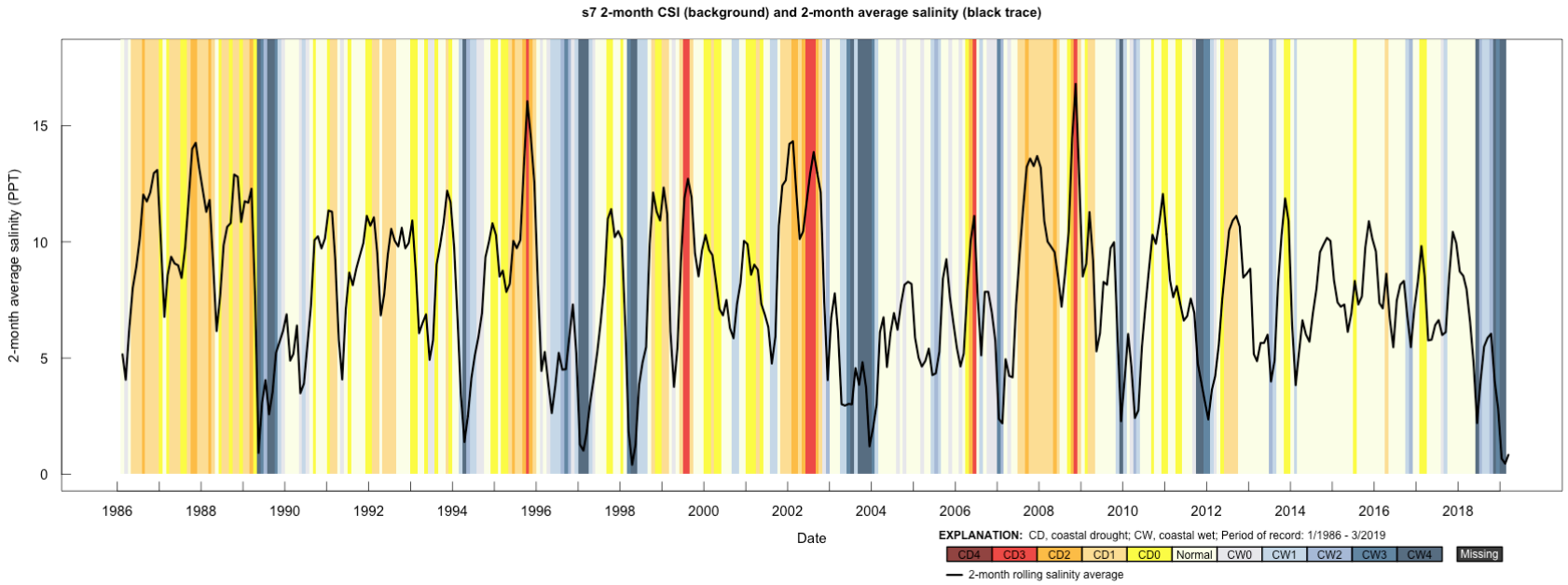

Figure S 3-15

1-month coastal salinity index (CSI) at station s8. Black line indicates 1-month rolling average salinity. Colors in background represent periods of drought (yellow to red colors) or periods of wetter conditions (light blue to dark blue). Green background indicates linearly interpolated data.

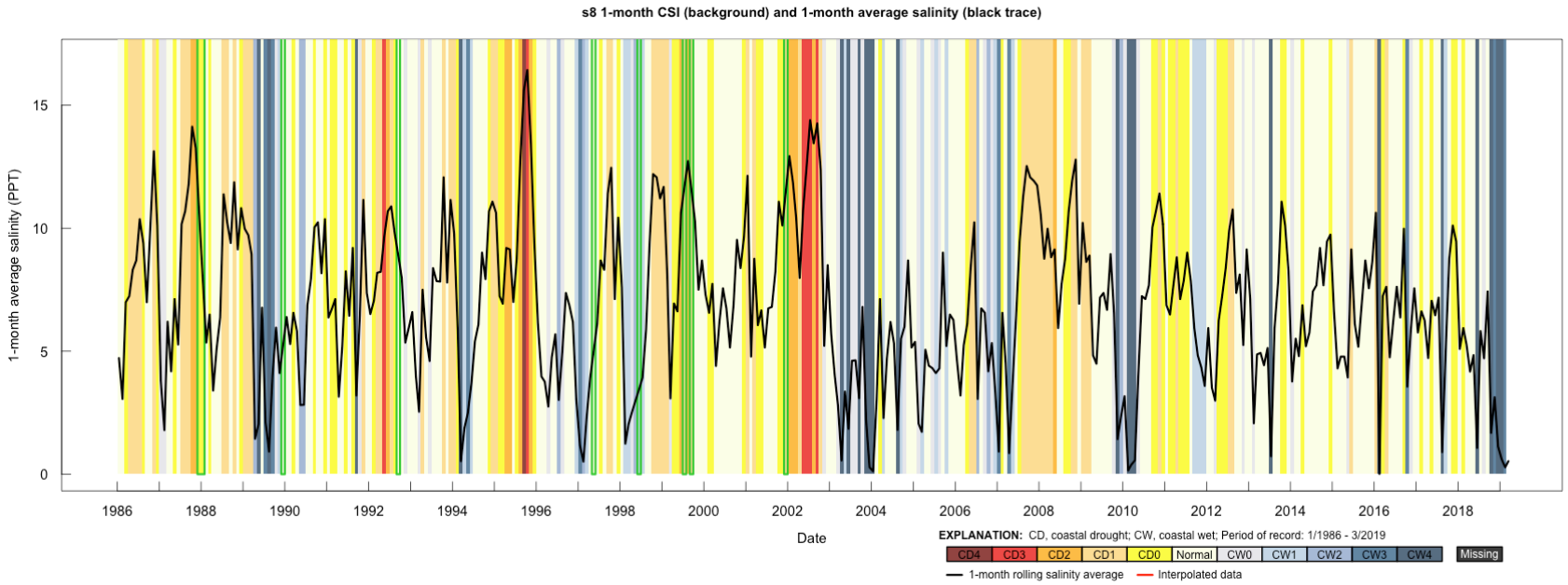

Figure S 3-16

2-month coastal salinity index (CSI) at station s8. Black line indicates 2-month rolling average salinity. Colors in background represent periods of drought (yellow to red colors) or periods of wetter conditions (light blue to dark blue).

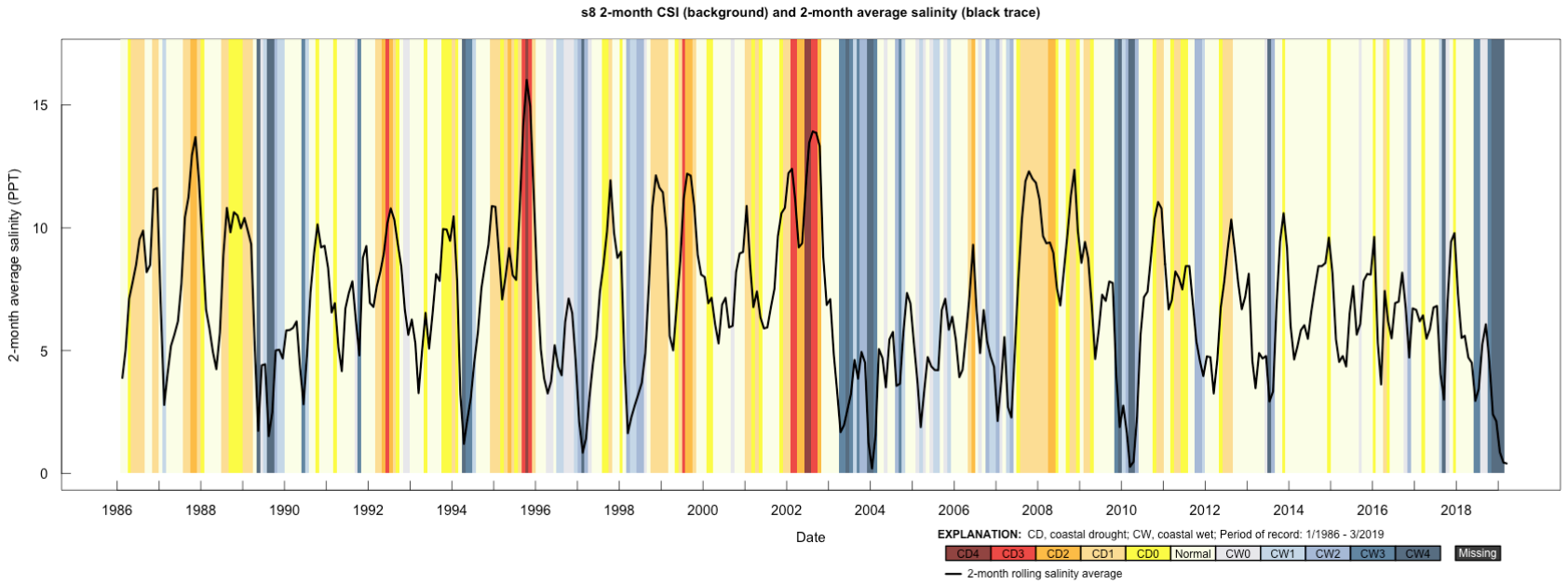

Figure S 3-17

1-month coastal salinity index (CSI) at station s9. Black line indicates 1-month rolling average salinity. Colors in background represent periods of drought (yellow to red colors) or periods of wetter conditions (light blue to dark blue). Green background indicates linearly interpolated data.

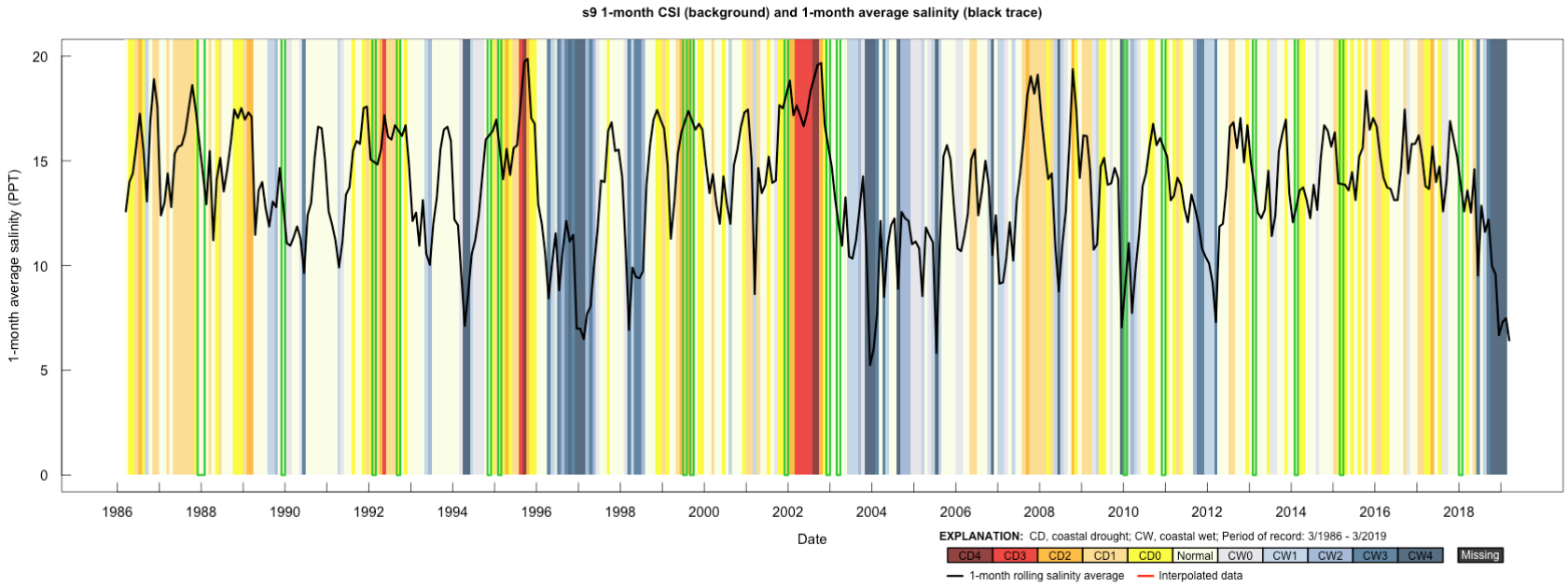

Figure S 3-18

2-month coastal salinity index (CSI) at station s9. Black line indicates 2-month rolling average salinity. Colors in background represent periods of drought (yellow to red colors) or periods of wetter conditions (light blue to dark blue).

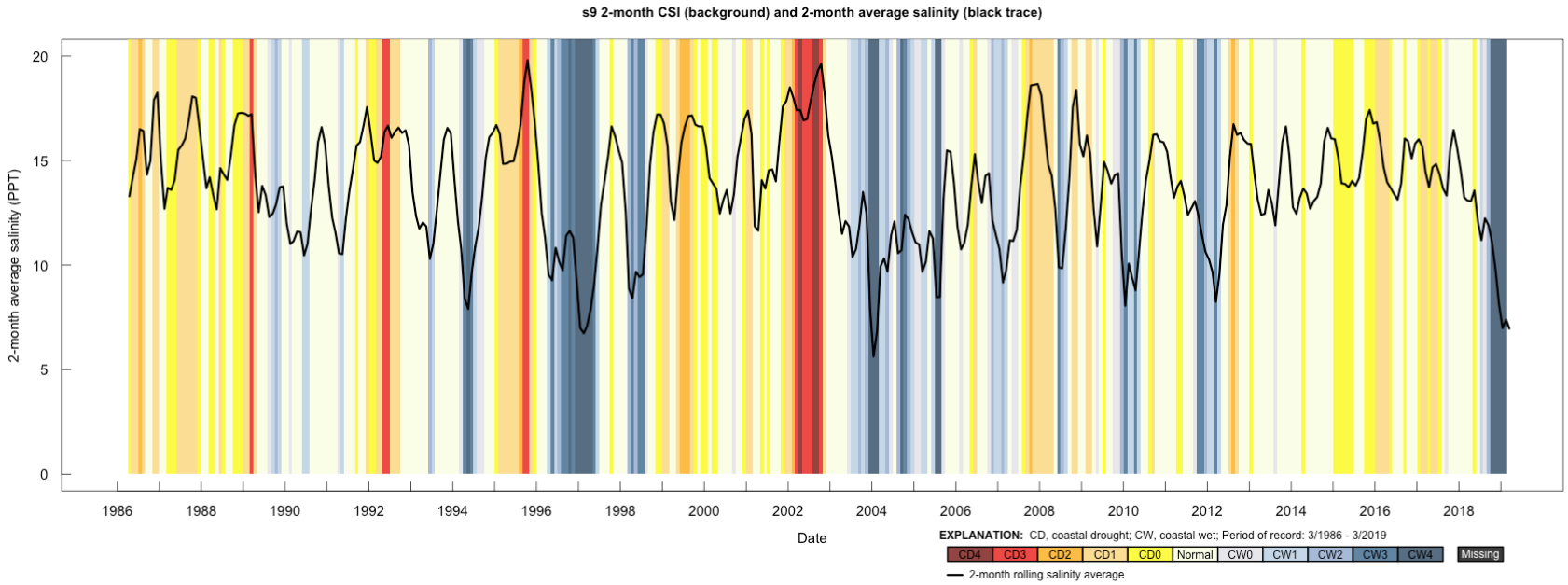

Figure S 3-19

1-month coastal salinity index (CSI) at station s10. Black line indicates 1-month rolling average salinity. Colors in background represent periods of drought (yellow to red colors) or periods of wetter conditions (light blue to dark blue). Green background indicates linearly interpolated data.

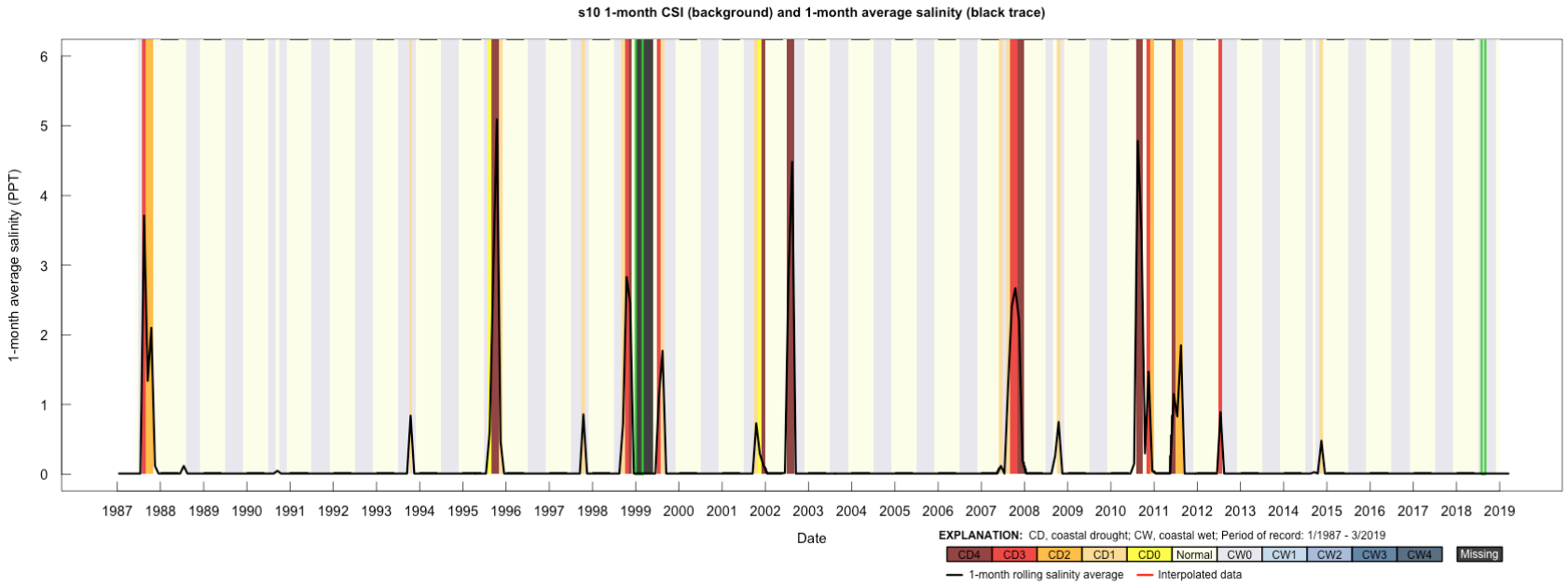

Figure S 3-20

2-month coastal salinity index (CSI) at station s10. Black line indicates 2-month rolling average salinity. Colors in background represent periods of drought (yellow to red colors) or periods of wetter conditions (light blue to dark blue).

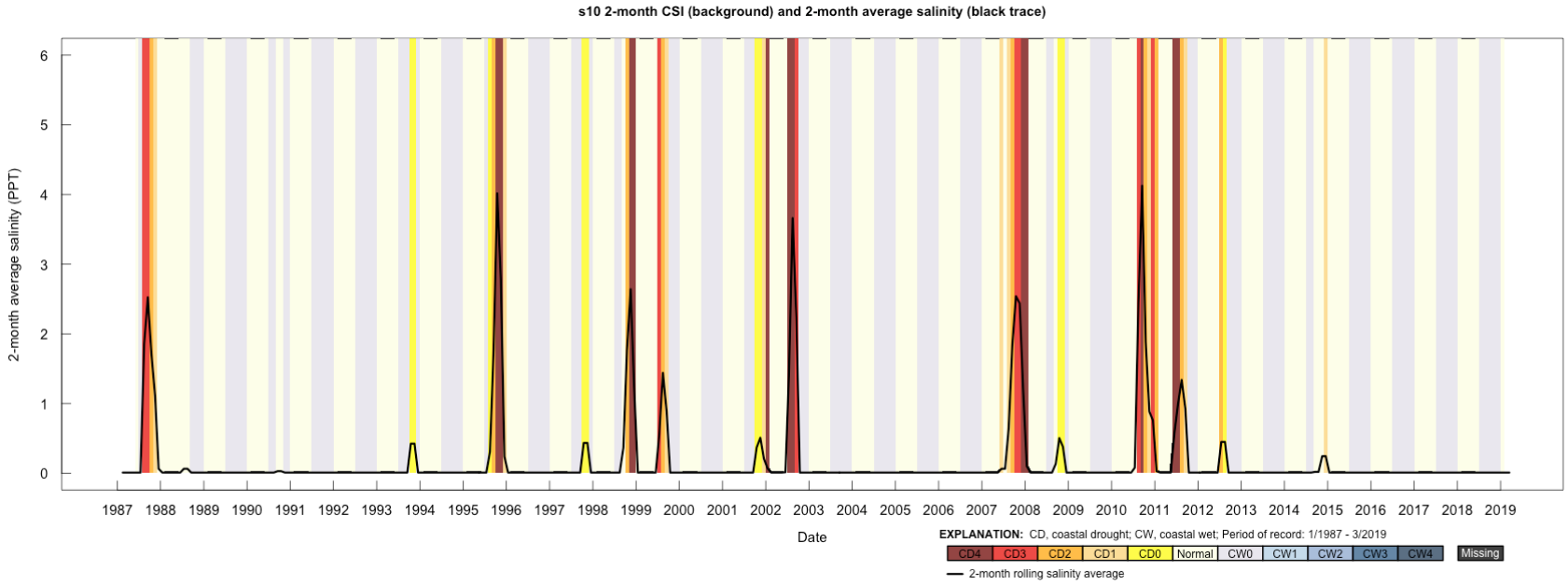

Chapter 4: Comprehensive works cited

Abler D, Shortle J, Carmichael J, Horan R (2002) Climate change, agriculture, and water quality in the Chesapeake Bay region. Clim Change 55:339–359. https://doi.org/10.1023/A:1020570526499

Allison LE, Bernstein L, Brown JW, et al (1954) Diagnosis and Improvement of Saline and Alkaline Soils. Washington D.C.

Ardón M, Helton AM, Scheuerell MD, Bernhardt ES (2017) Fertilizer legacies meet saltwater incursion : challenges and constraints for coastal plain wetland restoration. Elem Sci Anthr 5:41. https://doi.org/10.1525/elementa.236

Ardón M, Morse JL, Colman BP, Bernhardt ES (2013) Drought-induced saltwater incursion leads to increased wetland nitrogen export. Glob Chang Biol 19:2976–2985. https://doi.org/10.1111/gcb.12287

Arkema KK, Guannel G, Verutes G, et al (2013) Coastal habitats shield people and property from sea-level rise and storms. Nat Clim Chang 3:913–918. https://doi.org/10.1038/nclimate1944

Austin JA (2002) Estimating the mean ocean-bay exchange rate of the Chesapeake Bay. J Geophys Res C Ocean 107:13–1. https://doi.org/10.1029/2001jc001246

Baldwin AH, Kangas PJ, Megonigal JP, et al (2009) Coastal Wetlands of the Chesapeake Bay. In: Baldwin AH (ed) Wetland Habitats of North America - Ecology and Conservation Concerns, 1st edn. University of California Press, Berkeley, CA, pp 29–43

Bates D, Maechler M, Bolker B, et al (2018) lme4 Linear Mixed-Effects Models

using “Eigen” and S4. https://cran.r-project.org/web/packages/lme4/lme4.pdf

Beguería S, Latorre B, Reig F, Vicente-Serrano SM (2020) Standardized Precipitation Evapotranspiration Index Global Database. In: Cons. Super. Investig. Científicas. https://spei.csic.es/database.html. Accessed 1 Nov 2019

Bhattachan A, Emanuel RE, Ardon M, et al (2018) Evaluating the effects of land-use change and future climate change on vulnerability of coastal landscapes to saltwater intrusion. Elem Sci Anth 6:62. https://doi.org/10.1525/elementa.316

Bianchi TS (2007) Estuarine Science and Biogeochemical Cycles. In: Biogeochemistry of Estuaries. Oxford University Press, Oxford, pp 3–10

Boesch DF (2006) Scientific requirements for ecosystem-based management in the restoration of Chesapeake Bay and Coastal Louisiana. Ecol Eng 26:6–26. https://doi.org/10.1016/j.ecoleng.2005.09.004

Boesch DF, Brinsfield RB, Magnien RE (2001) Chesapeake Bay Eutrophication. J Environ Qual 30:303–320. https://doi.org/10.2134/jeq2001.302303x

Box GEP, Cox DR (1964) An analysis of transformations. J R Stat Soc Ser B 26:190–197

Brady NC, Weil RR (2016) The Nature and Properties of Soils, 15th edn. Pearson, Columbus

Brand-Klibanski S, Litaor MI, Shenker M (2007) Overestimation of Phosphorus Adsorption Capacity in Reduced Soils: An Artifact of Typical Batch Adsorption Experiments. Soil Sci Soc Am J 71:1128. https://doi.org/10.2136/sssaj2006.0222

Burgin AJ, Hamilton SK (2007) Have we overemphasized the role of denitrification in aquatic ecosystems? A review of nitrate removal pathways. Front Ecol

Environ 5:89–96. https://doi.org/10.1890/1540-9295(2007)5[89:HWOTRO]2.0.CO;2

Campbell PC, Bash JO, Nolte CG, et al (2019) Projections of Atmospheric Nitrogen Deposition to the Chesapeake Bay Watershed. J Geophys Res Biogeosciences 3307–3326. https://doi.org/10.1029/2019JG005203

Caraco N, Cole J, Likens GE (1990) A comparison of phosphorus immobilization in sediments of freshwater and coastal marine systems. Biogeochemistry 9:277–290. https://doi.org/10.1007/BF00000602

CBP Data Integrity Workgroup (DIWG), Nontidal Workgroup (2017) Methods and Quality Assurance for Chesapeake Bay Water Quality Monitoring Programs - CBP/TRS-319. In: Chesap. Bay Progr. Rep. https://www.chesapeakebay.net/documents/Methods_Manual.pdf

Chambers RM, Odum WE (1990) Porewater oxidation, dissolved phosphate and the iron curtain - Iron-phosphorus relations in tidal freshwater marshes. Biogeochemistry 10:37–52. https://doi.org/10.1007/BF00000891

Chesapeake Bay Program (2019) Chesapeake Bay Program: Water Quality Database. In: Chesap. Bay Progr. Website. https://www.chesapeakebay.net/what/downloads/cbp_water_quality_database_1984_present

Chesapeake Bay Program (2018) 2017 and 2025 Watershed Implementation Plans (WIPs). In: Chesap. Bay Progr. - Chesap. Prog. https://www.chesapeakeprogress.com/clean-water/watershed-implementation-plans. Accessed 29 Nov 2018

Clarke RA, Stanley CD, McNeal BL, MacLeod BW (2002) Impact of agricultural land use on nitrate levels in Lake Manatee, Florida. J Soil Water Conserv 57:106–111

Condron LM, Turner BL, Cade-Menun BJ (2005) 04 Chemistry and dynamics of soil organic phosphorus. Agron Monogr Phosphorus Agric Environ 46:87–120

Conrads PA, Darby LS (2017) Development of a coastal drought index using salinity data. Bull Am Meteorol Soc 98:753–766. https://doi.org/10.1175/BAMS-D-15-00171.1

Darke AK, Walbridge MR (1994) Estimating non-crystalline and crystalline aluminum and iron by selective dissolution in a riparian forest soil. Commun Soil Sci Plant Anal 25:2089–2101

Deegan LA, Johnson DS, Warren RS, et al (2012) Coastal eutrophication as a driver of salt marsh loss. Nature 490:388–392. https://doi.org/10.1038/nature11533

Di HJ, Cameron KC (2002) Nitrate leaching in temperate agroecosystems: Sources, factors and mitigating strategies. Nutr Cycl Agroecosystems 64:237–256. https://doi.org/10.1023/A:1021471531188

Diaz RJ, Rosenberg R (2008) Spreading dead zones and consequences for marine ecosystems. Science (80-) 321:926–929. https://doi.org/10.1126/science.1156401

Dierberg FE, DeBusk TA, Larson NR, et al (2011) Effects of sulfate amendments on mineralization and phosphorus release from South Florida (USA) wetland soils under anaerobic conditions. Soil Biol Biochem 43:31–45. https://doi.org/10.1016/j.soilbio.2010.09.006

Eshleman KN, Sabo RD (2016) Declining nitrate-N yields in the Upper Potomac River Basin: What is really driving progress under the Chesapeake Bay restoration? Atmos Environ 146:280–289. https://doi.org/10.1016/j.atmosenv.2016.07.004

Ezer T, Corlett WB (2012) Is sea level rise accelerating in the Chesapeake Bay? A demonstration of a novel new approach for analyzing sea level data. Geophys Res Lett 39:1–6. https://doi.org/10.1029/2012GL053435

Fanelli RM, Blomquist JD, Hirsch RM (2019) Point sources and agricultural practices control spatial-temporal patterns of orthophosphate in tributaries to Chesapeake Bay. Sci Total Environ 652:422–433. https://doi.org/10.1016/j.scitotenv.2018.10.062

Fowler DN, King SL, Weindorf DC (2014) Evaluating Abiotic Influences on Soil Salinity of Inland Managed Wetlands and Agricultural Croplands in a Semi-Arid Environment. Wetlands 34:1229–1239. https://doi.org/10.1007/s13157-014-0585-3

Gächter R, Müller B (2003) Why the phosphorus retention of lakes does not necessarily depend on the oxygen supply to their sediment surface. Limnol Oceanogr 48:929–933. https://doi.org/10.4319/lo.2003.48.2.0929

Gascho GJ, Parker MB (2001) Long-term liming effects on Coastal Plain soils and crops. Agron J 93:1305–1315. https://doi.org/10.2134/agronj2001.1305

Gburek WJ, Barberis E, Haygarth PM, et al (2005) Phosphorus Mobility in the Landscape. Phosphorus Agric Environ 941–979. https://doi.org/10.2134/agronmonogr46.c29

Gedan KB, Fernández-Pascual E (2019) Salt marsh migration into salinized agricultural fields: A novel assembly of plant communities. J Veg Sci 30:1007–1016. https://doi.org/10.1111/jvs.12774

Giblin AE, Tobias CR, Song B, et al (2013) The importance of dissimilatory nitrate reduction to ammonium (DNRA) in the nitrogen cycle of coastal ecosystems. Oceanography 26:124–131. https://doi.org/10.5670/oceanog.2013.54

Giesler R, Andersson T, Lövgren L, Persson P (2005) Phosphate Sorption in Aluminum-and Iron-Rich Humus Soils. Soil Sci Soc Am J 69:77–86. https://doi.org/10.2136/sssaj2005.0077

Glick P, Clough J, Nunley B (2008) Sea-Level Rise and Coastal Habitats in the Chesapeake Bay Region Technical Report. 1–121

Google Earth (2019) Google Earth imagery. http://www.earth.google.com. Accessed 4 Dec 2018

Goyne KW, Jun H-J, Anderson SH, Motavalli PP (2008) Phosphorus and nitrogen sorption to soils in the presence of poultry litter-derived dissolved organic matter. J Environ Qual 37:154–63. https://doi.org/10.2134/jeq2007.0141

Grubb KL, McGrath JM, Penn CJ, Bryant RB (2012) Effect of land application of phosphorus-saturated gypsum on soil phosphorus in a laboratory incubation. Appl Environ Soil Sci 2012:9–12. https://doi.org/10.1155/2012/506951

Grubb KL, McGrath JM, Penn CJ, Bryant RB (2011) Land application of spent gypsum from ditch filters: phosphorus source or sink? Agric Sci 02:364–374. https://doi.org/10.4236/as.2011.23048

Hamed KH, Rao AR (1998) A modified Mann-Kendall trend test for autocorrelated

data. J Hydrol 204:182–196. https://doi.org/10.1016/S0022-1694(97)00125-X

Hanin M, Ebel C, Ngom M, et al (2016) New Insights on Plant Salt Tolerance Mechanisms and Their Potential Use for Breeding. Front Plant Sci 7:1–17. https://doi.org/10.3389/fpls.2016.01787

Harding LW, Gallegos CL, Perry ES, et al (2016) Long-Term Trends of Nutrients and Phytoplankton in Chesapeake Bay. Estuaries and Coasts 39:664–681. https://doi.org/10.1007/s12237-015-0023-7

Harrel Jr. FE (2018) Package 'HMisc' for R

Hartzell JL, Jordan TE (2012) Shifts in the relative availability of phosphorus and nitrogen along estuarine salinity gradients. Biogeochemistry 107:489–500. https://doi.org/10.1007/s10533-010-9548-9

Hartzell JL, Jordan TE, Cornwell JC (2017) Phosphorus Sequestration in Sediments Along the Salinity Gradients of Chesapeake Bay Subestuaries. Estuaries and Coasts 40:1607–1625. https://doi.org/10.1007/s12237-017-0233-2

Harvey JW, Hall C (1992) Ammonium and Phosphate Dynamics in a Virginia Salt Marsh. Estuaries 15:349–359

Hauke J, Kossowski T (2011) Comparison of values of pearson's and spearman's correlation coefficients on the same sets of data. Quaest Geogr 30:87–93. https://doi.org/10.2478/v10117-011-0021-1

Helton AM, Ardón M, Bernhardt ES (2015) Thermodynamic constraints on the utility of ecological stoichiometry for explaining global biogeochemical patterns. Ecol Lett 18:1049–1056. https://doi.org/10.1111/ele.12487

Helton AM, Bernhardt ES, Fedders A (2014) Biogeochemical regime shifts in coastal

landscapes: The contrasting effects of saltwater incursion and agricultural pollution on greenhouse gas emissions from a freshwater wetland. Biogeochemistry 120:133–147. https://doi.org/10.1007/s10533-014-9986-x

Hilton TW, Najjar RG, Zhong L, Li M (2008) Is there a signal of sea-level rise in Chesapeake Bay salinity? J Geophys Res Ocean 113:1–12. https://doi.org/10.1029/2007JC004247

Hothorn T, Bretz F, Westfall P, et al (2017) Simultaneous Inference in General Parametric Models. https://cran.r-project.org/web/packages/multcomp/

Hussein AH, Rabenhorst MC (2010) Tidal Inundation of Transgressive Coastal Areas. Soil Sci Soc Am J 65:536. https://doi.org/10.2136/sssaj2001.652536x

IPCC (2013) IPCC, 2013: Summary for Policymakers

Irani F. (2015) Chesapeake Bay Watershed 2011 Edition Land Cover Data Release. In: U.S. Geol. Surv. data release. https://www.sciencebase.gov/catalog/item/557b238fe4b0c350d7b9abb8

Islam AKMS, Edwards DG, Asher CJ (1980) pH optima for crop growth. Plant Soil 54:339–357. https://doi.org/10.1007/BF02181830

Jessen S, Postma D, Thorling L, et al (2017) Decadal variations in groundwater quality: A legacy from nitrate leaching and denitrification by pyrite in a sandy aquifer. Water Resour Res 53:184–198. https://doi.org/10.1002/2016WR018995

Jia J, Bai J, Gao H, et al (2017) In situ soil net nitrogen mineralization in coastal salt marshes (Suaeda salsa) with different flooding periods in a Chinese estuary. Ecol Indic 73:559–565. https://doi.org/10.1016/j.ecolind.2016.10.012

Johnson SE, Loeppert RH (2006) Role of Organic Acids in Phosphate Mobilization

from Iron Oxide. Soil Sci Soc Am J 70:222. https://doi.org/10.2136/sssaj2005.0012

Jordan TE, Cornwell JC, Boynton WR, et al (2008) Changes in phosphorus biogeochemistry along an estuarine salinity gradient: The iron conveyer belt. Limnol Oceanogr 53:172–184

Jordan TE, Correll DL, Miklas J, Weller DE (1991) Nutrients and chlorophyll at the interface of a watershed and an estuary. Limnol Oceanogr 36:251–267. https://doi.org/10.4319/lo.1991.36.2.0251

Jordan TE, Weller DE, Pelc CE (2018) Effects of Local Watershed Land Use on Water Quality in Mid-Atlantic Coastal Bays and Subestuaries of the Chesapeake Bay. Estuaries and Coasts 41:38–53. https://doi.org/10.1007/s12237-017-0303-5

Kaplan D, Pruim R (2020) ggformula: Formula Interface to the Grammar of Graphics

Kemp WM, Boynton WR, Adolf JE, et al (2005) Eutrophication of Chesapeake Bay: historical trends and ecological interactions. Mar Ecol Prog Ser 303:1–29. https://doi.org/10.3354/meps303001

King KW, Williams MR, Macrae ML, et al (2015) Phosphorus Transport in Agricultural Subsurface Drainage: A Review. J Environ Qual 44:467–485. https://doi.org/10.2134/jeq2014.04.0163

Kirwan ML, Gedan KB (2019) Sea-level driven land conversion and the formation of ghost forests. Nat Clim Chang 9:450–457. https://doi.org/10.1038/s41558-019-0488-7

Kirwan ML, Kirwan JL, Copenheaver CA (2007) Dynamics of an Estuarine Forest and its Response to Rising Sea Level. J Coast Res 232:457–463.

https://doi.org/10.2112/04-0211.1

Kleinman PJA, Church C, Saporito LS, et al (2015) Phosphorus leaching from agricultural soils of the Delmarva Peninsula, USA. J Environ Qual 44:524–534. https://doi.org/10.2134/jeq2014.07.0301

Kleinman PJA, Sharpley AN, Buda AR, et al (2011) Soil controls of phosphorus in runoff: Management barriers and opportunities. Can J Soil Sci 91:329–338. https://doi.org/10.4141/cjss09106

Klemick H, Griffiths C, Guignet D, Walsh P (2018) Improving Water Quality in an Iconic Estuary: An Internal Meta-analysis of Property Value Impacts Around the Chesapeake Bay. Environ Resour Econ 69:265–292. https://doi.org/10.1007/s10640-016-0078-3

Koop-jakobsen K, Giblin AE (2010) The effect of increased nitrate loading on nitrate reduction via denitrification and DNRA in salt marsh sediments. Limnol Oceanogr 55:789–802

Koretsky CM, Van Cappellen P, Dichristina TJ, et al (2005) Salt marsh pore water geochemistry does not correlate with microbial community structure. Estuar Coast Shelf Sci 62:233–251. https://doi.org/10.1016/j.ecss.2004.09.001

Kraal P, Burton ED, Bush RT (2013) Iron monosulfide accumulation and pyrite formation in eutrophic estuarine sediments. Geochim Cosmochim Acta 122:75–88. https://doi.org/10.1016/j.gca.2013.08.013

Lilienfein J, Qualls RG, Uselman SM, Bridgham SD (2004) Adsorption of Dissolved Organic and Inorganic Phosphorus in Soils of a Weathering Chronosequence. Soil Sci Soc Am J 68:620–628

Lister TW, Perdue JL, Barnett CJ, et al (2011) Maryland's forests 2008. In: United States Dep. Agric. For. Serv. Rep. https://www.nrs.fs.fed.us/pubs/rb/rb_nrs58.pdf. Accessed 9 Sep 2019

Loughner CP, Tzortziou M, Shroder S, Pickering KE (2016) Enhanced dry deposition of nitrogen pollution near coastlines: A case study covering the chesapeake bay estuary and atlantic ocean coastline. J Geophys Res 121:14,221-14,238. https://doi.org/10.1002/2016JD025571

Markewich HW, Pavich MJ, Buell GR (1990) Contrasting soils and landscapes of the Piedmont and Coastal Plain, eastern United States. Geomorphology 3:417–447. https://doi.org/10.1016/0169-555X(90)90015-I

Marton JM, Herbert ER, Craft CB (2012) Effects of salinity on denitrification and greenhouse gas production from laboratory-incubated tidal forest soils. Wetlands 32:347–357. https://doi.org/10.1007/s13157-012-0270-3

Maryland Department of Natural Resources (1998) Maryland Watersheds - 8 Digit Watersheds. In: Maryland.gov Website. https://geodata.md.gov/imap/rest/services/Hydrology/MD_Watersheds/FeatureServer/1. Accessed 1 Feb 2020

Maryland Department of Natural Resources, NOAA [National Oceanic and Atmospheric Administration] (2008) Somerset County, Maryland: Rising Sea Level Guidance. https://dnr.maryland.gov/ccs/Publication/SeaLevel_Somerset.pdf. Accessed 1 May 2019

Maryland Department of the Environment (2018) Maryland's Integrated Report of

Surface Water Quality. https://mde.maryland.gov/programs/Water/TMDL/Integrated303dReports/Pages/2018IR.aspx. Accessed 20 Jun 2019

McCloskey B (2019) R - Coastal salinity index package

McDowell RW, Sharpley AN (2001) Soil phosphorus fractions in solution: Influence of fertiliser and manure, filtration and method of determination. Chemosphere 45:737–748. https://doi.org/10.1016/S0045-6535(01)00117-5

Megonigal JP, Neubauer SC (2009) Biogeochemistry of Tidal Freshwater Wetlands. Coast Wetl An Integr Ecosyst Approach 535–562. https://doi.org/10.1016/B978-0-444-53103-2.00019-3

Miller KG, Kopp RE, Horton BP, et al (2013) A geological perspective on sea-level rise and its impacts along the U.S. mid-Atlantic coast. Earth's Futur 1:3–18. https://doi.org/10.1002/2013ef000135

Moomaw WR, Chmura GL, Davies GT, et al (2018) Wetlands In a Changing Climate: Science, Policy and Management. Wetlands 38:183–205. https://doi.org/10.1007/s13157-018-1023-8

Moore PA, Miller DM (1994) Decreasing Phosphorus Solubility in Poultry Litter with Aluminum, Calcium, and Iron Amendments. J Environ Qual 23:325. https://doi.org/10.2134/jeq1994.00472425002300020016x

Moyer DL, Blomquist JD (2018) Summary of Nitrogen, Phosphorus, and Suspended-Sediment Loads and Trends Measured at the Nine Chesapeake Bay River Input Monitoring Stations: Water Year 2017 Update. In: United States Geol. Surv. Rep. https://cbrim.er.usgs.gov/data/RIM Load and Trend Summary

2017_Combined.pdf

Musolff A, Selle B, Büttner O, et al (2017a) Does iron reduction control the release of dissolved organic carbon and phosphate at catchment scales? Need for a joint research effort. Glob Chang Biol 23:e5–e6. https://doi.org/10.1111/gcb.13758

Musolff A, Selle B, Büttner O, et al (2017b) Unexpected release of phosphate and organic carbon to streams linked to declining nitrogen depositions. Glob Chang Biol 23:1891–1901. https://doi.org/10.1111/gcb.13498

Nair VD, Clark MW, Reddy KR (2015) Evaluation of Legacy Phosphorus Storage and Release from Wetland Soils. J Environ Qual 44:1956. https://doi.org/10.2134/jeq2015.03.0154

Nair VD, Reddy KR, DeLaune RD, et al (2013) Phosphorus Sorption and Desorption in Wetland Soils. In: Methods in Biogeochemistry of Wetlands. Madison, WI, pp 667–681

Najjar R, Patterson L, Graham S (2009) Climate simulations of major estuarine watersheds in the Mid-Atlantic region of the US. Clim Change 95:139–168. https://doi.org/10.1007/s10584-008-9521-y

National Oceanic and Atmospheric Administration - National Centers for Environmental Information [NOAA-NCEI] (2018) Climate Data Online. In: Natl. Ocean. Atmos. Adm. - Natl. Centers Environ. Inf. https://www.ncdc.noaa.gov/cdo-web/. Accessed 20 Nov 2018

Neubauer SC, Franklin RB, Berrier DJ (2013) Saltwater intrusion into tidal freshwater marshes alters the biogeochemical processing of organic carbon. Biogeosciences 10:8171–8183. https://doi.org/10.5194/bg-10-8171-2013

Ocampo CJ, Oldham CE, Sivapalan M (2006) Nitrate attenuation in agricultural catchments: Shifting balances between transport and reaction. Water Resour Res 42:1–16. https://doi.org/10.1029/2004WR003773

Paerl HW, Hall NS, Peierls BL, Rossignol KL (2014) Evolving Paradigms and Challenges in Estuarine and Coastal Eutrophication Dynamics in a Culturally and Climatically Stressed World. Estuaries and Coasts 37:243–258. https://doi.org/10.1007/s12237-014-9773-x

Patakamuri SK, O'Brien N (2019) modifiedmk: Modified Versions of Mann Kendall and Spearman's Rho Trend Tests

Perez MR (2015) Regulating Farmer Nutrient Management: A Three-State Case Study on the Delmarva Peninsula. J Environ Qual 44:402. https://doi.org/10.2134/jeq2014.07.0304

Qualls RG, Haines BL (1991) Geochemistry of Dissolved Organic Nutrients in Water Percolating through a Forest Ecosystem. Soil Sci Soc Am J 55:1112–1123

Qualls RG, Haines BL, Swank WT, Tyler SW (2000) Soluble Organic and Inorganic Nutrient Fluxes in Clearcut and Mature Deciduous Forests. Soil Sci Soc Am J 64:1068–1077

R Studio Team (2019) RStudio: Integrated Development for R

Reddy KR, DeLaune RD (2008) Biogeochemistry of Wetlands, 1st edn. CRC Press, Boca Raton, Florida

Rice KC, Hong B, Shen J (2012) Assessment of salinity intrusion in the James and Chickahominy Rivers as a result of simulated sea-level rise in Chesapeake Bay, East Coast, USA. J Environ Manage 111:61–69.

https://doi.org/10.1016/j.jenvman.2012.06.036

Roman CT, Burdick DM (2012) Tidal Marsh Restoration. Island Press/Center for Resource Economics, Washington, DC

Ross AC, Najjar RG, Li M, et al (2015) Sea-level rise and other influences on decadal-scale salinity variability in a coastal plain estuary. Estuar Coast Shelf Sci 157:79–92. https://doi.org/10.1016/j.ecss.2015.01.022

Rütting T, Boeckx P, Müller C, Klemedtsson L (2011) Assessment of the importance of dissimilatory nitrate reduction to ammonium for the terrestrial nitrogen cycle. Biogeosciences 8:1779–1791. https://doi.org/10.5194/bg-8-1779-2011

Ryberg KR, Blomquist JD, Sprague LA, et al (2018) Modeling drivers of phosphorus loads in Chesapeake Bay tributaries and inferences about long-term change. Sci Total Environ 616–617:1423–1430. https://doi.org/10.1016/j.scitotenv.2017.10.173

Sanford WE, Pope JP (2013) Quantifying groundwater's role in delaying improvements to Chesapeake Bay water quality. Environ Sci Technol 47:13330–13338. https://doi.org/10.1021/es401334k

Schoepfer VA, Bernhardt ES, Burgin AJ (2014) Iron clad wetlands: Soil iron-sulfur buffering determines coastal wetland response to salt water incursion. J Geophys Res Biogeosciences Res 119:2209–2219. https://doi.org/10.1002/2014JG002739

Sharpley AN, Daniel T, Sims T, et al (2003) Agricultural Phosphorus and Eutrophication Second Edition. United States Dep Agric - Agric Res Serv ARS-149:1–43

Sharpley AN, Jarvie HP, Buda AR, et al (2014) Phosphorus Legacy: Overcoming the

Effects of Past Management Practices to Mitigate Future Water Quality Impairment. J Environ Qual 42:1308–1326. https://doi.org/10.2134/jeq2013.03.0098

Sharpley AN, Kleinman PJA, Jordan P, et al (2006) Evaluating the success of phosphorus management from field to watershed. J Environ Qual 38:1981–1988. https://doi.org/10.2134/jeq2008.0056

Shepard A, Curson D, Patton K, Dubois N (2013) Sea-level Rise Is for the Birds: Landscape-level Conservation Planning to Protect Communities, Coastal Wetlands and Salt Marsh Birds. https://defenders.org/sites/default/files/publications/Lower-Shore-Tidal-Marsh-Climate-Adaptation-Project.pdf. Accessed 17 Dec 2017

Smith JAM (2013) The Role of Phragmites australis in Mediating Inland Salt Marsh Migration in a Mid-Atlantic Estuary. PLoS One 8:e65091. https://doi.org/10.1371/journal.pone.0065091

Soil Survey Staff (2018) Web Soil Survey. In: USDA-NRCS Web Soil Surv. Website. https://websoilsurvey.sc.egov.usda.gov/. Accessed 4 Dec 2018

Steinmuller HE, Chambers LG (2018) Can Saltwater Intrusion Accelerate Nutrient Export from Freshwater Wetland Soils? An Experimental Approach. Soil Sci Soc Am J 82:283. https://doi.org/10.2136/sssaj2017.05.0162

Tango PJ, Batiuk RA (2016) Chesapeake Bay recovery and factors affecting trends: Long-term monitoring, indicators, and insights. Reg Stud Mar Sci 4:12–20. https://doi.org/10.1016/j.rsma.2015.11.010

Tanner CC, Sukias JPS (2011) Multiyear Nutrient Removal Performance of Three

Constructed Wetlands Intercepting Tile Drain Flows from Grazed Pastures. J Environ Qual 40:620. https://doi.org/10.2134/jeq2009.0470

Tobias CR, Macko SA, Anderson IC, et al (2001) Tracking the fate of a high concentration groundwater nitrate plume through a fringing marsh: A combined groundwater tracer and in situ isotope enrichment study. Limnol Oceanogr 46:1977–1989. https://doi.org/10.4319/lo.2001.46.8.1977

Trimble SW (2008) Man-induced soil erosion on the Southern Piedmont, 1700-1970., 2nd edn. Soil and Water Conservation Society, Ankeny, IA

Tully KL, Gedan K, Epanchin-Niell R, et al (2019a) The Invisible Flood: The Chemistry, Ecology, and Social Implications of Coastal Saltwater Intrusion. Bioscience 69:368–378. https://doi.org/10.1093/biosci/biz027

Tully KL, Weissman D, Wyner WJ, et al (2019b) Soils in transition: saltwater intrusion alters soil chemistry in agricultural fields. Biogeochemistry 142:339–356. https://doi.org/10.1007/s10533-019-00538-9

Turner BL, Haygarth PM (2000) Phosphorus Forms and Concentrations in Leachate under Four Grassland Soil Types. Soil Sci Soc Am J 64:1090–1099. https://doi.org/10.2136/sssaj2000.6431090x

United States Department of Agriculture - National Agricultural Statistics Service [USDA-NASS] (2012) 2012 Census of Agriculture County Profile: Somerset County, Maryland. https://www.nass.usda.gov/Publications/. Accessed 1 May 2019

United States Environmental Protection Agency [USEPA] (2000) Ambient Water Quality Criteria Recommendations of State and Tribal Nutrient Criteria Lakes

and Reservoirs in Nutrient Ecoregion II. https://www.epa.gov/sites/production/files/documents/rivers14.pdf. Accessed 16 Dec 2018

USGS (2019) National Water Information System. In: U.S. Geol. Surv. https://nwis.waterdata.usgs.gov/nwis. Accessed 15 Oct 2019

Van Meter KJ, Basu NB, Van Cappellen P (2017) Two centuries of nitrogen dynamics: Legacy sources and sinks in the Mississippi and Susquehanna River Basins. Global Biogeochem Cycles 31:2–23. https://doi.org/10.1002/2016GB005498

Vicente-Serrano SM, Beguería S, López-Moreno JI, et al (2010) A new global 0.5° gridded dataset (1901-2006) of a multiscalar drought index: Comparison with current drought index datasets based on the palmer drought severity index. J Hydrometeorol 11:1033–1043. https://doi.org/10.1175/2010JHM1224.1

Viollier E, Inglett P., Hunter K, et al (2000) The ferrozine method revisited: Fe(II)/Fe(III) determination in natural waters. Appl Geochemistry 15:785–790. https://doi.org/10.1016/S0883-2927(99)00097-9

Waldrip HM, Pagliari PH, He Z, et al (2015) Legacy Phosphorus in Calcareous Soils: Effects of Long-Term Poultry Litter Application. Soil Sci Soc Am J 79:1601. https://doi.org/10.2136/sssaj2015.03.0090

Walsh S, Miskewitz R (2013) Impact of sea level rise on tide gate function. J Environ Sci Heal Part A 48:453–463. https://doi.org/10.1080/10934529.2013.729924

Wasson K, Woolfolk A, Fresquez C (2013) Ecotones as Indicators of Changing Environmental Conditions: Rapid Migration of Salt Marsh-Upland Boundaries.

Estuaries and Coasts 36:654–664. https://doi.org/10.1007/s12237-013-9601-8

Weinberg H (2008) Chesapeake Bay Salinity Maps. In: Chesap. Bay Progr. Website. https://www.chesapeakebay.net/what/maps/keyword/salinity. Accessed 30 Nov 2018

Weissman DS, Tully KL (2020) Saltwater intrusion affects nutrient concentrations in soil porewater and surface waters of coastal habitats. Ecosphere 11:. https://doi.org/10.1002/ecs2.3041

Weston NB, Dixon RE, Joye SB (2006) Ramifications of increased salinity in tidal freshwater sediments: Geochemistry and microbial pathways of organic matter mineralization. J Geophys Res Biogeosciences 111:1–14. https://doi.org/10.1029/2005JG000071

Weston NB, Vile MA, Neubauer SC, Velinsky DJ (2011) Accelerated microbial organic matter mineralization following salt-water intrusion into tidal freshwater marsh soils. Biogeochemistry 102:135–151. https://doi.org/10.1007/s10533-010-9427-4

White E, Kaplan D (2017) Restore or retreat? Saltwater intrusion and water management in coastal wetlands. Ecosyst Heal Sustain 3:e01258. https://doi.org/10.1002/ehs2.1258

White JW, Coale FJ, Sims JT, Shober AL (2010) Phosphorus Runoff from Waste Water Treatment Biosolids and Poultry Litter Applied to Agricultural Soils. J Environ Qual 39:314–323. https://doi.org/10.2134/jeq2009.0106

Williams AA, Lauer NT, Hackney CT (2014) Soil phosphorus dynamics and saltwater intrusion in a florida estuary. Wetlands 34:535–544.

https://doi.org/10.1007/s13157-014-0520-7

Williams MR, Filoso S, Longstaff BJ, Dennison WC (2010) Long-Term Trends of Water Quality and Biotic Metrics in Chesapeake Bay: 1986 to 2008. Estuaries and Coasts 33:1279–1299. https://doi.org/10.1007/s12237-010-9333-y

Wilson AM, Morris JT (2012) The influence of tidal forcing on groundwater flow and nutrient exchange in a salt marsh-dominated estuary. Biogeochemistry 108:27–38. https://doi.org/10.1007/s10533-010-9570-y

Zak D, Rossoll T, Exner H-J, et al (2009) Mitigation of sulfate pollution by rewetting of fens — A conflict with restoring their phosphorus sink function? Wetlands 29:1093–1103. https://doi.org/10.1672/09-102D.1

Zhang Q, Murphy RR, Tian R, et al (2018) Chesapeake Bay's water quality condition has been recovering: Insights from a multimetric indicator assessment of thirty years of tidal monitoring data. Sci Total Environ 637–638:1617–1625. https://doi.org/10.1016/j.scitotenv.2018.05.025